UNIVERSIDADE FEDERAL DE MATO GROSSO DO SUL – UFMS
Campus de CAMPO GRANDE
PROGRAMA MULTICÊNTRICO DE PÓS-GRADUAÇÃO EM BIOQUÍMICA E
BIOLOGIA MOLECULAR – PMBqBM – SBBq

LUÍS HENRIQUE DE OLIVEIRA ALMEIDA

**Desenvolvimento de um novo peptídeo com atividade
antimicrobiana (bactérias e leveduras) e antiproliferativa em células
neoplásicas: análises *in silico*, *in vitro* e *in vivo***

CAMPO GRANDE – MS
Outubro – 2023

LUÍS HENRIQUE DE OLIVEIRA ALMEIDA

Desenvolvimento de um novo peptídeo com atividade antimicrobiana (bactérias e leveduras) e antiproliferativa em células neoplásicas: análises *in silico*, *in vitro* e *in vivo*

Tese de Doutorado apresentado ao Programa Multicêntrico de Pós-Graduação em Bioquímica e Biologia Molecular - PMBqBM - SBBq, da Universidade Federal de Mato Grosso do Sul, como requisito para a obtenção do grau de Doutor.

Orientadora: Dra. Maria Lígia Rodrigues Macedo

Coorientador: Dr. Marlon Henrique e Silva Cardoso

CAMPO GRANDE – MS
Outubro – 2023

TERMO DE APROVAÇÃO

LUÍS HENRIQUE DE OLIVEIRA ALMEIDA

Desenvolvimento de um novo peptídeo com atividade antimicrobiana (bactérias e leveduras) e antiproliferativa em células neoplásicas: análises *in silico*, *in vitro* e *in vivo*

Tese de Doutorado apresentado ao Programa Multicêntrico de Pós-Graduação em Bioquímica e Biologia Molecular – PMBqBM – SBBq, da Universidade Federal de Mato Grosso do Sul, para a obtenção do título de Doutor em Bioquímica e Biologia Molecular.

Campo Grande – MS, 23 de outubro de 2023.

Comissão Examinadora:

_____
Dr.ª Maria Lígia Rodrigues Macedo – UFMS

_____
Dr.ª Fabiana Fonseca Zanoelo – UFMS

_____
Dr. Adilson Beatriz – UFMS

_____
Dr. Douglas Chodi Masui

_____
Dr. Ludovico Migliolo

"É bom lembrar que contra o preconceito, a intolerância, a mentira, a tristeza, já existe vacina: é o afeto. É o amor."

Paulo Gustavo

AGRADECIMENTOS

RESUMO

A resistência antimicrobiana (RAM) adquirida por microrganismos, seja naturalmente ou devido ao uso indiscriminado de antimicrobianos, e a resistência a múltiplas drogas (RMD) adquirida pelos microrganismos e também por células cancerígenas, tornou-se um grave problema de saúde pública em todo o mundo. Os microrganismos, além serem capazes de sobrepujar os efeitos dos antimicrobianos, ainda apresentam como forma de resistência a formação de biofilmes, o que dificulta ainda mais o tratamento de infecções microbianas. Dessa forma destaca-se a importância da descoberta e/ou desenvolvimento de novos agentes antimicrobianos e anticancerígenos. Dentre as classes de biomoléculas, os peptídeos têm se destacado devido ao seu amplo espectro de atividades biológicas. Tendo em vista isso, neste estudo foi desenvolvido um novo peptídeo antimicrobiano (PAM), a partir de um peptídeo encriptado na sequência do inibidor de tripsina de sementes de *Inga laurina* (ILTI). Para obtenção do PAM, a sequência de ILTI foi fragmentada *in silico,* obtendo-se 169 fragmentos, e *o* fragmento que apresentou maior potencial antimicrobiano foi escolhido para estudo. Alterações de posicionamento de resíduos de aminoácidos e troca de resíduos de aminoácidos, da sequência selecionada, foram realizadas, obtendo assim um PAM com 19 resíduos de aminoácidos denominado KWI-19. As avaliações *in silico* das características físico-químicas da sequência peptídica obtida mostraram parâmetros desejáveis para um PAM. Feito isso, foram realizadas a modelagem por homologia, a validação do modelo de menor energia (mais estável) e posteriormente a síntese do peptídeo pela metodologia em fase sólida (SPFS), seguida de sua purificação por cromatografia líquida de alta eficiência (CLAE) e determinação da sua massa por espectrometria de massas pela técnica *matrix assisted laser dessorption/ionization time-of-flight* (MALDI-TOF). A avaliação da citotoxicidade do peptídeo *in vitro* e *in vivo* foi realizada e verificou-se que o peptídeo apresentou uma concentração hemolítica em 50% dos eritrócitos na concentração de 6,54 µmol L^{-1}. Com relação ao ensaio de toxicidade aguda *in vivo* em larvas de *Galleria mellonella*, não foi observado nenhum efeito tóxico. Os ensaios *in vitro* foram realizados com bactérias Gram-positivas e negativas, e com leveduras pertencentes ao gênero *Candida*. KWI-19 inibiu o crescimento bacteriano com as concentrações inibitórias e bactericidas mínimas (CIM e CBM) variando entre 1,25 a 10 µmol L^{-1}. Das espécies de leveduras testadas, KWI-19 inibiu o crescimento concentração inibitórias e fungicidas mínimas (CIM e CFM) variando entre 2,5 a 20 µmol L^{-1}. Devido os resultados obtidos, foram escolhidas as espéccies de *Pseudomonas aeruginosa*, *Staphylococcus saprophyticus* e *C. tropicalis* para aprofundamento dos estudos. Para essas espécies, realizamos os ensaios de cinética de morte, onde verificou-se que KWI-19 inibe o crescimento bacteriano e fúngico, na CBM e CFM, a partir de 30 min para *S. saprophyticus*, em 120 minutos para *P. aeruginosa* e em 60 min para *C. tropicalis*. Ensaios de determinação do modo de ação do peptídeo foram realizados, e no ensaio de liberação de ácidos nucleicos, em bactérias, observou-se que há uma maior quantidade de DNA e RNA presente no meio extracelular, quando as cepas foram tratadas com KWI-19. Já no ensaio de captação do cristal violeta, não foi possível observar diferença estatística entre as bactérias tratadas e não tratadas com KWI-19. Para investigar o modo de ação de KWI-19 em leveduras, foram realizados ensaios utilizando a sonda SYTOX™ Green e outro utilizando ergosterol e sorbitol. Nesses ensaios pode-se verificar que KWI-19 atua sobre a membrana plasmática de leveduras. Os efeitos do KWI-19 na inibição da formação do biofilme e na erradicação do biofilme maduro das cepas selecionadas também foram avaliados e a viabilidade do biofilme foi quantificada com o número total de unidades formadoras de colônia (UFC) viáveis, onde KWI-19 inibiu e erradicou parte do biofilme de todas as cepas de estudo. Ensaios de viabilidade celular com a linhagem B16F10-Nex2, de melanoma murino, foram realizados e o peptídeo mostrou uma IC_{50} de 22,1 µmol L^{-1}, onde foi verificado, por citometria de fluxo, que o principal processo de morte celular ativado por KWI-19 é necrose.

Palavras-chave: peptídeo encriptado, antibacteriano, antifúngico, antibiofilme, anticâncer.

ABSTRACT

Antimicrobial resistance (AMR) acquired by microorganisms, whether naturally or due to the indiscriminate use of antimicrobials, and multidrug resistance (MRD) acquired by microorganisms and also by cancer cells, has become a serious public health problem throughout the world. world. Microorganisms, in addition to being able to overcome the effects of antimicrobials, also present biofilm formation as a form of resistance, which makes the treatment of microbial infections even more difficult. This highlights the importance of discovering and/or developing new antimicrobial and anticancer agents. Among the classes of biomolecules, peptides have stood out due to their broad spectrum of biological activities. With this in mind, in this study a new antimicrobial peptide (AMP) was developed, based on a peptide encrypted in the sequence of *Inga laurina* seed trypsin inhibitor (ILTI). To obtain the AMP, the ILTI sequence was fragmented *in silico*, obtaining 169 fragments, and the fragment that presented the greatest antimicrobial potential was chosen for study. Changes in the positioning of amino acid residues and exchange of amino acid residues in the selected sequence were carried out, thus obtaining a AMP with 19 amino acid residues called KWI-19. *In silico* evaluations of the physicochemical characteristics of the peptide sequence obtained showed desirable parameters for a AMP. Once this was done, homology modeling was carried out, the validation of the lower energy model (more stable) and subsequently the synthesis of the peptide using solid phase methodology (SPSP), followed by its purification by high performance liquid chromatography (HPLC) and determination of its mass by mass spectrometry using the technique matrix assisted laser desorption/ionization time-of-flight (MALDI-TOF). The evaluation of the cytotoxicity of the peptide *in vitro* and *in vivo* was carried out and it was found that the peptide presented a hemolytic concentration in 50% of erythrocytes at a concentration of 6.54 µmol L^{-1}. Regarding the *in vivo* acute toxicity test on *Galleria mellonella* larvae, no toxic effects were observed. *In vitro* tests were carried out with Gram-positive and negative bacteria, and with yeasts belonging to the *Candida* genus. KWI-19 inhibited bacterial growth with minimum inhibitory and bactericidal concentrations (MIC and MBC) ranging from 1.25 to 10 µmol L^{-1}. Of the yeast species tested, KWI-19 inhibited growth at minimum inhibitory and fungicidal concentrations (MIC and CFM) ranging from 2.5 to 20 µmol L^{-1}. Due to the results obtained, the species of *Pseudomonas aeruginosa*, *Staphylococcus saprophyticus* and *C. tropicalis* were chosen for further studies. For these species, we carried out death kinetic assays, where it was found that KWI-19 inhibits bacterial and fungal growth, in MBC and MFC, from 30 min for *S. saprophyticus*, in 120 minutes for *P. aeruginosa* and in 60 min for *C. tropicalis*. Assays to determine the peptide's mode of action were carried out, and in the nucleic acid release assay, in bacteria, it was observed that there is a greater amount of DNA and RNA present in the extracellular environment, when the strains were treated with KWI-19 . In the crystal violet uptake assay, it was not possible to observe a statistical difference between bacteria treated and not treated with KWI-19. To investigate the mode of action of KWI-19 in yeast, assays were carried out using the SYTOX^{TM} Green probe and another using ergosterol and sorbitol. In these assays it can be seen that KWI-19 acts on the yeast plasma membrane. The effects of KWI-19 on inhibiting biofilm formation and eradicating mature biofilm from selected strains were also evaluated and biofilm viability was quantified with the total number of viable colony forming units (CFU), where KWI-19 inhibited and eradicated part of the biofilm from all study strains. Cell viability assays with the murine melanoma line B16F10-Nex2 were performed and the peptide showed an IC_{50} of 22.1 µmol L^{-1}, where it was verified, by flow cytometry, that the main cell death process activated by KWI-19 is necrosis.

Keywords: encrypted peptide, antibacterial, antifungal, antibiofilm, anticancer.

LISTA DE FIGURAS

LISTA DE ANEXOS

Anexo 1 – Depósito de pedido de patente

Anexo 2 – Cadastro no SISGEN

LISTA DO CÓDIGO DOS AMINOÁCIDOS

Aminoácido	Código
Alanina	A
Arginina	R
Asparagina	N
Aspartato	D
Cisteína	C
Fenilalanina	F
Glicina	G
Glutamato	E
Glutamina	Q
Histidina	H
Isoleucina	I
Leucina	L
Lisina	K
Metionina	M
Prolina	P
Serina	S
Tirosina	Y
Treonina	T
Triptofano	W
Valina	V

LISTA DE ABREVIATURAS E SIGLAS

AHL   Acil Homoserina Lactona

AI-2   Auto Indutor – 2

ANA   Artificial Neural Network

APD   Antimicrobial Peptide Database

$CAMP_{R3}$ Collection of Anti-Microbial Peptides

CBM   Concentração Bactericida Mínima

CFM   Concentração Fungicida Mínima

CIM   Concentração Inibitória Mínima

CLAE   Cromatografia Líquida de Alta Eficiência

DA   Discriminant Analysis

DBM   Demanda Biológica de Oxigênio

DFI   Doença Fúngica Invasiva

DNA   Ácido Desoxirribonucleico

EUA   Estados Unidos da América

FCH   Fator de Crescimento de Hepatócitos

GLASS   Sistema de Vigilância de Uso de Antimicrobiano e Resistência Antimicrobiana Global

ILIT   Inibidor de Tripsina de Inga laurina

INCA   Instituto Nacional do Câncer

IP   Inibidor de Proteinase

ITU   Infecção do Trato Urinário

kDa   Kilo Dalton (unidade de medida)

MAT   Tumor Assocciado ao Tumor

MPM   Metaloprotease de Matriz

OMS   Organização Mundial da Saúde

PAI   Peptídeo Auto Indutor

PAM   Peptídeo Antimicrobiano

RAM   Resistência Antimicrobiana

RF   Random Forest

RMD   Resistência a Múltiplas Drogas

RNA   Ácido Ribonucleico

SPE   Substância Polimérica Extracelular

SVM   Support Vector Machine

UFC   Unidades Formadoras de Colônia

UTI   Unidade de Terapia Intensiva

UV   Radiação Ultravioleta

SUMÁRIO

1. INTRODUÇÃO

O uso indevido de antibióticos e antifúngicos fez com que microrganismos patogênicos desenvolvessem resistência antimicrobiana (RAM) e resistência a múltiplas drogas (RMD), sendo essa última também observada em diferentes tipos de câncer (ANAND *et al.*, 2020; HUBER *et al.*, 2010).

O uso prolongado de antimicrobianos e seus elevados custos, são alguns dos principais fatores pelos quais não há o surgimento de novas drogas contra microrganismos resistentes, sejam elas naturais ou sintéticas (ANAND *et al.*, 2020).

E assim como as infecções causadas por microrganismos, o câncer afeta os sistemas globais de saúde pública, respondendo por cerca de 8,7 milhões de mortes anualmente (ANTONI *et al.,* 2016). Em 2018, 18 milhões de casos foram diagnosticados em todo o mundo e projeta-se que o número de casos aumente para 29 milhões até 2040, ou seja, um aumento de 63% (WHO*,* 2018).

Apesar do progresso na redução das taxas de mortalidade por câncer e de mudanças na terapia nos últimos anos, o desenvolvimento de novas abordagens terapêuticas continua a ser prioridade (ROUDI *et al.,* 2017). Embora a quimioterapia tenha como objetivo controlar este processo descontrolado de divisão celular, muitas drogas utilizadas contra o câncer não possuem especificidade para as células cancerígenas (KOLBERG *et al.*, 2005; KATO *et al.*, 2015). Consequentemente, elas também matam células saudáveis, resultando em efeitos colaterais.

Outra limitação da quimioterapia é o desenvolvimento de resistência pelas células tumorais (TAMBURRINO *et al.,* 2013). Assim, uma alternativa eficaz consiste no desenvolvimento de outras classes de drogas com a propriedade de atingir especificamente as células cancerosas sem toxicidade para as células normais. Outro requisito para aumentar a eficiência é possuir uma menor tendência para o

desenvolvimento de resistência, em comparação com as drogas convencionais. Nesse sentido, os peptídeos antimicrobianos (PAMs) são moléculas com potencial anticâncer.

Os PAMs representam um grupo de compostos amplamente distribuídos na natureza. Devido ao seu amplo espectro de atividades, tais como antibacteriano, anticâncer, antiviral, antifúngico, propriedades anti-inflamatórias e imunomoduladoras, os PAMs tornaram-se um modelo para o desenvolvimento de novas drogas (BHADRA *et al.,* 2018).

Os PAMs são pequenas moléculas anfipáticas (que possuem regiões hidrofóbicas e hidrofílicas), carregadas positivamente ou negativamente e de composição e comprimento variáveis (de 10 a 60 aminoácidos) (HUAN *et al.*, 2020). Com base na sua estrutura secundária, os PAMs são agrupados em quatro classes principais: β-folha, α-hélice, circulares e *random coil*. Em 20 de novembro de 2023 constam depositadas 3.569 sequências de PAMs, naturais e sintéticos, com sequências diferentes, estão depositados no banco de dados *Antimicrobial Peptide Database* (APD) (WANG & WANG, 2004; WANG, LI e WANG, 2009; WANG, LI e WANG, 2016). Em humanos, os PAMs inatos mais proeminentes são as catelicidinas (por exemplo, o peptídeo LL-37) e defensinas, produzidas primariamente pelas células do sistema imune, que possuem atividades antibacterianas, antifúngicas, antivirais e imunomoduladoras, inibindo a proliferação de microrganismos (PETERS *et al.*, 2010). Além dos PAMs naturais, com o desenvolvimento e aprimoramento da ciência e da tecnologia, novos PAMs sintéticos são projetados com auxílio computacional, através de ferramentas de bioinformática (PORTO *et al.*, 2018).

Para a projeção de novas sequências peptídicas com potenciais atividades biológicas são necessárias avaliações das atividades antimicrobiana, hemolítica,

antibiofilme e anticâncer por meio de análises *in silico*, das quais são possíveis obter as predições das atividades biológicas citadas, tendo assim redução de custos e de recursos humanos.

Para o desenvolvimento e obtenção de novos PAMs, pode-se fazer o desenho da sequência primária encontrando padrões de posicionamento de resíduos de aminoácidos de PAMs com sequências depositadas nos bancos de dados, pode-se fazer o desenho guiado por carcaterísticas físico-químicas e também ter uma proteína ou um peptídeo como modelo (CARDOSO *et al.*, 2020).

Partindo de uma proteína modelo para obtenção de PAMs, é interessante utilizar uma proteína que tenha seu sequenciamento completo e que já tenha alguma atividade biológica de interesse, pois dessa forma pode-se explorar ainda suas aplicações biotecnológicas.

Dos diversos tipos de proteínas, os inibidores de proteinases (IPs) são uma classe de compostos que podem ser amplamente explorados devido a sua diversidade de composição e estrutural.

Um IP de serina do tipo Kunitz, que já possui sua sequência completa elucidada e apresenta alto potencial de uso biotecnológico é o inibidor de tripsina de *Inga laurina* (ILTI). O ILTI é uma proteína constituída por 178 resíduos de aminoácidos que foi isolado e purificado das sementes de *Inga laurina,* uma espécie de árvore nativa do Brasil (MACEDO *et al.*, 2007).

Dentre as atividade biológicas avaliadas em ILTI, verificou-se que o mesmo inibe tripsina bovina (MACEDO *et al.*, 2007), inibe a atividade de enzimas proteolíticas do sistema digestivo de insetos (MACEDO *et al.*, 2011), tem atividade inseticida (RAMOS *et al.*, 2012), atividade antimicrobiana (MACEDO *et al.*, 2016), atividade antibiofilme e antitumoral (CARNEIRO *et al.*, 2018), e foi modelo para obtenção para

peptídeos curtos, inspirados na sua sequência, que apresentaram atividade inseticida contra insetos da ordem Lepidoptera ((MERIÑO-CABRERA *et al.*, 2020) e um outro peptídeo (IKR-18) apresentou atividade antibacteriana e antibiofilme (RAMALHO *et al.*, 2022)

Tendo em vista todos esses resultados de atividades biológicas positivos utilizando ILTI, direta ou indiretamente, essa sequência proteica foi escolhida como modelo para obtenção de um novo PAM que tenha atividade antimicrobiana e antiproliferativa frente células neoplásicas de melanoma murino.

2. REVISÃO DE LITERATURA

2.1. *Resistência antimicrobiana*

A RAM é um fenômeno que ocorre quando microrganismos, sejam bactérias, fungos, vírus ou parasitas, adquirem a capacidade de crescer mesmo na presença de substâncias que antes interferiam no seu ciclo de vida, ou seja, conseguem sobrepujar o efeito das substâncias que atuavam sobre eles (DADGOSTAR, 2019).

A RAM é classificada como uma ameaça significativa para os sistemas de saúde pública global, atingindo não só países em desenvolvimento, mas também os já desenvolvidos (DADGOSTAR, 2019). E essa classificação de ameaça se deve ao fato de que as doenças infecciosas, por não apresentarem mais respostas positivas aos tratamentos com drogas convencionais, representam um futuro desconhecido para humanidade (DADGOSTAR, 2019).

A grande quantidade de casos de infecções bacterianas causadas por microrganismos resistentes no mundo é grave, pois, nesses casos, os principais acometidos são pacientes que foram submetidos à cirurgia, os que apresentam infecções persistentes e também os imunocomprometidos (PULINGAM *et al.*, 2022). E toda essa problemática gera elevados custos e alta taxa de mortalidade.

O surgimento da resistência é multifatorial, porém, a principal causa é o uso excessivo de antibióticos, em diversos setores da saúde e também na agropecuária (Figura 1) (PULINGAM *et al.*, 2022). O uso indiscriminado dos antibióticos pode ser facilmente verificado no período de 2000 a 2015, em que houve um aumento de 65% do seu uso em todo o mundo, principalmente nos países em desenvolvimento (WALSH *et al.*, 2023).
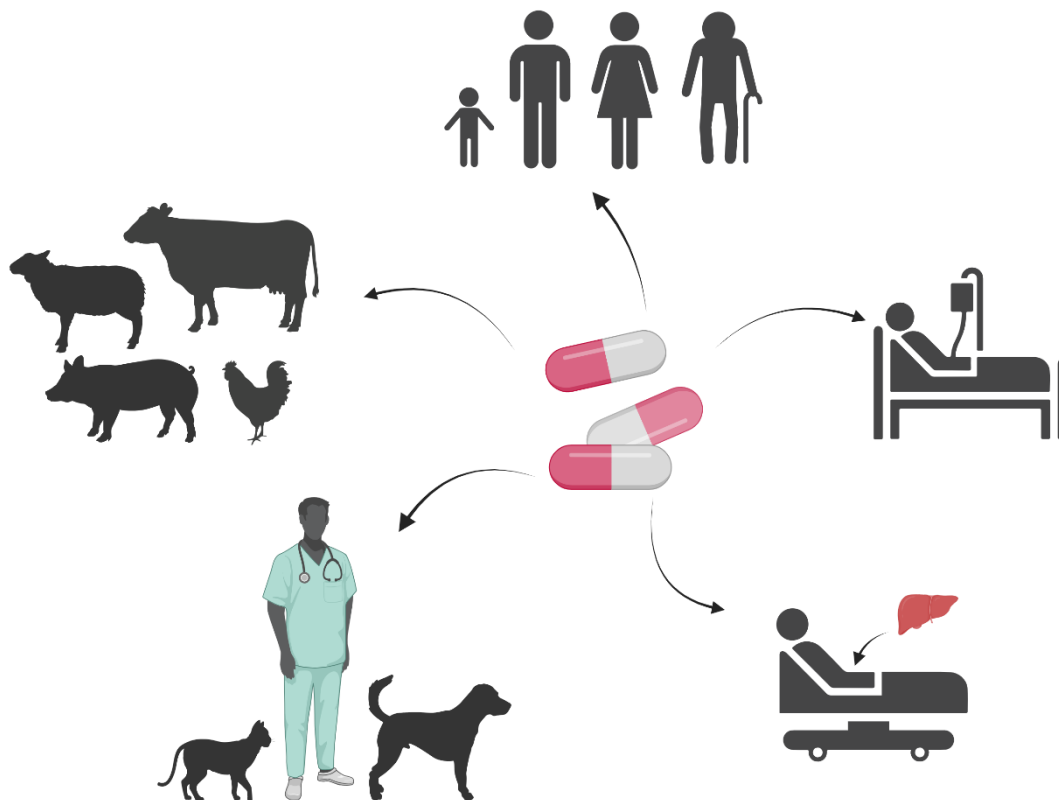
Figura 1 – Usos comuns de antibióticos na clínica veterinária, na agropecuária, tratamento de infecções bacterianas na população de forma geral, tratamento de infecções em pacientes hospitalizados e transplantados. (Fonte: de autoria própria utilizando BioRender)

Outro fenômeno que surgiu com os microrganismos resistentes é a resistência a múltiplas drogas (RMD), que ocorre quando um microrganismo apresenta mecanismos de desenvolvimento de resistência a pelo menos três classes diferentes de antimicrobianos, microrganismos estes que são encontrados com facilidade em ambientes hospitalares (TERRENI, TACCANI e PREGNOLATO, 2021).

O Relatório Global de Resistência Antimicrobiana e Sistema de Vigilância de Uso de Antimicrobiano (GLASS, em inglês), publicado pela Organização Mundial da Saúde (OMS) em 2022, mostra que no ano de 2020 houve elevados níveis de

resistência (> 50%) em microrganismos patogênicos que causam sepse frequentemente em hospitais (WHO, 2022). Desses microrganismos causadores de sepse que apresentaram resistência destacam-se as bactérias *K. pneumoniae* e *Acinetobacter spp.*, em que o tratamento é baseado no uso de antibióticos de último recurso, como carbapenêmicos, para infecções graves (WHO, 2022). Porém, das sepses causadas por *K. pneumoniae*, 8% apresentaram resistência a classe dos carbapenêmicos, o que dificulta muito o processo de cura, aumentando assim o número de óbitos por uma infecção intratável (WHO, 2022).

Ainda de acordo com o relatório publicado pela OMS em 2022, as infecções bacterianas comuns estão se tornando resistentes aos antibióticos, por exemplo, 60% das cepas de *Neisseria gonorreia* apresentaram resistência a ciprofloxacina, assim como mais de 20% das cepas de *E. coli* apresentaram resistência a ampicilina, co-trimoxazol e fluoroquinolonas (WHO, 2022).

Para as bactérias há três modos de aquisição da resistência, podendo ser intrínseca, adquirida ou adaptativa (CHRISTAKI, MARCOU, TOFARIDES, 2019).

A resistência intrínseca surge devido carcaterísticas inerentes da própria bactéria, como por exemplo, a resistência aos glicopeptídeos nas bactérias Gram-negativas, que surge devido a impermeabilidade à membrana externa (CHRISTAKI, MARCOU, TOFARIDES, 2019). Já a resistência adquirida surge quando uma bactéria sensível passa por uma mutação ou então adquire um material genético novo, de fonte exógena (transferência horizontal de genes) (CHRISTAKI, MARCOU, TOFARIDES, 2019). E por fim, a resistência adaptativa surge devido algum processo de sinalização externo, ambiental, como por exemplo, estresse, pH, concentrações de íons, níveis subinibitórios de antibióticos, dentre outros (CHRISTAKI, MARCOU, TOFARIDES, 2019).

Dentre as bactérias resistentes que são grandes responsáveis pelas infecções nosocomiais destaca-se um grupo composto por cinco espécies de bactérias Gram-positivas e negativas. Esse grupo de "superbactérias" é chamado ESKAPE, sigla utilizada para referir aos patógenos *Enterococcus faecium*, *Staphylococcus aureus*, *K. pneumoniae*, *A. baumannii*, *P. aeruginosa* e espécies de *Enterobacter* (SANTAJIT & INDRAWATTANA, 2016). Vale ainda ressaltar que essa nomenclatura (ESKAPE) foi dada por Rice, em 2008, devido também esses microrganismos conseguirem "escapar" da ação dos antibióticos, uma vez que adquiriram resistência (RICE, 2008)

Os microrganismos ESKAPE são encontrados frequentemente em ambientes hospitalares, o que favorece o desenvolvimento de vários mecanismos de resistência aos antibióticos. Os diferentes mecanismos adquiridos por esses patógenos são classificados em quatro grupos: (a) inativação ou alteração da molécula com atividade antimicrobiana; (b) modificação do sítio alvo bacteriano; (c) redução do acúmulo/penetração dos antibióticos e (d) formação de biofilmes bacterianos (OLIVEIRA *et al.*, 2020).

Esses patógenos contribuem significativamente nos números registrados de doenças infecciosas tanto em países desenvolvidos quanto em países em desenvolvimento (DENISSEN *et al.*, 2022). Os microrganismos ESKAPES estão associados à diversas infecções nosocomiais, como por exemplo, bacteremia, infecções do trato urinário (ITU), pneumonia, meningite e infecções de feridas, acometendo principalmente pacientes em unidades de terapia intensiva (UTI), sendo uma das principais causas de mortalidade e morbidade mundial (DENISSEN *et al.*, 2022).

Como descrito anteriormente, além das bactérias, outros microrganismos também são causadores de diversas infecções e merecem uma atenção nos cuidados

e prevenção. Os fungos, por exemplo, causam diversas doenças nos seres humanos, desde síndromes alérgicas simples, lesões superficiais até a doenças fúngicas invasivas (DFIs), que muitas das vezes levam a pessoa a óbito. Todas essas e demais doenças infecciosas causadas por fungos afetam mais de 1 bilhão de pessoas em todo o mundo (FISHER *et al.*, 2022).

Das doenças causadas por esses microrganismos, a micose do tipo candidíase invasiva é a mais comum e possui alta morbidade e mortalidade, causando infecções mais severas, assim como as bactérias resistentes, em pessoas com o sistema imunológico comprometido (PEREZ-RODRIGUEZ *et al.*, 2022).

Dentre as espécies causadores de candidíase invasiva, a *C. albicans* é o agente etiológico mais prevalente, porém, têm-se verificado muitas notificações de infecções por outras espécies como *C. tropicalis*, *C. parapsilosis*, *C. glabrata* e a *C. auris* (PEREZ-RODRIGUEZ *et al.*, 2022).

Algumas dessas espécies conseguiram sobrepujar o efeito dos antifúngicos de ação sistêmica, surgindo espécies resistentes à essas drogas. Os fármacos disponíveis atualmente para terapia antifúngica são os polienos, os azóis, as equinocandinas e os análogos da pirimidina, mas devido aos mecanismos de resistência adquiridos por esses microrganismos, a eficácia dessas drogas foi reduzida e, além disso, há o fator da toxicidade, uma vez que a maioria dessas drogas apresentam elevada hepatotoxicidade (FISHER *et al.*, 2022; PEREZ-RODRIGUEZ *et al.*, 2022).

Para cada uma das classes de antifúngicos citadas acima os patógenos desenvolveram diferentes tipos de mecanismo de resistência. Os azóis aumentam o efluxo de droga, modificam a via de biossíntese de esteróis e promovem a superexpressão do alvo da droga (FISHER *et al.*, 2022). Os polienos alteram a

permeabilidade da membrana celular fúngica através da formação de um complexo polieno-ergosterol e a resistência é causada devido mutações nos genes da biossíntese do ergosterol (FISHER *et al.*, 2022). As equinocandinas promovem estresse na membrana e na parede celular, o que desencadeia uma cascata que afeta reguladores intracelulares, que confere tolerância a essa classe de medicamento (FISHER *et al.*, 2022). Já os análogos da pirimidina inibem a síntese de DNA e de RNA, onde a resistência surge através de mutações específicas no gene FCY1 (FISHER *et al.*, 2022).

Apesar de a resistência antimicrobiana ser adquirida pelas células dos patógenos na sua forma planctônica, uma das formas de resistência antimicrobiana mais crítica é quando há a formação dos biofilmes, sejam eles monoespécies ou multiespécies (OLIVEIRA *et al.*, 2020; CIOFU *et al.*, 2022).

Os biofilmes são comunidades microbianas que vivem em uma substância polimérica extracelular (SPE) que é composta por diversas macromoléculas (polissacarídeos, proteínas, lipídeos e ácidos nucleicos) e por moléculas menores e mais simples, como os açúcares (CIOFU *et al.*, 2022; LI *et al.*, 2020).

Um processo recentemente desenvolvido utiliza reatores de biofilme para purificar águas residuais através da biotecnologia, onde é possível, por meio desse processo remover a demanda biológica de oxigênio (DBO), purificar água e realizar o processo de nitrificação (LI *et al.*, 2020). Porém, os biofilmes não ficam restritos apenas na sua ação benéfica. Os biofilmes são amplamente conhecidos devido aos enormes problemas e custos que geram em ambientes hospitalares, causando inúmeras infecções e mortes em todo o mundo (LI *et al.*, 2020).

Os biofilmes são formados por meio da adesão de células planctônicas em uma superfície ou por meio da agregação em tecidos, onde após ocorre o processo de

maturação e proliferação com a produção de uma matriz extracelular e desenvolvimento de uma estrutura tridimensional, que após todo esse processo dá início a fase de dispersão, que é desencadeado por fatores ambientais (Figura 2) (CIOFU *et al.*, 2022).
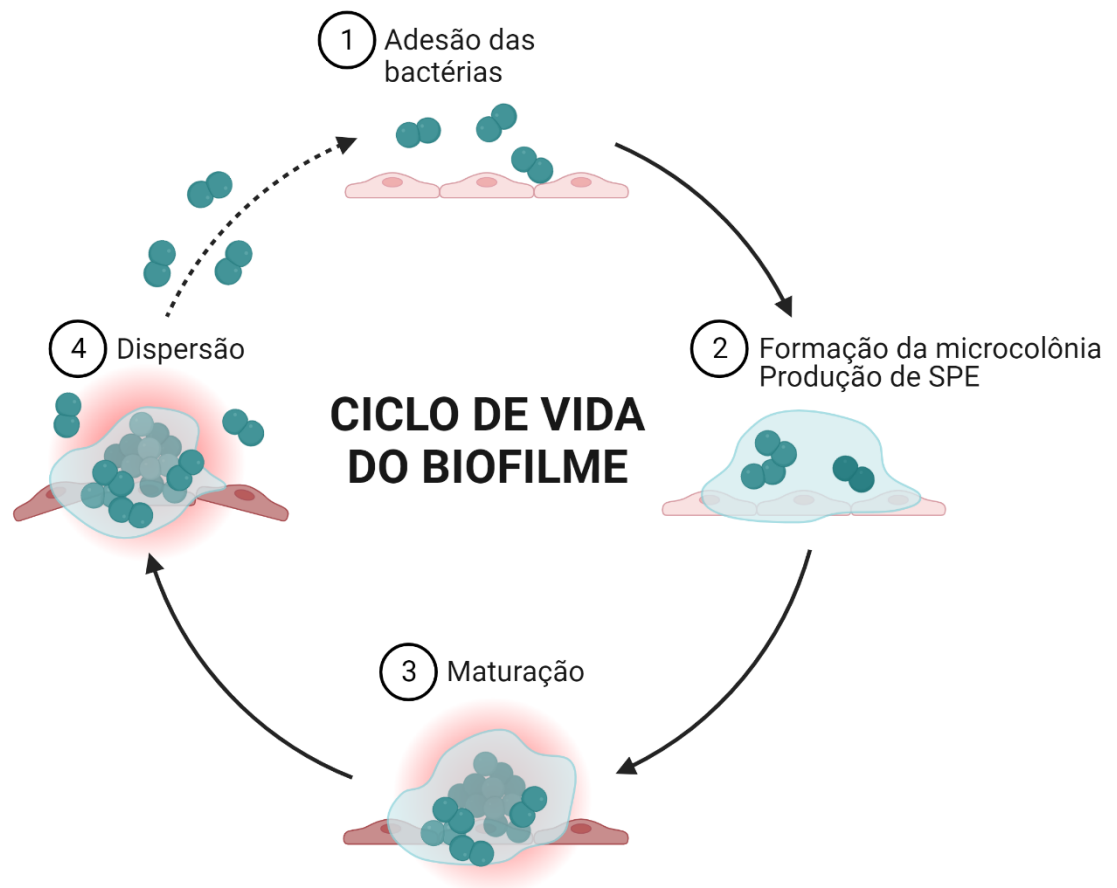
Figura 2 – Processo de formação de um biofilme. 1) ocorre a adesão e agregação das células planctônicas na superfície do tecido ou de algum corpo estranho; 2) a partir da adesão são originadas microcolônias que passam a produzir SPE; 3) dentro da matriz extracelular as células bacterianas se multiplicam levando ao processo de maturação do biofilme; 4) e por fim ocorre a dispersão, onde as células que estavam presentes dentro da matriz do biofilme são expelidas, na forma planctônica, iniciando novamente ao processo de adesão. (Fonte: de autoria própria utilizando BioRender)

Devido a capacidade de serem resistentes aos antibióticos, do sistema imune do hospedeiro não conseguir combater esse tipo de infecção e de serem extremamente resistentes a diversas ações externas, os biofilmes são um sério problema de saúde pública, uma vez que são causadores de infecções crônicas persistentes (SHARMA *et al.*, 2019).

As principais infecções causadas por biofilmes microbianos são os biofilmes dentários, também conhecidos como placas bacterianas, como também em biofilmes em cateteres intravasculares, próteses articulares e em feridas crônicas (CIOFU *et al.*, 2022). Essas infecções não são causadas por um tipo específico de microrganismo, mas qualquer patógeno, quando o hospedeiro oferece um fator predisponente, é capaz de formar os agregados que dão início no ciclo de formação dos biofilmes (CIOFU *et al.*, 2022).

Dentre as bactérias formadoras de biofilme, as que são encontradas comumente nos ambientes hospitalares, são *S. epidermidis*, *S. aureus*, *P. aeruginosa* e espécies da família Enterobacteriaceae (CIOFU *et al.*, 2022). Já nas espécies de fungos, as principais espécies formadoras de biofilme são as pertencentes aos gêneros *Candida* e *Cryptococcus*, das espécies de leveduras, e dos fungos filamentosos as espécies pertencentes ao gênero *Aspergillus* (ROUDBARY *et al.*, 2022).

Assim como na resistência antimicrobiana desenvolvida por células planctônicas, os biofilmes bacterianos e fúngicos também desenvolvem mecanismos de defesa. Nos biofilmes, a resistência é um fenômeno multifatorial, podendo ocorrer através de barreiras físicas, como por exemplo, o aumento da matriz extracelular, como também por meio de processos regulatórios complexos, que levam a superexpressão de uma determinada molécula alvo, expulsão dos compostos

antimicrobianos por bomba de efluxo, dentre outros mecanismos (ROUDBARY *et al.*, 2022).

Tendo em vista que diversas infecções causadas por microrganismos são devidas a formação de biofilmes e que os mesmos adquiriram resistência as drogas de uso comum, métodos alternativos para o tratamento dessas infecções devem ser desenvolvidos com urgência.

Quando comparadas concentrações inibitórias mínimas (CIM) dos antibióticos e antifúngicos em células planctônicas *versus* biofilme, verifica-se que é necessária uma maior concentração da droga para o combate do biofilme (ROUDBARY *et al.*, 2022). Porém, deve-se tomar cuidado com as altas concentrações dessas drogas devido aos efeitos colaterais e aos efeitos tóxicos, principalmente no caso dos antifúngicos (ROUDBARY *et al.*, 2022). Com isso, verifica-se que o uso dos antibióticos convencionais não é o suficiente para eliminar por completo os biofilmes, mas sim para apenas diminuir, o que resulta numa infecção crônica. Portanto, métodos alternativos devem ser aplicados para o controle da infecção, que pode ocorrer de duas formas: na inibição da formação do biofilme e na erradicação dos biofilmes já formados (CIOFU *et al.*, 2022; LI *et al.*, 2020; ROUDBARY *et al.*, 2022).

Dentre os métodos alternativos aplicados há a terapia combinada, formas de revestimento de superfícies, produtos naturais, moléculas reduzidas do quórum, probióticos, terapia fotodinâmica e ferramentas baseadas em CRISPR (ROUDBARY *et al.*, 2022).

Dos métodos alternativos a terapia combinada é uma das estratégias mais promissoras para dispersar, inibir e até mesmo erradicar biofilmes, na qual visa o uso conjunto de dispersores de biofilme com antibióticos de uso convencional (HAWAS, VERDEROSA e TOTSIKA, 2022). Dentre os agentes dispersores de biofilme

encontram-se inibidores de detecção de quórum, óxido nítrico e os peptídeos antimicrobianos, que são combinados à diversas classes de antibióticos (HAWAS, VERDEROSA e TOTSIKA, 2022).

Um outro método alternativo ao uso de antibióticos convencionais é o uso de moléculas reduzidas do sistema de detecção do quórum (traduzido para o português de *quorum sensing*), também chamado de sensor de densidade, que é a forma de comunicação, através de sinalização química, entre as células planctônicas no processo de formação do biofilme (PREDA & SANDULESCU, 2019). O quórum é responsável por regular a atividade metabólica das células planctônicas e induzir a formação do biofilme, aumentando assim a sua virulência (PREDA & SANDULESCU, 2019).

Há três tipos de sistemas de detecção do quórum, que se diferenciam de acordo com o tipo de microrganismo. O primeiro é o sistema de detecção de acil-homoserina lactona (AHL), que é encontrado na bactérias Gram-negativas e são uma classe de compostos que possuem em comum um anel lactona homosserina (PREDA & SANDULESCU, 2019). O segundo tipo de sistema é o de detecção de peptídeo auto indutor (PAI), presente em bactérias Gram-positivas e secretadas por transportadores de membrana (PREDA & SANDULESCU, 2019). À medida que a concentração ambiental de PAIs aumenta, estes se ligam ao sensor de histidina quinase, que fosforila e altera a expressão do gene alvo (PREDA & SANDULESCU, 2019). O último tipo de sistema de detecção de quórum é o autoindutor-2 (AI-2), presente em bactérias Gram-negativas e positivas, que é capaz de estabelecer cooperação e comunicação com cepas distintas do patógeno por meio da tradução do sinal químico, sendo catalisado pela LuxS sintase, que está diretamente envolvido na ativação do ciclo de

metilação, controlando diversas expressões de genes de interesse que auxiliam na adesão à superfície (PREDA & SANDULESCU, 2019).

Tendo em vista a importância do sistema de detecção do quórum na formação do biofilme, uma estratégia para controle desse tipo de infecção é inibir a comunicação entre as células utilizando moléculas reduzidas do próprio sistema do quórum, fazendo com que não se tenha a aglomeração de células e nem a aquisição de nutrientes para manutenção do ciclo, além de que dessa forma não haverá produção de certos metabólitos secundários essenciais para comunicação (PREDA & SANDULESCU, 2019).

Além do problema da RAM, patógenos, como bactérias e fungos, podem causar vários tipos de câncer devido à infecção persistente, falta de resposta do sistema imunológico e inflamação crônica (YUSUF, SAMPATH e UMAR, 2023). Esses eventos podem levar à proliferação celular desordenada e aumentar o risco de transformação oncogênica, mesmo em indivíduos imunocompetentes (YUSUF, SAMPATH e UMAR, 2023)

2.2. *Câncer causado por infecções microbianas persistentes e resistência aos quimioterápicos*

O câncer é um termo que engloba mais de 100 diferentes tipos de neoplasias, as quais apresentam em comum o crescimento desordenado de células que podem migrar e invadir tecidos e órgãos diferentes da sua origem (INCA, 2022). As causas do câncer podem ser classificadas em externas e internas. Como causas externas existem os fatores ambientais, como água, terra, ar, estresse, alimentação, entre outros (INCA, 2023). Já os fatores internos são aqueles relacionados aos hormônios, sistema imunológico, mutações genéticas e infecções persistentes (INCA, 2023)

De acordo com Kouzu e colaboradores (2021), têm surgido, nos últimos anos, claras evidências de que uma resposta inflamatória, causada por infecções microbianas, estimulam o potencial metastático das células tumorais (KOUZU *et al.*; 2021). Kouzu e colaboradores investigaram acerca do desenvolvimento dos tumores malignos originados no trato gastrointestinal. Em suas análises, foi verificado que ainda não se tem conhecimento de como ocorre a interação entre a inflamação microbiana e o surgimento e desenvolvimento do câncer gastrointestinal, mas sabe-se que a infecção bacteriana persistente induz ao câncer, como por exemplo, infecções causadas por *Helicobacter pylori*, que está diretamente associada ao desenvolvimento de câncer de estômago por meio da ativação da via TLR4 (receptor do tipo Toll 4) (KOUZU *et al.*, 2021).

Após a infecção pelo patógeno ocorre o processo de inflamação local. Nesse processo células do tipo monócitos, presentes no sangue periférico, se deslocam até o local da inflamação e se diferenciam em macrófagos, que por sua vez produzem uma grande quantidade de mediadores bioativos que afetam diretamente no crescimento desordenado das células (KOUZU *et al.*, 2021).

Os macrófagos existentes nos tecidos tumorais são chamados de macrófagos associados ao tumor (MAT) (KOUZU *et al.*; 2021). Os MAT são responsáveis pela produção dos fatores de crescimento tecidual, como IL-6, TNFα, fatores angiogênicos, metaloproteases de matriz (MPMs) e fatores imunossupressores (KOUZU *et al.*; 2021). Todos esses fatores descritos permitem que o potencial metastático seja ampliado e que haja uma proliferação de células neoplásicas muito mais desordenada.

Um outro fator muito importante do processo de desenvolvimento de câncer relacionado a pacientes que estão em estado de estresse cirúrgico e sepse é a

produção do fator de crescimento de hepatócitos (FCH). O FCH é secretado pelas células mesenquimais e atua diretamente sob células epiteliais e endoteliais (KOUZU *et al.*; 2021). E a secreção do FCH é um grande problema pois ele se liga ao receptor de c-MET e a ativação de MET suprime a apoptose, favorecendo assim a sobrevivência das células neoplásicas (KOUZU *et al.*; 2021).

Diversos tipos de câncer podem se desenvolver a partir das infecções microbianas persistentes, como por exemplo o câncer de pele. De acordo com Woo e colaboradores (2022), o melanoma (câncer de pele) é a neoplasia mais comum no Estados Unidos (EUA), e sua incidência tem crescido mundialmente com o decorrer dos anos (WOO *et al.*, 2022). Sabe-se que a o principal fator do desenvolvimento do melanoma é a exposição sem proteção a radiação ultravioleta (UV), mas, outros fatores também são responsáveis pelo surgimento da doença, por exemplo, infecções cutâneas como dermatite atópica, acne, rosácea, entre outros tipos de inflamações na pele (WOO *et al.*, 2022).

No Brasil, o melanoma encontra-se entre os principais tipos de câncer diagnosticado, onde segundo a Estimativa de Incidência de Câncer no Brasil. 2023-2025, haverá 8.980 de novos casos registrados, o que representa 1,85% o somatório de todas as neoplasias, exceto câncer de pele não melanoma (SANTOS *et al.*, 2023).

Dados da última estimativa em 2020, segundo o Instituto Nacional de Câncer do Ministério da Saúde do Brasil (INCA), revelaram que o câncer se tornou o principal problema de saúde pública mundial, estando entre as principais causas de mortes prematuras. Segundo estimativa de 2018, foram registrados no mundo mais de 18 milhões de novos casos e cerca de 9,5 milhões de óbitos (BRAY *et al.*, 2018).

E o problema do câncer se agrava ainda mais quando nos referimos ao tratamento, uma vez que a resistência também é um problema que atinge o tratamento

das células cancerígenas, uma vez que essas células desenvolvem a RMD após a sua exposição aos quimioterápicos (WANG *et al.*, 2017). A RMD observada nas células cancerígenas não possui relação estrutural ou funcional, e se tornou o principal motivo dos tratamentos com os quimioterápicos não terem maior eficácia, levando ao ressurgimento de tumores malignos, podendo levar os pacientes à óbito (WANG *et al.*, 2017).

Existem diversos mecanismos que levam ao surgimento da RMD, entre eles temos: (a) aumento do efluxo de drogas; (b) aumento dos reparos de danos ao DNA; (c) redução da morte celular via apoptose; (d) autofagia; e (e) alteração do metabolismo celular (WANG *et al.*, 2017).

Com o intuito de ampliar e melhorar a eficácia dos quimioterápicos nos tratamentos de diversos tipos de câncer, estudos e métodos variados têm sido amplamente explorados nos últimos anos (WANG *et al.*, 2017).

Considerando a grande elevação dos registros de óbitos ocasionados tanto por infecções causadas por microrganismos resistentes aos antimicrobianos quanto pelos óbitos ocasionados pelo câncer, há urgência em encontrar e/ou desenvolver novas drogas que combatam ambas as doenças, evitando-se principalmente efeitos colaterais, ou seja, é necessário a descoberta de novas drogas que tenham como alvos específicos os microrganismos ou que tenham uma especificidade maior pelas células cancerígenas do que pelas células normais/saudáveis.

2.3. *Desenvolvimento de novos agentes antimicrobianos e anticâncer*

Atualmente a tecnologia é uma grande aliada na descoberta e desenvolvimento de novos agentes antimicrobianos e anticâncer. Novas estratégias para obtenção de moléculas ativas têm sido desenvolvidas, incluindo o uso de ferramentas

computacionais no auxílio da construção, determinação estrutural de qualidade e predição de atividades biológicas *in silico* (CARDOSO *et al.*, 2020).

Uma classe de substâncias que tem sido amplamente estudada como uma alternativa promissora no controle de infecções causadas por microrganismos e no combate ao câncer é a classe dos peptídeos antimicrobianos (PAMs). E para obtenção dessas sequências peptídicas podem ser aplicadas diversas metodologias que utilizam ferramentas computacionais variadas (CARDOSO *et al.*, 2020).

Hoje em dia muitos estudos são guiados pelos resultados obtidos *in silico*, o que gera economia de recursos materiais e humanos. Por exemplo, para obtenção de fragmentos peptídicos de uma proteína e avaliação de diversas atividades biológicas, inicialmente pode-se fazer a clivagem e a predição das atividades biológicas utilizando *softwares* disponíveis online e de forma gratuita.

Um *software* utilizado para clivagem *in silico* de proteínas é o CAMP$_{R3}$ (*Collection of Anti-Microbial Peptides*), que além de gerar os fragmentos pelo método de janela deslizante, utiliza os algoritmos *Support Vector Machine* (SVM), *Random Forest* (RF), *Artificial Neural Network* (ANA) e *Discriminant Analysis* (DA) para gerar uma predição da atividade antimicrobiana para cada um dos fragmentos obtidos (THOMAS *et al.*, 2010; WAGHU *et al.*, 2014; WAGHU *et al.*, 2015)

A análise da disposição dos resíduos de aminoácidos também é de grande importância, uma vez que através da posição dos resíduos que será possível verificar se a sequência possui ou não um caráter anfipático e se tem ou não tendência em formar estrutura secundárias em α-hélice, que é a mais comumente encontrada em PAMs. Um, dos diversos, *software* para realizar essa análise é o HeliQuest, que além de mostrar a distribuição dos resíduos em uma roda helicoidal, ainda faz o cálculo de algumas carcaterísticas físico-químicas da sequência e faz o rastreamento de

segmentos de proteínas que possuam características semelhantes (GAUTIER *et al.*, 2008).

Outra ferramenta que é uma grande aliada no desenvolvimento de novos agentes biológicos são os bancos de dados. Para os PAMs existem diversos bancos, dentre eles o *The Antimicrobial Peptide Database* (APD), que em sua biblioteca possui 3.569 peptídeos antimicrobianos com sequências depositadas (WANG & WANG, 2004; WANG, LI e WANG, 2009; WANG, LI e WANG, 2016).

Softwares que utilizam de algoritmos de ponta para predizer a atividade biológica também são usados, e a partir deles pode-se ter um direcionamento para iniciar os ensaios *in vitro* após a obtenção da molécula. Diversos *softwares* para as mais distintas atividades biológicas estão disponíveis, como por exemplo, o ACPred para predição da atividade anticâncer (SCHADUANGRA *et al.*, 2019), ToxinPred para predição da atividade tóxica (GUPTA *et a*l., 2013; GUPTA *et al.*, 2015) e o dPABBs para predição da atividade antibiofilme (SHARMA *et al.*, 2016), sendo todos esses citados para predições das atividades de peptídeos.

Além de *softwares* pensados para auxiliar na busca da sequência e na predição das atividades biológicas, muitas ferramentas computacionais também surgiram para obtenção dos modelos tridimensionais teóricos das moléculas estudadas. Antes, para se saber como era a estrutura tridimensional de moléculas como proteínas e peptídeos era necessárias análises experimentais por ressonância magnética nuclear (RMN), cristalografia de raios-X e microscopia crioeletrônica (crio-EM) (REZENDE *et al.*, 2023). Já na última década, devido abordagens de aprendizado de máquina, é possível construir modelos mais precisos e por diferentes métodos, seja por modelagem comparativa, *threading* ou *ab inition* (REZENDE *et al.*, 2023).

Dentre as ferramentas utilizadas para obtenção de modelos confiáveis podemos citar o MODELLER para modelagem comparativa (SALI & BLUNDELL, 1993; FISER, DO, e SALI, 2000; MARTI-RENOM *et al.*, 2000; WEBB & SALI, 2016),o I-TASSER para modelagem pelo método *threading* (YANG & ZHANG, 2015; ZHENG *et al.*, 2021; ZHOU *et al.*, 2022), e para a modelagem *ab inition* o *software* AlphaFold 2 (JUMPER *et al.*; 2021)

E devido a todo esse suporte na inovação das ferramentas computacionais para o desenho de moléculas bioativas, o desenho de novos compostos se tornou uma área de grande importância e interesse da química medicinal, uma vez que busca a criação de novos produtos farmacêuticos com uma maior especificidade pelas células dos microrganismos e pelas células cancerígenas do que pelas células eucarióticas normais (PORTO *et al.*, 2012).

Na projeção de novos PAMs pode-se fazer ou não o uso de uma sequência modelo, de origem natural ou não. Quando não se faz o uso de um modelo para projeção de um novo PAM, o método computacional utilizado é o desenho *de novo* (CARDOSO *et al.*, 2020). Nesse método são geradas diversas sequências usando aminoácidos em posições específicas de acordo com a repetição que os mesmos aparecem em outras fragmentos peptídicos que já se encontram depositadas em banco de dados específicos (CARDOSO *et al.*, 2020). Dessa forma, é permitido gerar sequências com uma enorme diversidade de composição de aminoácidos, estrutura tridimensional e mecanismos de ação (CARDOSO *et al.*, 2020).

2.4. *Peptídeos Antimicrobianos*

Os PAMs são uma classe de compostos que se destacam pois podem ter ação antimicrobiana de amplo espectro e em alguns casos ainda podem apresentar atividade anticâncer, além da baixa incidência de resistência microbiana, atividade

biológica em concentrações baixas (micromolar e nanomolar) e diversos mecanismos de ação (SILVA *et al.*, 2022).

Os PAMs constituem a resposta imune inata, presentes em diversas classes de seres vivos, e que por serem constituídos por aminoácidos, apresentam uma enorme diversidade, tanto quanto a estrutura quanto a sua funcionalidade (SILVA *et al.*, 2022). Os PAMs podem apresentar atividades antibacteriana, anticâncer, antiviral, antifúngica, anti-inflamatória e imunomoduladora, e devido a isso tornaram-se um modelo para o desenvolvimento de novas drogas (BHADRA, P. et al., 2018).

PAMs são pequenas moléculas anfipáticas (que possuem regiões hidrofóbicas e hidrofílicas), carregadas positivamente ou negativamente e de composição e comprimento variáveis (10 a 60 aminoácidos) (HUAN *et al.*, 2020).

Além dos PAMs naturais, com o desenvolvimento e aprimoramento da ciência e da tecnologia, novos PAMs sintéticos são projetados com auxílio computacional, através de ferramentas de bioinformática (PORTO *et al.*, 2018).

Apesar dos PAMs serem promissores no controle de microrganismos e câncer, ainda existem muitos desafios a serem enfrentados até o uso clínico. Entre as principais dificuldades encontradas para que os PAMs tenham uso clínico, temos a sua rápida eliminação no organismo, mas principalmente a sua rápida degradação (SILVA *et al.*, 2022). Porém, aplicações biotecnológicas têm conseguido mudar esse cenário, tendo diversos estudos com utilização de lipossomas e a conjugação de PAMs a outras moléculas (mais estáveis), como polímeros, nanopartículas ou outras moléculas de baixo peso molecular, fazendo com os efeitos terapêuticos dos PAMs sejam potencializados (SILVA *et al.*, 2022).

Devido ao enorme número de peptídeos diferentes que podem existir, os mesmos podem ser classificados de diversas formas. Abordaremos as classificações

de acordo com: fonte; atividade; características estruturais e tipos de aminoácidos (HUAN *et al.*,2020).

De acordo com o banco de dados APD, os peptídeos antimicrobianos podem ser oriundos de organismos, como mamíferos, anfíbios, bactérias, fungos, animais marinhos ou de insetos (HUAN *et al.*, 2020). Ainda de acordo com o banco de dados APD, existem 25 classes de peptídeos antimicrobianos, quando os mesmos são agrupados de acordo com a sua atividade, dentre as principais classes encontram-se os peptídeos antibacterianos, peptídeos antibiofilme, peptídeos antivirais, peptídeos antifúngicos, peptídeos anti-HIV, peptídeos antiparasitários, peptídeos anticâncer, dentre outros (WANG & WANG, 2004; WANG, LI e WANG, 2009; WANG, LI e WANG, 2016).

Outra classificação é quanto a composição de aminoácidos. Os PAMs podem ser classificados em peptídeos ricos em prolina, ricos em triptofano, ricos em histidina ou ricos em glicina (HUAN *et al.*, 2020).

Os PAMs também podem ser classificados de acordo com sua estrutura secundária em: α-hélice; β-folha; circulares ou *random coils* (HUAN *et al.*, 2020).

Uma das principais vantagens do uso clínico dos PAMs é a capacidade que eles possuem de sobrepujar os mecanismos de defesa dos microrganismos, uma vez que essa classe de compostos pode possuir diferentes modos de ação frente um único alvo. A maior parte dos PAMs possuem ação direta e rápida causando a ruptura e/ou comprometendo a integridade física da membrana celular dos microrganismos, ou podem interagir com a membrana, permear a mesma e atuar em alvos intracelulares, como por exemplo inibindo a síntese da membrana, inibindo a ação de enzimas necessárias para sobrevivência do microrganismo, na transcrição do DNA, entre outros (MAHLAPUU *et al.*, 2016; HANCOCK & SAHL, 2006).

Para que os PAMs atuem nas células dos microrganismos é necessário que eles consigam estabelecer incialmente uma interação com a membrana. Essa interação ocorre devidos forças eletrostáticas originadas pelas cargas dos peptídeos e pela carga da membrana celular. Os PAMs geralmente possuem carga positiva (são catiônicos) e as superfícies das membranas bacterianas, fúngicas ou neoplásicas são carregadas negativamente.

Direcionando primeiramente o modo de ação na membrana bacteriana é importante ressaltar que há diferenças nas membranas citoplasmática das bactérias Gram-negativas e positivas. As bactérias Gram-positivas possuem uma camada espessa de peptidoglicano, na sua membrana citoplasmática, e ainda há a presença de ácidos teicóicos. Já nas bactérias Gram-negativas há também uma camada de peptidoglicano e há os lipopolissacarídeo (LPS) presentes na membrana externa, o que favorece a interação com os PAMs carregados positivamente, uma vez que esses compostos possuem carga negativa (MAHLAPUU *et al.*, 2016). E tanto as membranas citoplasmáticas das bactérias Gram-negativas quanto das Gram-positivas, há a presença de fosfolipídios, fosfatidilglicerol, cardiolipina e fosfatidilserina, que possuem um grupamento polar carregado negativamente na sua extremidade (MAHLAPUU *et al.*, 2016).

Já as células de mamíferos são constituídas por fosfolipídios zwiteriônicos, como fosfatidiletanolamina, fosfatidilcolina e esfingomielina, os quais deixam a membrana com um equilíbrio entre as cargas, além de possuírem um alto teor de colesterol, o que reduz a interação dos PAMs com a bicamada lipídica de mamíferos, impedido a ação dos PAM (MAHLAPUU *et al.*, 2016).

Quando os PAMs se aproximam da membrana citoplasmática dos microrganismos, eles adquirem a estrutura secundária mais estável, o que permite

que os grupos hidrofílicos estabeleçam interações com a cabeça polar dos fosfolipídios, enquanto a parte hidrofóbica dos PAMs estabelecem interações com as cadelas apolares dos fosfolipídios (MAHLAPUU *et al.*, 2016).

Estudos propõem alguns modelos de ação dos PAMs frente membranas citoplasmáticas de bactérias, como por exemplo, a formação de poros toroidais, a ruptura da membrana através do modelo carpete, o extravasamento de material intracelular pelo modelo barril, além de que os PAMs podem ser translocados, permeando a bicamada lipídica da membrana citoplasmática e atuar em alvos intracelulares que comprometam a sobrevivência das células bacterianas (MAHLAPUU *et al.*, 2016).

Além de atuarem diretamente nas células dos microrganismos, os PAMs podem atuar recrutando o sistema imune para combater esses invasores do organismo infectado. A atividade imunomudulatória dos PAMs incluem a estimulação de quimiotaxia, modulação de células imunes, diferenciação da imunidade adaptativa e supressão e/ou produção de citocinas (MAHLAPUU *et al.*, 2016).

Assim como nos microrganismos, os PAMs possuem diversos modos de ação, ao combater as células cancerígenas os PAMs também apresentam diversos modos de ação, os quais ainda estão em fase de elucidação, mas já se sabe que um PAM com atividade anticâncer pode atuar de diversas formas contra um único tipo de célula (GASPAR *et al.*, 2013).

Dentre os principais mecanismos de ação dos PAMs frente células cancerígenas temos a indução de apoptose e/ou necrose através da ruptura da membrana citoplasmática, há também o recrutamento de células do sistema imune, os PAMs podem atuar diretamente sob os receptores de membrana das células

cancerígenas, podem inibir a síntese de DNA e impedir a vascularização do tumor a ser formado, ou seja, atuar na angiogênese (GASPAR *et al.*, 2013).

Tendo em vista a extensa aplicação dos PAMs, muitos pesquisadores têm buscado inspiração em moléculas bioativas naturais para projeção de novos compostos, porém com tamanhos reduzidos. Um exemplo disso é a utilização de proteínas como modelo. A partir da sequência primária de uma proteína pode ser obtidos vários fragmentos e esses serem analisados *in silico* e *in vitro*, obtendo assim uma molécula menor, o que gera menos custos na síntese (ao se pensar em síntese de larga escala), e com atividade potencializada, pois ao fazer a clivagem da proteína *in silico*, também pode-se fazer alterações na sequência para aferir melhores carcaterísticas físico-químicas e dessa forma poder aumentar significativamente a potencial atividade biológica.

2.5. *Inibidor de tripsina de Inga laurina (ILTI)*

Como já discutido no tópico anterior, os PAMs naturais podem ser obtidos de uma grande variedade de organismos vivos, sendo pertencentes a imunidade inata desses organismos, que possuem como função proteger e combater contra patógenos (KIM et al., 2009).

Os PAMs fazem parte da primeira linha de defesa quando há invasão de microrganismos patogênicos em plantas e em animais, porém, além dos peptídeos, proteínas de várias fontes vegetais também possuem atividade antimicrobiana, inibindo o crescimento e proliferação de microrganismos (KIM *et al.*, 2009). Essas proteínas são classificadas em doze subfamílias: quitinases, β-1,3-glucanases, proteínas semelhantes à taumatina, inibidores de proteinase, endoproteinases, peroxidases, proteínas semelhantes a ribonuclease, γ-tionina e defensinas vegetais,

oxalato oxidases, proteínas semelhantes à oxalato oxidase e outras proteínas de propriedades biológicas desconhecidas (KIM et al., 2009).

Das subfamílias de proteínas, os IPs são amplamente encontrados em tubérculos e sementes de plantas, e em grandes quantidades, possuindo como função armazenamento de nitrogênio e defesa (KIM *et al.*, 2009). Essa classe de proteínas também se destaca pelo amplo espectro de atividade biológica, como inseticida, antimicrobiana e anticâncer (KIM *et al.*, 2009).

Os IPs são classificados de acordo com seu mecanismo de ação, uma vez que formam complexos estáveis com as proteinases alvo, e dessa forma bloqueia, altera ou impede o acesso das enzimas proteolíticas (MACEDO *et al.*, 2007). Os IPs são classificados como inibidores de serina, cisteína aspártico ou metaloproteases (MACEDO *et al.*, 2007). Dessa classificação, os IP de serina são os mais estudados e podem ser classificados em Bowman-Birk, Kunitz, Batata I, Batata II, Cucúrbita, Cereal, Tipo Taumatina e Ragi A1 (MACEDO *et al.*, 2007). A classificação do tipo de IP de serina é baseada no peso molecular, quantidade de ligações de dissulfeto, estrutura tridimensional e estabilidade térmica (MACEDO *et al.*, 2007).

Os inibidores vegetais de Kunitz são proteínas com peso molecular compreendido entre 18 e 24 kDa, possuindo uma ou duas cadeias polipeptídicas e baixo teor de cisteína, geralmente com quatro resíduos de cisteína dispostos em duas pontes dissulfeto (MACEDO *et al.*, 2007). Esses IPs são capazes de inibir, principalmente, proteases como tripsina, quimotripsina, subtilisina e calicreína (MACEDO *et al.*, 2007).

Como exemplo de um IP de serina do tipo Kunitz podemos citar o inibidor de tripsina isolado das sementes de *I. laurina* (ILTI). O *I. laurina* é uma árvore pertencente a subfamília Mimosoideae das Leguminosae, de ampla distribuição na América

Central e na América do Sul (MACEDO *et al.*, 2007). O ILTI é uma proteína composta por 178 resíduos de aminoácidos, com peso molecular de 19,8 kDa e sua estrutura terciária é composta por estruturas em β-olha (Figura 3).
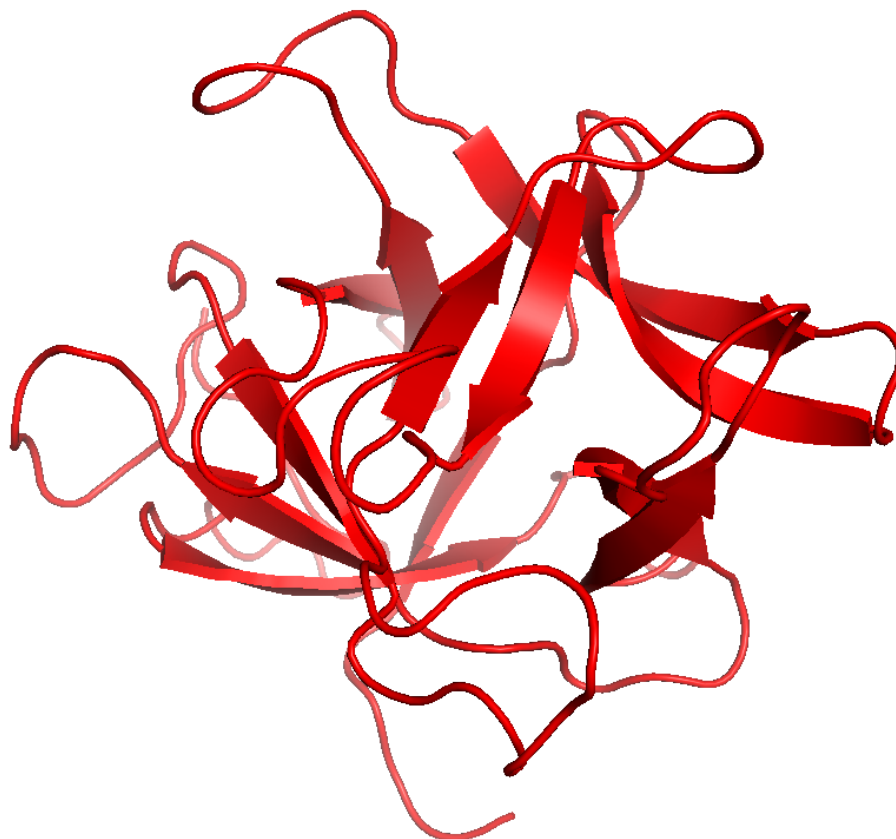
Figura 3 – Estrutura tridimensional teórica do inibidor de tripsina de *Inga laurina* (ILTI). (Fonte: de autoria própria utilizando PyMOL)

Algumas atividades biológicas de ILTI já foram comprovadas e descritas na literatura, uma vez que ele foi capaz de inibir de tripsina bovina (MACEDO *et al.*, 2007), enzimas proteolíticas presentes no sistema digestivo de insetos (MACEDO *et al.*, 2011), atividade inseticida (RAMOS *et al.*, 2012), atividade antimicrobiana (MACEDO *et al.*, 2016) e atividade antibiofilme e antitumoral (CARNEIRO *et al.*, 2018).

E tendo em vista suas aplicações, também foram realizados estudos que objetivaram a redução do tamanho de ILTI, uma vez que a aplicação de proteínas

grandes, tanto no campo agrícola (atividade inseticida) quanto aplicada a saúde, é limitada devido ao elevado custo de síntese (MERIÑO-CABRERA *et al.*, 2020). Então a partir da sequência primária de ILTI foram obtidos peptídeos miméticos a ele, com o intuito de manter ou potencializar a atividade que a proteína íntegra já possuía. Esse processo de obtenção de peptídeos que tiveram como modelo a proteína ILTI gerou peptídeos que foram avaliados tanto contra pragas da ordem Lepdoptera (MERIÑO-CABRERA *et al.*, 2020), como também gerou o peptídeo IKR-18, que possui atividade antibacteriana e não tóxica (RAMALHO *et al.*, 2022). Para obtenção desses peptídeos foram utilizados *softwares* que fizeram a clivagem *in silico* da sequência primária de ILTI e então realizadas modificações para que as novas sequências obtivessem as carcaterísticas desejadas.

Como os PAMs obtidos a partir da sequência de ILTI têm mostrado resultados positivos com relação a sua obtenção e com relação as suas aplicações, uma nova sequência de um PAM encriptado na sequência de ILTI foi analisado nesse trabalho. Uma sequência encriptada é aquela que se encontra inserida na sequência da proteína utilizada como modelo, portanto, desenvolvemos um novo PAM que teve como modelo um fragmento de ILTI. O novo PAM, denominado KWI-19, é composto por 19 resíduos de aminoácidos, possui carga líquida positiva (+6), adota conformação α-hélice em ambientes hidrofóbicos, não apresentou toxicidade aguda frente larvas de *G. mellonella*, possui atividade antifúngica, antibacteriana, antibiofilme e antiproliferativa frente uma linhagem de células de melanoma murino.

REFERÊNCIAS

ANAND, U.; NANDY, S.; MUNDHRA, A.; DAS, N.; PANDEY, D. K.; DEY, A. A review on antimicrobial botanicals, phytochemicals and natural resistance modifying agents from Apocynaceae family: Possible therapeutic approaches against multidrug resistance in pathogenic microorganisms. **Drug Resistance Updates**, v. 51, 2020. DOI: 10.1016/j.drup.2020.100695.

ANTONI, S.; SOERJOMATARAM, I.; MØLLER, B.; BRAY, F.; FERLAY, J. An assessment of GLOBOCAN methods for deriving national estimates of cancer incidence. **Bulletin of the World Health Organization**, v. 94, p.174–84, 2016. DOI: 10.2471/BLT.15.164384.

BHADRA, P.; YAN, J.; LI, J.; FONG, S.; SIU, S.W.I.. AmPEP: Sequence-based prediction of antimicrobial peptides using distribution patterns of amino acid properties and random forest. **Nature**, v. 8, n. 1697, 2018. DOI: 10.1038/s41598-018-19752-w.

BRAY, F.; FERLAY, J.; SOERJOMATARAM, I.; SIEGEL, R. L.; TORRE, L. A.; JEMAL, A. Global cancer statistics 2018: GLOBOCAN estimates of incidence and mortality worldwide for 36 cancers in 185 countries. **CA: A Cancer Journal of Clinicians**. 2018. DOI: 10.3322/caac.21492.

CARDOSO, M. H.; OROZCO, R. Q.; REZENDE, S. B.; RODRIGUES, G.; OSHIRO, K. G. N.; CÂNDIDO, E. S.; FRANCO, O. L. Computer-Aided Design of Antimicrobial

Peptides: Are We Generating Effective Drug Candidates? **Frontiers in Microbiology**, 2020. DOI: 10.3389/fmicb.2019.03097.

CARNEIRO, F. C.; WEBER, S. S.; SILVA, O. N.; JACOBOWSKI, A. C.; RAMADA, M. H. S.; MACEDO, M. L. R.; FRANCO, O. L.; PARACHIN, N. S. Recombinant *Inga laurina* trypsin inhibitor (ILTI) production in *Komagataella phaffii* confirms its potential anti-biofilm effect and reveals an anti-tumoral activity. **Microorganisms**, 2018. DOI: 10.3390/microorganisms6020037.

CHRISTAKI, E.; MARCOU, M.; TOFARIDES, A. Antimicrobial resistance in bacteria: machanisms, evolution and persistence. **Journal of Molecular Evolution**, 2019. DOI: 10.1007/s00239-019-09914-3

CIOFU, O.; MOSER, C.; JENSEN, P. O.; HOIBY, N. Tolerance and resistance of microbial biofilms. **Nature Reviews Microbiology**, 2022. DOI: 10.1038/s41579-022-00682-4

DADGOSTAR, P. Antimicrobial Resistance: Implications and Costs. **Infection and Drug Rersistance**, 2019. DOI: 10.2147/IDR.S234610

DENISSEN, J.; REYNEKE, B.; WASO-REYNEKE, M.; HAVENGA, B.; BARNARD, T.; KHAN, S.; KHAN, W. Prevalence of ESKAPE pathogens in the environment: Antibiotic resistance status, community-acquired infection and risk to human health, International **Journal of Hygiene and Environmental Health**, v, 244, 2022. DOI:10.1016/j.ijheh.2022.114006.

FISER, A.; DO, R. K.; SALI, A. Modeling of loops in protein structures. **Protein Science**, v. 9. 1753-1773, 2000. DOI: 10.1110/ps.9.9.1753.

FISHER, M. C.; ALASTRUEY-IZQUIERDO, A.; BERMAN, J. et al. Tackling the emerging threat of antifungal resistance to human health. **Nature Reviews Microbiology,** 2022. DOI: 10.1038/s41579-022-00720-1

GASPAR, D.; VEIGA, A. S.; CASTANHO, M. A. From antimicrobial to anticancer peptides. A review. **Frontiers in Microbiology**. 2013. DOI: 10.3389/fmicb.2013.00294.

GAUTIER, R.; DOUGUET, D.; ANTONNY, B.; DRIN, G. HELIQUEST: a web server to screen sequences with specific α-helical Properties. **Bioinformatics**, 2008. DOI: 10.1093/bioinformatics/btn392

GUPTA et al. In silico approach for predicting toxicity os peptides and proteins. **PLoS ONE**, 2013. DOI: 10.1371/journal.pone.0073957

GUPTA, s.; KAPOOR, P.; CHAUDHARY, K.; GAUTAM, A.; KUMAR, R.; RAGHAVA, G. P. S. Peptide toxicity prediction. **Methods in Molecular Biology**, 2015. DOI: 10.1007/978-1-4939-2285-7_7

HANCOCK, R. E.; SAHL, H. G. Antimicrobial and host-defense peptides as new anti-infective therapeutic strategies. **Nature Biotechnology**. 2006. DOI: 10.1038/nbt1267.

HAWAS, S.; VERDEROSA, A. D.; TOTSIKA, M. Combination therapies for biofilm inhibition and erradiction: a comparative review of laboratory and preclinical studies. **Frontiers in Cellular Infection Microbiology**, 2022. DOI: 10.3389/fcimb.2022.850030

HUAN, Y.; KONG, Q.; MOU, H.; YI, H. Antimicrobial peptides: classification, design, application and research progress in multiple fields. **Frontiers in Microbiology**, 2020. DOI: 10.3389/fmicb.2020.582779

HUBER, P. C.; MARUIAMA, C. H.; ALMEIDA, W. P. Glicoproteína-P, resistência a múltiplas drogas (MDR) e relação estrutura-atividade de moduladores. **Química Nova**, v. 33, n. 10, 2010.

INSTITUTO NACIONAL DO CÂNCER (Brasil). O que causa o câncer?. [Brasília, DF]: Instituto Nacional do Câncer, 2023. Disponível em: < https://www.gov.br/inca/pt-br/assuntos/causas-e-prevencao-do-cancer/o-que-causa-o-cancer >. Acesso em: 23 set. 2023.

INSTITUTO NACIONAL DO CÂNCER (Brasil). O que é câncer?. [Brasília, DF]: Instituto Nacional do Câncer, 2022. Disponível em: < https://www.gov.br/inca/pt-br/assuntos/cancer/o-que-e-cancer >. Acesso em: 23 set. 2023.

JUMPER, J.; EVANS, R.; PRITZEL, A; *et al*. Highly accurate protein structure prediction with AlphaFold. **Nature**, 2021. DOI: https:10.1038/s41586-021-03819-2

KATO Y, SATO J, KATO R, TAKATA R, OBARA W. Side effect and supportive care to combination of gemcitabine and cisplatin chemotherapy for the advanced urothelial cancer. **Nihon Rinsho**, v. 73, p. 609–613, 2015. PMID: 25831832

KIM, J. Y.; PARK, S. C.; HWANG, I.; CHEONG, H.; NAH, J. W.; HAHM, K. S.; PARK, Y. Protease inhibitors from plants with antimicrobial activity. **International Journal Molecular Sciences**, 2009. DOI: 10.3390/ijms10062860

KOLBERG, H. C.; VILLENA-HEINSEN, C.; DEML, M. M.; KRAEMER, S.; DIEDRICH, K.; FRIEDRICH, M. Relationship between chemotherapy with paclitaxel, cisplatin, vinorelbine and titanocene dichloride and expression of proliferation markers and tumour suppressor gene p53 in human ovarian cancer xenografts in nude mice. **European Journal Gynaecological Oncology**, v. 26, p.398–402, 2005. PMID: 16122187.

KOUZU, K.; TSUJIMOTO, H.; KISHI, Y.; UENO, H.; SHINOMIYA, N. Role of Microbial Infection-Induced Inflammation in the Development of Gastrointestinal Cancers. **Medicines** 2021, *8*, 45. DOI: 10.3390/medicines8080045

LI, Y.; XIAO, P.; WANG, Y.; HAAO, Y. Mechanisms and control measures of mature biofilm resistance to antimicrobial agents in the clinical context. **American Chemical Society Omega**, 2020. DOI: 10.1021/acsomega.0c02294

MACEDO, M. L. R.; RIBEIRO, S. F. F.; TAVEIRA, G. B.; GOMES, V. M.; BARROS, K. M. C. A.; NETO, S. M. Antimicrobial activity of ILTI, a Kunitz-type trypsin inhibitor from *Inga laurina* (SW.) Willd. **Current Microbiology**, 2016. DOI: 10.1007/s00284-015-0970-z.

MACEDO, M. L. R.; FREIRE, M. G. M.; FRANCO, O. L.; MIGLIOLO, L.; OLIVEIRA, C. F. R. Practical and theorical characterization of *Inga laurina* Kunitz inhibitor on the control of *Homalinotus coriaceus*. **Biochemistry and Molecular Biology**, v. 158, n. 2, p. 164-172, 2011. DOI: 10.1016/j.cbpb.2010.11.005.

MACEDO, M. L. R.; GARCIA, V. A.; FREIRE, M. G. M.; RICHARDSON, M. Characterization of a Kunitz trypsin inhibitor with a single disulfide bridge from seeds of *Inga laurina* (SW.) Willd. **Phytochemistry**, v.68, n. 8, p.1104-1111, 2007. DOI: 10.1016/j.phytochem.2007.01.024.

MAHLAPUU, M.; HAKANSSON, J.; RINGSTAD, L.; BJORN, C. Antimicrobial Peptides: An Emerging Category of Therapeutic Agents. **Frontiers in Cellular and Infection Microbiology**, 2016. DOI: 10.3389/fcimb.2016.00194.

MARTI-RENOM, M. A.; STUART, A.; FISER, A.; SÁNCHEZ, R.; MELO, F.; SALI, A. Comparative protein structure modeling of genes and genomes. **Annual Review Biophysics and Biomolecular Structure**. 29, 291-325, 2000. DOI: 10.1146/annurev.biophys.29.1.291.

MERIÑO-CABRERA, Y.; CASTRO, J. G. S.; DIEZ, J. D. R.; MACEDO, M. L. R.; MENDES, T. A. O.; OLIVEIRA, M. G. A. Rational design of mimetic peptides based on the interaction between *Inga laurina* inhibitor and trypsins for *Spodoptera cosmioides* pest control. **Insect Biochemistry and Molecular Biology**, v. 122, 2020. DOI: 10.1016/j.ibmb.2020.103390.

OLIVEIRA, D. M. P.; FORDE, B. M.; KIDD, T. J.; HARRIS, P. N. A.; SCHEMBRI, M. A.; BEATSON, S. A.; PATERSON, D. L.; WALKER, M. J. Antimicrobial Resistance in ESKAPE Pathogens. **Clinical Microbiology Reviews**. 2020. DOI: 10.1128/CMR.00181-19.

PEREZ-RODRIGUEZ, A.; ERASO, E.; QUINDÓS, G.; MATEO, E. Antimicrobial Peptides with Anti-Candida Activity. **International Journal of Molecular Sciences**, 2022, *23*, 9264. DOI: 10.3390/ijms23169264

PETERS, B.M.; SHIRTLIFF, M.E.; JABRA-RIZK, M.A. 2010. Antimicrobial Peptides: Primeval Molecules or Future Drugs? **PLoS Pathogens**, 2010. DOI: 10.1371/journal.ppat.1001067.

PORTO, W. F.; IRAZAZABAL, L.; ALVES, E.S.F.; RIBEIRO, S.M.; MATOS, C.O.; PIRES, A.S.;FENSTERSEIFER, I.C.M.; MIRANDA, V.J.; HANEY, E.F.; HUMBLOT, V.; TORRES, M.D.T.; HANCOCK, R.E.W., LIAO, L.M.; LADRAM, A.; LU, T.K.; FUENTE-NUNEZ, C.; FRANCO, O.L. In silico optimization of a guava antimicrobial peptide enables combinatorial exploration for peptide design. **Nature Communications**, v. 9, n. 1490, 2018. DOI: 10.1038/s41467-018-03746-3.

PORTO, W. F.; PIRES, A. P.; FRANCO, O. L. CS-AMPPred: An Updated SVM Model for Antimicrobial Activity Prediction in Cysteine-Stabilized Peptides. **PLoS ONE**, 2012. DOI: 10.1371/journal.pone.0051444.

PREDA, V. G.; SANDULESCU, O. Communication is the key: biofilms, quórum sensing, formation and prevetion. **Discoveries (Craiova)**, 2019. DOI: 10.15190/d.2019.13

PULINGAM, T.; PARUMASIVAM, T.; GAZZALI, A. M.; SULAIMAN, A. M.; CHEE, J. Y.; LAKSHMANAN, M.; CHIN, C. F.; SUDESH, K. Antimicrobial resitance: prevalence, economic burden, mechanisms of resistance and strategies to overcome. European **Journal of Pharmaceutical Sciences**, 2022. DOI: 10.1016/j.ejps.2021.106103

RAMALHO, S. R.; SARDI, J. C. O.; JÚNIOR, E. C.; MARCHETTO, R.; WENDER, H.; VARGAS, L. F. P.; MIRANDA, A.; ALMEIDA, C. V.; ALMEIDA, L. H. O.; OLIVEIRA, C. F. R.; MACEDO, M. L. R. The synthetic antimicrobial peptide IKR18 displays anti-infectious properties in *Galleria mellonella in vivo* model. **Biochimica et Biophysica Acta (BBA) – General Subjects**, 2022. DOI: 10.1016/j.bbagen.2022.130244.

RAMOS, V. S.; CABRERA, O. G.; CAMARGO, E. L. O.; AMBRÓSIO, A. B.; VIDAL, R. O.; SILVA, D. S., GUIMARÃES, L. C.; MARANGONI, S.; PARRA, J. R. P.; PEREIRA, A. G.; MACEDO, M. L. R. Molecular cloning and insecticidal effect of *Inga laurina* trypsin inhibitor on *Diatrae saccharalis* and *Heliothis virescens*. **C: Toxicology & Pharmacology**, v. 156, n. 3-4, p. 148-158, 2012. DOI: 10.1016/j.cbpc.2012.07.007.

REZENDE, S. B.; LIMA, L. R.; MACEDO M. L. R.; FRANCO, O. L. and CARDOSO M. H. Advances in Peptide/Protein Structure Prediction Tools and their Relevance for Structural Biology in the Last Decade. **Current Bioinformatics** 2023. DOI: 10.2174/1574893618666230412080702

RICE, L. B. Federal funding for the study of antimicrobial resistance in nosocomial pathogens: no ESKAPE. **The Journal of Infectious Diseases**. 197:1079–81, 2008. DOI: 10.1086/533452

ROUDBARY, M.; VAHEDI-SHAHANDASHTI, R.; DOS SANTOS. A. L. S.; MOHAMMADI, S. R.; ASLANI, P.; LASS-FLÖRL C.; RODRIGUES, C. F. Biofilm formation in clinically relevant filamentous fungi: A therapeutic challenge. **Critical Reviews in Microbiology**, 2022;48:197–221. DOI: 10.1080/1040841X.2021.1950121

ROUDI, R., SYN, N.L., ROUDBARY, M. Antimicrobial Peptides as Biologic and Immunotherapeutic Agents Against Cancer: a Comprehensive Overview. **Frontiers in Immunology**. v.8, 2017. DOI: 10.3389/fimmu.2017.01320.

SALI, A.; BLUNDELL. T. L. Comparative protein modelling by satisfaction of spatial restraints. **Journal of Molecular Biology** 234, 779-815, 1993. DOI: 10.1006/jmbi.1993.1626.

SANTAJIT, S.; INDRAWATTANA, N. Mechanisms of antimcirobial resistance in ESKAPE pathogens. **BioMed Research International**, 2016. DOI: 10.1155/2016/2475067

SANTOS, M. O.; LIMA, F. C. S.; MARTINS, L. F. L.; OLIVEIRA, J. F. P.; ALMEIDA, L. M.; CANCELA, M. C. Estimativa de Incidência de Câncer no Brasil, 2023-2025. **Revista Brasileira de Cancerologia**, v. 23, n. 1, 2023. DOI: 10.32635/2176-9745.RBC.2023v69n1.3700

SCHADUANGRAT, N.; NANTASENAMAT, C.; PRACHAYASITTIKUL, V.; SHOOMBUATONG, W. ACPred: A Computational Tool for the Prediction and Analysis of Anticancer Peptides. **Molecules**. 2019. DOI: 10.3390/molecules24101973.

SHARMA, A.; GUPTA, P.; KUMAR, R. et al. dPABBs: A Novel in silico Approach for Predicting and Designing Anti-biofilm Peptides. **Scientific Reports**, 2016. DOI: 10.1038/srep21839

SILVA, A. R. P.; GUIMARÃES, M. S.; RABELO, J.; BELÉN, L. H.; PERECIN, C. J.; FARIAS, J. G.; SANTOS, J. H. P. M.; RANGEL-YAGUI, C. O. Redcent advances in the design of antimicrobial peptide conjugates. **Journal of Materials Chemistry B**, 2022. DOI: 10.1039/d1tb02757c

TAMBURRINO A, PIRO G, CARBONE C, TORTORA G, MELISI D. Mechanisms of resistance to chemotherapeutic and anti-angiogenic drugs as novel targets for

pancreatic cancer therapy. **Frontiers in Pharmacology**, v.4, p.56, 2013. DOI: 10.3389/fphar.2013.00056.

TERRENI, M.; TACCANI, M.; PREGNOLATO, M. New antibiotics for multidrug-resistant bacterial strains: latest research developments and future perspectives. **Molecules**, 2021. DOI: 10.3390/molecules26092671

WAGHU, F. H.; BARAI, R. S.; GURUNG, P.; IDICULA-THOMAS, S. CAMPR3: a database on sequences, structures and signatures of antimicrobial peptides**. Nucleic Acids Research**, v. 44, 2015. DOI: 10.1093/nar/gkv1051.

WALSH, T. R.; GALES, A. C.; LAXMINARAYANR.; DODD, P. C. Antimicrobial resistance: addressing a global threat to humanity. **Plos Medicine**, 2023. DOI: 10.1371/ journal.pmed.1004264

WANG, J.; SEEBACHER, N.; SHI, H.; KAN, Q.; DUAN, Z. Novel strategies to prevent the development of multidrug resistance (MDR) in cancer. **Oncotarget**. 2017. DOI: 10.18632/oncotarget.19187.

WANG, G., LI, X.; WANG, Z. APD3: the antimicrobial peptide database as a tool for research and education. **Nucleic Acids Research**, v. 44, 2016. DOI: 10.1093/nar/gkv1278.

WANG, G.; LI, X.; WANG, Z. APD2: the updated antimicrobial peptide database and its application in peptide design. **Nucleic Acids Research** v. 37, 2009. DOI: 10.1093/nar/gkn823.

WANG, Z.; WANG, G. APD: the antimicrobial peptide database. **Nucleic Acids Research**, v. 32, 2004. DOI: 10.1093/nar/gkh025.

WEBB, B.; SALI, A. Comparative Protein Structure Modeling Using Modeller. **Current Protocols in Bioinformatics**, 2016. DOI: 10.1002/cpbi.3.

WOO, Y. R.; CHO, S. H.; LEE, J. D.; KIM, H. S. The human microbiota and skin cancer. **International Journal of Molecular Sciences**, 2022. DOI: 10.3390/ijms23031813

WORLD HEALTH ORGANIZATION, 2022. Global antimicrobial resistance and use surveillance system (GLASS) report: 2022. Disponível em: < https://www.who.int/publications/i/item/9789240062702>. Acessado em: 29 agosto 2023.

WORLD HEALTH ORGANIZATION. International Agency for Research on Cancer 2018. Disponível em: <http://gco.iarc.fr/today>. Acessado em: 29 agosto 2023.

YANG, J.; ZHANG, Y. I-TASSER server: new development for protein structure and function predictions. **Nucleic Acids Research**, 43: W174-W181, 2015.

YUSUF, K.; SAMPATH, V.; UMAR, S. Bacterial infections and cancer: exploring this association and its implications for cancer patients. **International Journal of Molecular Sciences**, 2023. DOI: 10.3390/ijms24043110

ZHENG, W.; ZHANG, C.; LI, Y.; PEARCE, R.; BELL,E. W.; ZHANG, Y. Folding non-homology proteins by coupling deep-learning contact maps with I-TASSER assembly simulations. **Cell Reports Methods**, 1: 100014, 2021.

ZHOU, X.; ZHENG, W.; LI, Y.; PEARCE, R.; ZHANG, C.; BELL, E. W.; ZHANG, G.; ZHANG, Y. I-TASSER-MTD: a deep-learning-based platform for multi-domain protein structure and function prediction. **Nature Protocols**, 17: 2326-2353 (2022).

3. OBJETIVOS

3.1. Objetivo Geral

Projetar um peptídeo antimicrobiano sintético, com o auxílio de ferramentas computacionais, baseado em fragmentos obtidos da sequência primária de um inibidor de proteinase vegetal e avaliar a atividade antimicrobiana, a atividade antiproliferativa em células de melanoma murino e determinar seu mecanismo de ação.

3.2. Objetivos Específicos

- Desenhar com auxílio de ferramentas computacionais uma sequência peptídica e averiguar características estruturais e físico-químicas *in silico* do peptídeo;

- Determinar a estrutura tridimensional *in silico* e *in vitro* do peptídeo obtido;

- Avaliar a atividade antibacteriana, antifúngica, antibiofilme e determinar seu provável mecanismo de ação *in vitro*;

- Avaliar a citotoxicidade *in vitro* e a toxicidade aguda *in vivo* do peptídeo obtido;

- Avaliar a atividade antiproliferativa e determinar o tipo de morte celular desencadeada pelo peptídeo in vitro;

- Averiguar a indução do processo de morte celular imunogênica *in vitro*.

CAPÍTULO I –DESENHO DO PEPTÍDEO ANTIMICROBIANO E AVALIAÇÃO ATIVIDADE ANTIFÚNGICA

A potent candicidal peptide designed based on an encrypted peptide from a proteinase inhibitor

Luís Henrique de Oliveira Almeida[a*], Suellen Rodrigues Ramalho[a], Claudiane Vilharroel Almeida[a], Camila de Oliveira Gutierrez[a], Janaína de Cassia Orlandi Sardi[a], Antonio de Miranda[b], Ricardo Abreu de Oliveira[a], Samilla Beatriz de Rezende[c], Edson Crusca[d], Octávio Luiz Franco[c,e], Caio Fernando Ramalho de Oliveira[a], Marlon Henrique Cardoso[a,c,e] and Maria Lígia Rodrigues Macedo[a]

[a]*Laboratório de Purificação de Proteínas e suas Funções Biológicas, FACFAN, Universidade Federal de Mato Grosso do Sul, Campo Grande, Brazil;*

[b]*Departamento de Biofísica da Universidade Federal de São Paulo – SP, Brazil;*

[c]*S-Inova Biotech, Programa de Pós-Graduação em Biotecnologia, Universidade Católica Dom Bosco, MS, Brazil;*

[d] *Instituto de Química, Departamento de Bioquímica e Química Tecnológica, Universidade Estadual Paulista Júlio de Mesquita Filho, Araraquara, São Paulo, Brazil.*

[d]*Centro de Análises Proteômicas e Bioquímicas, Programa de Pós-Graduação em Ciências Genômicas e Biotecnologia, Universidade Católica de Brasília, DF, Brazil.*

* Correspondence:

Prof. Maria Lígia Rodrigues Macedo

Email: ligiamacedo18@gmail.com

ABSTRACT

Antimicrobial peptides (AMP) represent an alternative in the treatment of fungal infections associated with countless deaths. Here, we report a new AMP, named KWI-19, which was designed based on a peptide encrypted in the sequence of an *Inga laurina* Kunitz-type inhibitor (ILTI). KWI-19 inhibited the growth of *Candida* species and acted as a fungicidal agent from 2.5 to 20 µmol L^{-1}, also showing synergistic activity with amphotericin B. Kinetic assays showed that KWI-19 killed *Candida tropicalis* cells within 60 minutes. We also report the membrane-associated mechanisms of action of KWI-19 and its interaction with ergosterol. KWI-19 was also characterized as a potent antibiofilm peptide, with activity against *C. tropicalis*. Finally, non-toxicity was reported against *Galleria mellonella* larvae, thus strengthening the interest in all the bioactivities mentioned above. This study extends our knowledge on how AMPs can be engineered from peptides encrypted in larger proteins and their potential as candicidal agents.

Keywords: antifungal agents, candidiasis, peptide-based drugs, antimicrobial peptides.

Abbreviations: [1]MDR: Multidrug Resistance; [2]AMP: Antimicrobial Peptides; [3]ILTI: *Inga laurina* Trypsin Inhibitor; [4]NCBI: National Center for Biotechnology Information; [5]CAMP$_{R3}$: Collection of Antimicrobial Peptides; [6]SVM: Support Vector Machine; [7]RF: Random Forest; [8]DA: Discriminant Analysis; [9]ANN: Artificial Neural Network; [10]DBAASP: Database of Antimicrobial Activity and Structure of Peptides; [11]MD: Molecular Dynamics; [12]STM: Sense The Moment; [13]SPC: single point charge; [14]APD3: Antimicrobial Peptide Database; [15]dPABBs: Design Peptide Against Bacterial Biofilms; [16]MALDI-TOF/MS: Matrix-Assisted Laser Desorption Ionization Time-of-Flight; [17]HPLC: High-Performance Liquid Chromatography; [18]CD: Circular Dichroism; [19]SDS: sodium dodecyl sulfate; [20]TFE: 2,2,2-trifluoretanol; [21]PME: Particle Mesh Ewald; [22]RMSD: root mean square deviation; [23]RMSF: root mean square fluctuation; [24]DMEM: Dulbecco's Modified Eagle Medium; [25]RPMI: Roswell Park Memorial Institute; [26]FBS: fetal bovine serum; [27]DMSO: dimethylsulfoxide; [28]ATCC: American Type Culture Collection; [29]SD: Sabouraud; [30]MIC: Minimum Inhibitory Concentration; [31]MFC: Minimum Fungicide Concentration; [32]CLSI: Clinical and Laboratory Standards Institute; [33]CFU: colony forming units; [34]PI: Propidium Iodide; [35]OD: optical density; [36]SISGEN: Sistema Nacional de Gestão do Patrimônio Genético e do Conhecimento Tradicional Associado.

1. INTRODUCTION

The increasing number of infections caused by multidrug-resistant microorganisms has become a threat to the global public health system, leading to the death of thousands of people worldwide annually [1]. Consequently, the search for new antimicrobial agents has become an urgent need, where research groups and pharmaceutical industries have focused on the development of new therapeutic agents to fight pathogenic microorganisms [1].

Diseases caused by yeasts have become a serious threat to human health, affecting more than one billion people worldwide [2]. Fungal infections are more concerning in immunocompromised patients and those with autoimmune diseases, as well as patients that have undergone cancer chemotherapy or organ transplantation [3]. The main fungal agents that cause infections in humans are *Candida albicans, Candida tropicalis*, *Cryptococcus neoformans* and *Aspergillus fumigatus* [3]. In certain conditions, planktonic fungal cells can develop fungal biofilms, which have been associated with high rates of morbidity and mortality, mainly due to antibiotic resistance [4]. Misuse of antibiotics has caused pathogenic microorganisms to develop multidrug resistance (MDR) [5]. Thus, an effective alternative consists in developing other classes of antimicrobial drugs with high cell selectivity, low toxicity and with well-known molecular targets.

Antimicrobial peptides (AMPs) are molecules with a potential application in controlling fungal infections. AMPs comprise amphipathic molecules with 5 to 50 amino acid residues in length, and are usually rich in positively charged residues [6]. Based on their secondary structure, AMPs are grouped into four main classes: β-sheet, α-helix, loop and extended. In humans, the most prominent innate AMPs are cathelicidins and defensins, produced primarily by cells of the immune system [7]. As well as

naturally occurring AMPs, new synthetic AMPs have been designed with the aid of bioinformatics tools [8].

One of the ways to find new AMPs is through the search for cryptic sequences. Cryptic peptides are amino acid sequences found within a larger protein sequence, and which may have antimicrobial properties [9]. From plant proteins, for instance, it is possible to find one or more scrambled peptide sequences (*e.g.*, randomly rearranged peptides) that have high antimicrobial prediction. These cryptic peptides can also be used as model molecules for design strategies, aiming at improved antibacterial and/or antifungal activities.

Previously, a Kunitz trypsin inhibitor, named ILTI, was isolated from seeds of *Inga laurina* (Fabaceae, Mimosoideae), a native Brazilian tree [10]. ILTI is a protein composed of 178 amino acid residues [10] and displays multiple roles, including trypsin inhibition [10,11], insecticidal activity [12], antimicrobial (antifungal) activity [13], antibiofilm activity, and anticancer properties [14]. Considering the huge biotechnological potential displayed by ILTI, here we used bioinformatics tools to screen for possible encrypted AMPs that could be further used as template peptides for the optimization of candicidal properties. ILTI amino acid segments were extracted through a sliding-window protocol (Table S1), and the resulting fragments were submitted to a suit of antimicrobial activity predictors, with a core focus on antifungal activities. The final sequence with the most promising predictions was submitted to physicochemical properties-guided design strategies, thus generating peptide KWI-19 (Figure 1). KWI-19 was here characterized as a potent candicidal agent as a monotherapy and in synergy with other antifungal agents. The interest in all these activities is further strengthened by the moderate toxicity towards mammalian models *in vitro* and absence of acute toxicity *in vivo*.
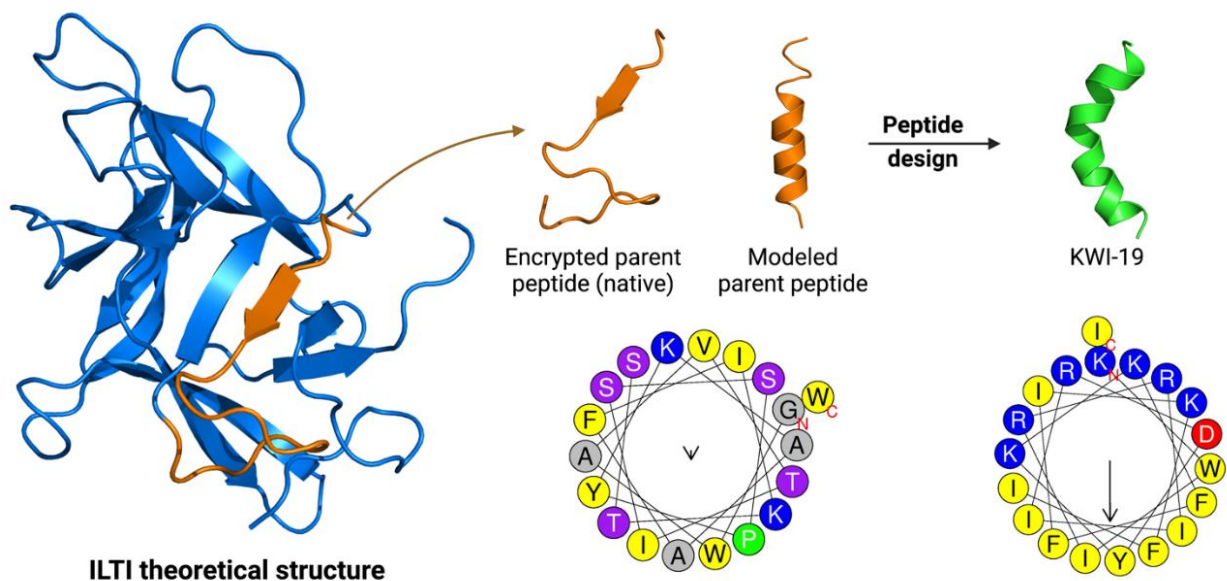
Figure 1. Lowest free energy three-dimensional structure obtained for ILTI, highlighting in orange the encrypted parent peptide (positions 54-72) and its theoretical model, presenting three turns of α-helix. After the physicochemical-guided design, peptide KWI-19 (green) was obtained with higher net positive charge and hydrophobic moment than its parent peptide, as shown in the helical wheel diagrams (black vectors indicate the hydrophobic moment for each peptide).

2. MATERIAL AND METHODS

2.1. Peptides encrypted in ILTI

The amino acid sequence of ILTI is deposited in the National Center for Biotechnology Information (NCBI) database, under the GenBank code: AFG28551.1. Computational analysis using the Phobius server [15] confirmed that the initial sequence for ILTI was free of signal peptide and propeptide regions. Subsequently, the ILTI primary structure was cleaved into numerous 19-amino-acid-residue peptides using a sliding-window approach. The peptides' size was determined aiming at obtaining potential α-helical peptides with at least three stable α-helical turns. The ILTI sequence cleavage was performed using the Collection of Antimicrobial Peptides

(CAMP$_{R3}$) server, and its 19-mer fragments were further submitted to four antimicrobial peptide predictors, including Support Vector Machine (SVM), Random Forest (RF), Discriminant Analysis (DA) and Artificial Neural Network (ANN) [16]. Additionally, two other prediction tools were used, including the Database of Antimicrobial Activity and Structure of Peptides (DBAASP) server (specific microbial species (filter: *C. albicans*)) [17]; and Sense The Moment (STM) – Eisenberg Scale [18]. Finally, the helical wheel diagrams, net charge, hydrophobicity (%) and hydrophobic moment <μH> were obtained from HeliQuest [19], which assisted in the physicochemical properties-guided design of our lead peptide, named KWI-19.

To further investigate the 19-amino-acid-residue peptides encrypted in ILTI in terms of three-dimensional structure, ILTI was submitted to comparative molecular modeling. For this, ILTI was modeled through the satisfaction of the spatial restraints using MODELLER v.10.2 [20]. The crystal structure of the trypsin inhibitor 1 from *Senna obtusifolia* (PDB ID: 6KV2) was used as a template structure. A total of 200 theoretical models were generated and ranked according to their free energy (DOPE score). The lowest free energy theoretical model was then selected for structural statistics analyses, including fold quality using ProSaWeb [21], and stereochemistry using PROCHECK [22]. Structural refinement was performed through molecular dynamics (MD) simulations using the GROMACS 5.0.4 computational package, as described below.

2.2. ILIT structure refinement through MD simulations

The structural refinement of ILIT was performed in water using atomistic MD simulations, as previously described [23]. All simulations were done using the GROMACS 5.0.4 computational package. The GROMOS96 43a1 force field was set

for all simulations, followed by the addition of single point charge (SPC) water molecules [24]. The system was neutralized by the addition of chloride and sodium ions. Moreover, additional ions were added until the 0.15 mol L^{-1} NaCl ionic strength was reached. The systems were submitted to energy minimization using the steepest descent algorithm (50,000 steps). Temperature and pressure normalization were performed at 310 K and 1 bar using the velocity rescaling thermostat (NVT) and the Parrinello-Rahman barostat (NPT), respectively. Structural refinement though MD simulations was performed during 100 ns. From the final MD structure (Figure 1), the atomic coordinates for the 19-amino-acid-residue peptide encrypted in ILIT were extracted and further used as a structural parameter for the design of an improved peptide with potential candicidal activity (Figure 1).

2.3. *Antifungal peptide designed from an encrypted peptide in ILTI*

Up to this point, we obtained the refined three-dimensional structural for ILIT, as well as its 19 amino acid residue encrypted peptide with higher antimicrobial prediction. Nevertheless, aiming at designing a more potent and candicidal peptide, this encrypted peptide was used as a model molecule for the physicochemical properties-guided design of a lead peptide candidate. The alterations carried out included changes in the positioning of the amino acid residues and also the substitution of residues present in the structure for others that imposed more favorable characteristics on the molecule, thus obtaining a new peptide sequence, which presented 36.84% of identity with the parental peptide. These modifications in the parental peptide were guided by the HeliQuest server [19], in which we verified the arrangement of amino acid residues in a helical wheel. To obtain an amphipathic sequence, 11 amino acid residues were replaced, in which three apolar residues were replaced by positively charged polar

residues, one apolar residue was replaced by a negatively charged polar residue, three apolar residues were replaced by other apolar residues that conferred greater stability to the molecule, one uncharged polar residue was replaced by a positively charged polar residue and, finally, three remaining uncharged polar residues were replaced by nonpolar residues. These changes resulted in a new peptide sequence, called KWI-19 (lysine-tryptophan-isoleucine (KWI) C-terminus; 19 amino acids long). The physicochemical parameters for peptide KWI-19 were measured in APD3 [25]. Moreover, to predict the antimicrobial and antifungal activity, we used $CAMP_{R3}$ and DBAASP server software (specific microbial species (filter: *C. albicans*)) [16, 17] and STM, as described above. Once KWI-19 was designed, searches were performed in non-redundant databases to check for possible homologous sequences [16, 25]. In addition to antimicrobial and antifungal activity, predictions of antibiofilm activity were also performed using the dPABBs software [26].

2.4. Peptide synthesis

Peptide KWI-19 was synthesized in collaboration with Prof. Antônio de Miranda, from the Department of Biophysics, Universidade Federal de São Paulo – SP, Brazil. The peptide molecular mass and purity (> 95%) were confirmed by t Matrix-Assisted Laser Desorption Ionization Time-of-Flight (MALDI-TOF/MS) and High-Performance Liquid Chromatography (HPLC), respectively.

2.5. Secondary structure characterization using circular dichroism

Spectra were recorded on a Jasco J-815 circular dichroism spectropolarimeter in a quartz cuvette with an optical path of 1 mm at 30 ºC. Far-UV analyses were obtained from 190 to 250 nm measurement range, 100 nm min^{-1} scanning speed, 0.5

nm bandwidth, 4s response time and 12 accumulations. The peptide's secondary structure at 40 µmol L^{-1} was investigated in water, 40 mmol L^{-1} sodium dodecyl sulfate (SDS), and 50% TFE in water (v/v). Spectral analyses were carried out with Dichroweb [27], using the SELCON3 method [28] and dataset 4 [29].

2.6. KWI-19 MD simulations under similar CD conditions

MD simulations were carried out in water, 50% TFE/water (v/v; 1:4 molar ratio), and in contact with an SDS micelle, according to Cardoso et al. [24]. The single point charge (SPC) water model was used. The simulations were performed using the GROMOS96 43A1 force field from the GROMACS v.5.0.4 computational package [23]. The validated tridimensional theoretical model for KWI-19 (comparative modeling using PDB ID: 6Z2J as template structure) was used as the initial structure in the simulations. SDS micelles were built, and their topologies generated using the CHARMM-GUI server [30]. Chloride ions were added to neutralize the system's charge in each of the simulations, which were performed under 0.15 mol L^{-1} NaCl ionic strength. Simulations in 50% TFE/water (molar ratio 1:4) were also performed in cubic boxes, the peptide immersed in single point charge water molecules, until the ideal concentration was reached. The geometry of water molecules was constrained using the SETTLE algorithm [31]. Moreover, the LINCS algorithm was used to link all the atom bond lengths. Particle Mesh Ewald (PME) was used for electrostatic corrections with a radius cut-off of 1.4 nm to minimize the computational simulation time. The same radius cut-off was used for the Van der Waals interactions. The list of neighbors of each atom was updated every 10 simulation steps of 2 fs each. The steepest descent algorithm (50,000 steps) was applied for energy minimization. The systems underwent a normalization of temperature and pressure to 310 K and 1 bar using the velocity

rescaling thermostat (NVT) and the Parrinello-Rahman barostat (NPT), respectively, for 100 ps. The systems with minimized energy and balanced temperature and pressure were submitted to MD simulations for 500 ns. MD simulations were analyzed using root mean square deviation (RMSD), root mean square fluctuation (RMSF), number of hydrogen bonds, hydrogen bonds occupancy and structure snapshots.

2.7. Hemolytic activity

The hemolytic activity of peptide KWI-19 was measured using a 1% erythrocyte solution [32]. For this, peptide dilutions from 400 to 1.5 μmol L^{-1} were prepared in 1.5 mL microtubes. Afterwards, 50 µL of each peptide concentration was incubated with 50 µL of erythrocyte solution at 37 °C, for 1 h. The microtubes were then centrifuged for 10 min at 2455 × g, and the supernatant was transferred to 96-well microplates. The content of free hemoglobin was determined at 414 nm in a Varioskan Lux microplate reader (Thermo Scientific).

2.8. Cell viability assays with murine macrophages

Aliquots of RAW 264.7 cells were stored in cryovials in a -80°C freezer until use. For thawing, the cryovials were heated in a water bath and transferred to a falcon tube, DMEM culture medium was added and centrifuged for 5 min, at 2000 rpm. After centrifugation, the supernatant was aspirated to the smallest volume possible without disturbing the cell sediment, and then resuspended in DMEM supplemented with 10% fetal bovine serum (FBS) and 1% antibiotics (penicillin 5 mg mL^{-1}, streptomycin 5 mg mL^{-1} and neomycin 10 mg mL^{-1}). The cells were incubated in atmospheric air enriched with 5% CO_2, at 37 °C. Cell viability in the presence of peptide KWI-19 was evaluated through the MTT assay [33]. Cells were seeded (5 x 10^3 cells $well^{-1}$) in 96-well

microplates and treated with increasing KWI-19 concentrations (from 0.25 to 64 µmol L^{-1}), diluted in culture medium without FBS, and incubated for 24 h. After 24 h, the culture medium was removed from the microplate. One hundred µL of MTT reagent (0.5 mg mL^{-1}) prepared in culture medium containing 10% FBS) was added to the wells and incubated for 4 h, at 37 °C. The medium was removed from the plate and this plate received 100 µL of dimethylsulfoxide (DMSO), responsible for solubilizing the formed formazan crystals. Absorbances were determined at 630 nm in a Varioskan Lux microplate reader (Thermo Scientific) and cell viability was calculated using SkanIt 6.0 software (Thermo Scientific). Data were presented as mean ± standard deviation. The half maximal inhibitory concentration (IC$_{50}$) values were calculated using GraphPad Prism 8.0 software.

2.9.   In vivo acute toxicity assay on Galleria mellonella

The acute toxicity of KWI-19 was also determined *in vivo* using *Galleria mellonella* larvae, as described by Megaw et al. 2015 [34]. Ten *G. mellonella* larvae weighting 200-300 mg were selected for each experimental group (KWI-19 at 50 µmol L^{-1}, 25 µmol L^{-1}, and 12.5 µmol L^{-1}, amphotericin B at 5.4 µmol L^{-1} and 0.54 µmol L^{-1}, saline 0.9% and DMSO 100%). Ten µL was administered for each treatment condition into the hemocoel of each larva through the last left propaw with a Hamilton syringe. Larvae were kept at room temperature and their survival rate were recorded for 72 h.

2.10. Cultivation of yeast cells

C. albicans ATCC 90028, *Candida glabrata* ATCC 90030, *Candida krusei* ATCC 6258, *Candida parapsilosis* ATCC 2209, *C. tropicalis* ATCC 750 and *Candida guillermondii* ATCC 6260 strains were used in this study. The strains were kept at –80

°C until use. For the assays, a single colony was inoculated in RPMI 1640 medium at 37 °C for 24 h, after which it was transferred to Sabouraud (SD) agar and incubated at 37 °C for 24 h, followed by the fungal inoculum preparation.

2.11. MIC and MFC determination

The minimum inhibitory concentration (MIC) of KWI-19 was determined using the broth microdilution technique, according to the protocols of the Clinical and Laboratory Standards Institute (CLSI) [35]. The peptide was dissolved in sterile 0.9% NaCl solution and assayed from 20 μmol L^{-1} to 0.02 μmol L^{-1}. Amphotericin B was used as positive control. The fungal suspension incubated in culture medium was used as negative control. RPMI 1640 culture medium without the addition of antifungal agents was used as sterility control. The fungal inoculum was prepared by suspending the colony forming units (CFU) in sterile 0.9% NaCl solution and adjusting its optical density (0.08 to 0.1) at 620 nm. From this inoculum, 10 µL was diluted in 4990 µL of RPMI 1640 medium, and 100 µL was transferred to a 96-well microplate, resulting in a density ranging from 2.5×10^3 to 2.5×10^4 cells mL^{-1}. The microplate was incubated for 24 h at 37 °C. A visual reading of the results was performed, where the MIC was determined in the wells in which there was no fungal growth (no turbidity). To determine the minimum fungicidal concentration (MFC), 10 µL aliquots were cultured on SD agar plates, and incubated for 24 h at 37 °C. The MFC was determined as the lowest concentration of the peptide in which there was no visible growth in the solid medium.

2.12. Peptide action on fungal cell wall (sorbitol) and plasma membrane (ergosterol) of Candida tropicalis

The sorbitol assay was performed according to the methodology described by Frost et al. [36], with modifications. For this, the MIC values previously determined were used as the starting concentrations in additional MIC assays using RPMI 1640 medium supplemented with 0.8 mol L^{-1} sorbitol (cell wall). The same was performed for RPMI 1640 medium supplemented with 1.01 mol L^{-1} ergosterol (plasma membrane). The peptide was dissolved in sterile 0.9% NaCl solution and assayed from 20 μmol L^{-1} to 0.02 μmol L^{-1}. In the same microplate, 100 µL of medium containing the treatments with KWI-19, amphotericin B, and negative control were added. The 96-well microplate was then incubated for 24 h at 37°C, and a visual reading of the results was performed.

2.13. Time-dependent fungicidal activity

The fungicidal activity was evaluated against *C. tropicalis* ATCC 750 using the KWI-19 peptide's MFC, according to Mitić-Ćulafić et al. (2005), with modifications [37]. Three types of assays were performed: one with non-supplemented RPMI 1640 medium; RPMI 1640 medium supplemented with 1.01 mmol L^{-1} ergosterol; and RPMI 1640 medium supplemented with 0.8 mol L^{-1} sorbitol. Amphotericin B was used as positive control. RPMI 1640 medium without the addition of any other agent was used as sterility control. The fungal inoculum was prepared as described previously. Peptide KWI-19 was tested at a final concentration of 5.0 µmol L^{-1} (MFC). A volume of 10 µL from each sample was transferred to Sabouraud agar plates at 0, 30, 60, 90, 120, 180 and 240 min intervals. The plates were incubated for 24 h at 37 °C. After the incubation period, CFUs were counted.

2.14. Synergistic effect between KWI-19 and amphotericin B

The synergism assay was performed following the checkerboard method [38], with peptide concentrations ranging from 5.0 µmol L^{-1} to 9.76 nmol L^{-1}, and amphotericin B from 0.5 µmol L^{-1} to 3.39 nmol L^{-1}. The assay was carried out with *C. tropicalis* ATCC 750, as previously mentioned. After 24 h at 37 ºC, a visual reading was performed and the wells in which there was total inhibition of fungal growth were determined. After obtaining the data, the calculations were made to determine the FIC$_A$ and FIC$_B$, and then the determination of the $\sum FIC$, using the equations below:

$$FIC_{(KWI-19)} = \frac{MIC_{combination}}{MIC_{individual}}$$

$$FIC_{(amphotericin\,B)} = \frac{MIC_{combination}}{MIC_{individual}}$$

$$\sum FIC = FIC_{(KWI-19)} + FIC_{(amphotericin\,B)}$$

2.15. Effects of KWI-19 on formation inhibition and eradication on C. tropicalis biofilm

The effects of KWI-19 on yeast biofilm were evaluated against *C. tropicalis* ATCC 750, according to Coffey and Anderson (2014) [39]. The peptide was dissolved in sterile 0.9% NaCl solution at 5.0 µmol L^{-1} and 2.5 µmol L^{-1}. Amphotericin B was used as a positive control at 0.5 µmol L^{-1} and 0.25 µmol L^{-1}. BHI broth culture medium supplemented with 1% glucose was used as sterility control. The fungal inoculum was prepared by suspending *C. tropicalis* ATCC 750 in sterile 0.9% saline solution and adjusting its OD from 0.08 to 0.1, at 620 nm. A 1:10 dilution was prepared (inoculum: RPMI 1640). 170 µL of BHI broth medium supplemented with 1% glucose, 20 µL of the

yeast cell suspension (1:100 dilution), and 10 µL of the peptide solution were placed in a 96-well microplate, and incubated for 24 h at 37 °C. In the biofilm eradication assay, 180 µL of BHI broth medium supplemented with 1% glucose and 20 µL of yeast cell suspension were added to the wells of the 96-well microplate and then it was incubated for 24 h at 37 °C. After incubation, the supernatant was aspirated and 190 µL of BHI broth medium supplemented with 1% glucose and 10 µL of peptide were added and the microplate was again incubated for 24 h at 37 °C. After the incubation time, the supernatant was aspirated, the wells were washed and 125 µL of 0.1% crystal violet solution were added and incubated for 10 min. The supernatant was aspirated, the wells washed twice with distilled water and the microplate was left to dry at room temperature for 2 h. The biofilm was dissolved in 150 µL of a 30% acetic acid solution and the OD determined at 550 nm in a Varioskan Lux microplate reader (Thermo Scientific).

2.16. Effects of KWI-19 on cells present in the Candida tropicalis biofilm

The cell viability of *C. tropicalis* biofilm treated with KWI-19 was performed according to Sardi *et al*. [40]. In this assay, 200 µL aliquots of cell suspension, with optical density from 0.08 - 0.1 at 620 nm were added to a 96-well microplate for the pre-adhesion step, for 2 h at 37 °C without agitation. After this period, the supernatant was removed, and the respective treatments (KWI-19 or amphotericin B) were added to BHI broth supplemented with 1% glucose at concentrations of MIC. Wells containing only BHI supplemented with 1% glucose were used as biofilm formation negative control. The microplate was incubated for 24 h at 37 °C without agitation. Following this period, the supernatant was removed, and the wells were washed twice with 0.9% saline. A volume of 50 µL of 0.9% saline was added to wells that were scraped off

using a micropipette tip. The scraped suspension was transferred to a microtube containing 450 µL of 0.9% saline solution and 50 µL of this solution was transferred to another 450 µL of 0.9% saline solution and so on, making a serial dilution, obtaining 10 different concentrations at the end. From each dilution, 10 µL was cultured on SD agar and the plates incubated for 24 h at 37 °C. The CFUs were counted, and the percentage of cell survival was quantified by means of CFU mL^{-1}. The viability test of the cells present in the pre-formed biofilm was carried out in a similar way, where the modification in the protocol is in the first incubation period, which instead of being only 2 hours for pre-adhesion of the cells, the incubation for 24 hours, and after the treatments and other stages of the process.

2.17. *Effects of KWI-19 on C. tropicalis biofilm using fluorescence microscopy*

The assay was performed in a sterile 24-well microplate containing a removable circular coverslip at the bottom. Five hundred µL of fungal suspension in 0.9% saline with an optical density of 0.1 at 620 nm was added, following pre-adhesion for 2 h at 37 °C. Then, the supernatant was removed and 500 µL of BHI broth supplemented with 1% glucose was added and used as a biofilm growth control. The wells were treated with 500 µL of BHI broth supplemented with 1% glucose and KWI-19 or amphotericin B at MIC. The microplate was incubated for 24 h at 37 °C. The non-adhered cells were washed from the coverslip using 500 µL of sterile 0.9% saline. The Live/DEAD BacLight (Invitrogen™) kit was used to investigate the biofilm viability, following the manufacturer's instructions. The coverslips were incubated with 500 µL of SYTO9/Propidium Iodide (PI) for 10 min, at 37 ºC and under low light. The excess of dye was washed in 0.9% saline solution and the coverslip analyzed in a Leica DM 2000 LED microscope, equipped with a Leica DFC 7000 camera (SYTO9: excitation

at 490 nm and emission at 520 nm; PI: excitation at 490 nm and emission at 635 nm). The images were analyzed in the LAS V4.12 software.

2.18. Fungal plasma membrane permeability using the microplate reader method

Membrane permeability was investigated using SYTOX™ green, as described by Mohanram & Bhattacharjya (2016) [41], with modifications as proposed by Almeida et al. (2021) [42]. Three types of assays were performed: one with non-supplemented RPMI 1640 medium; RPMI 1640 medium supplemented with 1.01 mmol L^{-1} ergosterol; and RPMI 1640 medium supplemented with 0.8 mol L^{-1} sorbitol. For this assay, a *C. tropicalis* ATCC 750 suspension was grown in SD broth for 24 h, at 37 °C. After that, striation was performed on an SD agar plate to obtain CFUs, and subsequently incubated for 24 h, at 37 °C. The fungal inoculum was then prepared with an OD reading of 0.5 at 620 nm in 10 mmol L^{-1} sodium phosphate buffer, pH 7.0. Further, 280 μL of the fungal suspension was transferred to 96-well black microplates, where 12 μL of SYTOX™ green at 30 μmol L^{-1} was added and incubated for 10 min at 37 °C. Subsequently, 10 μL of the KWI-19 peptide at a concentration 30 times greater than the MIC was added to each well, and the kinetic assay was performed for 240 min, at 5 min reading intervals. The assay was performed with fluorescence reading, excitation at 485 nm and emission at 520 nm in a Varioskan Lux microplate reader (Thermo Scientific). Negative membrane damage control was performed with *C. tropicalis* incubated with 10 μL of sodium phosphate buffer, pH 7.0, at 10 mmol L^{-1}.

2.19. Fungal plasma membrane permeability assay using fluorescence microscopy

In this assay, following the procedure described in the MIC, the permeability of the plasma membrane was investigated through the uptake of SYTOX[TM] green, according to Thevissen *et al.* (1996) [43]. Each microplate well received 1.7 μmol L^{-1} of SYTOX[TM] green. The incubation time for fungi + SYTOX[TM] green was 30 min at 25 °C, with constant stirring (500 rpm). Twenty µL aliquots were placed between a glass slide and a coverslip and the cells were analyzed in a Leica DM 2000 LED fluorescence microscope, equipped with a Leica DFC 7000 T camera (excitation wavelength 450-490 nm, emission wavelength 500 nm).

2.20. Access to genetic heritage

Access to genetic heritage was registered in the Sistema Nacional de Gestão do Patrimônio Genético e do Conhecimento Tradicional Associado (SISGEN, the National Genetic Heritage and Traditional Knowledge System), under ID number A315278.

2.21. Statistical analysis

Statistical analyses were performed using one-way analysis of variance (ANOVA) followed by Dunnett's or Tukey's multiple comparison tests using GraphPad Prism version 8.0.0 for Windows, GraphPad Software, San Diego, California, USA.

3. RESULTS

Peptide design, antifungal activity prediction and physicochemical properties

By cleaving the ILTI sequence *in silico* we obtained 160 peptide fragments containing 19 amino acid residues (Supplementary Material – Table 1). Each fragment was analyzed for its theoretical probability of showing antimicrobial activity. The

peptide encrypted in the ILTI sequence found at position 54-72 (NH_2-GWAVTISSPYKAAFIKTSW-COOH – parental peptide) presented an average antimicrobial prediction of 88.6% based on the algorithms shown in Table 1. Additionally, the parental peptide prediction for antibiofilm properties (Table 1) indicated no possible activity. Thus, modifications in the parental peptide amino acid sequence were carried out to increase its helicity, hydrophobicity, amphipathicity and positive net charge. Five uncharged amino acids (Thr, Ser, Ser, Thr, and Ser) were replaced by charged polar amino acids or nonpolar amino acids (Arg, Ile, Ile, Phe and Ile). Two lysine residues and one arginine residue were inserted in positions occupied by hydrophobic amino acids (Gly, Val, and Ala), and three substitutions of hydrophobic amino acids (Ala, Ala, and Trp) were replaced by other hydrophobic residues (Ile, Phe, and Ile) to equilibrate the peptide's amphipaticity. Finally, a proline residue was removed to favor an α-helical structure and replaced by an aspartic acid residue. Therefore, the resulting sequence, NH_2-KWIRRIIRDYKKFFIKFII-COOH, is loosely based on the parent peptide and was named KWI-19. The antimicrobial predictions for this peptide analog are described in Table 1.

The antimicrobial activity predicted by $CAMP_{R3}$ has a broad spectrum, and to refine our search for a sequence with antifungal activity, we submitted peptide KWI-19 to the DBAASP server [17], applying a filter for anti-*C. albicans* activity. We found that the parental peptide is not expected to act on *C. albicans* (Table 1). By contrast, peptide KWI-19 presents a prediction of antifungal activity against *C. albicans* with a positive predictive value (PPV) of 0.74 (Table 1). Furthermore, KWI-19 was predicted as an antibiofilm molecule in the WEKA algorithm (Table 1).

Table 1 – Antimicrobial activity predictions for the parental peptide and its modified derivative, KWI-19, using the $CAMP_{R3}$ server. Antibiofilm activity predictions for the parental peptide and for peptide KWI-19 were calculated using the Support Vector Machine (SVM) and Weka (machine learning) algorithms, which are part of the

dPABBs server. Another analysis regarding antibiofilm activity was performed using the BIOFIN server, which generates a score for each sequence analyzed and classifies them as biofilm inhibitor or non-inhibitor. The DBAAPS server classified sequences for specific microorganisms and revealed that changes in the parental peptide resulted in a peptide that was theoretically active against species from the *Candida* genus.

CAMP$_{R3}$	Sequence	Algorithm				AVERAGE
		SVM	RF	ANN	DA	
	GWAVTISSPYKAAFIKTSW	0.863	0.868	AMP	0.927	0.886
	KWIRRIIRDYKKFFIKFII	0.989	0.933	AMP	0.969	0.964

DPABBs	Sequence	Algorithm			
		SVM		WEKA	
		Score	Prediction	Probability	Prediction
	GWAVTISSPYKAAFIKTSW	-0.02	Biofilm-inactive	0.35	Biofilm-inactive
	KWIRRIIRDYKKFFIKFII	-0.08	Biofilm-inactive	0.71	Biofilm-active

BIOFIN	Sequence	Score	Prediction
	GWAVTISSPYKAAFIKTSW	-1.09	Negative
	KWIRRIIRDYKKFFIKFII	0.61	Biofilm Inhibitory

DBAAPS	Sequence	Strain Type	Class	Predictive value (Type)
	GWAVTISSPYKAAFIKTSW	*C. albicans*	Not Active	0.54
	KWIRRIIRDYKKFFIKFII	*C. albicans*	Active	0.74

SVM = Support Vector Machine; RF = Random Forest; ANN = Artificial Neural Network; DA = Discriminant Analysis.

Comparing the physicochemical features of the parental peptide and its modified derivative, KWI-19, the modifications resulted in an amphipathic structure, as well as increases in the positive net charge, hydrophobicity and in the Boman index, as displayed in Table 2. Therefore, the physicochemical properties-guided design of KWI-19 prompted more favorable features for this peptide in terms of antimicrobial effects.

Table 2 – Physicochemical properties calculated the parental peptide and its modified derivative, KWI-19.

Physicochemical properties	Parental peptide	KWI-19
Total Net Charge	+2	+6
Boman index	-0.07 Kcal mol^{-1}	1.85 Kcal mol^{-1}

Isoelectric Point	10.40	11.80
Molar Mass (theoretical)	2.113.44 g mol^{-1}	2.584.24 g mol^{-1}
Hydrophobic Relationship	47.37%	52.00%

Structural studies

The structural characterization of peptide KWI-19 was initially investigated through CD spectroscopy, followed by MD simulations under similar experimental conditions. CD analyses revealed that, in phosphate buffer, the peptide assumed a disordered structure, commonly observed for short, linear AMPs in this condition (Figure 2). In the presence of 50% tetrafluoroethylene (TFE), peptide KWI-19 adopted a well-defined α-helix conformation, characterized by a positive band around 190 nm and two negative bands at 208 and 222 nm (Figure 2). A similar pattern was observed in the presence of sodium dodecyl sulfate (SDS) micelles (Figure 2). The highest helicity was recorded in SDS (79.9%), followed by 30% TFE (58.7%) and in aqueous solution (5.29%), thus revealing that the secondary structure of KWI-19 is environment-dependent.

To support our CD data in a three-dimensional level, molecular modeling simulations were carried out, followed by MD simulations. One hundred theoretical models were generated for KWI-19, out of which only the lowest free-energy model was selected for structural statistics analyses. The lowest free-energy theoretical model for KWI-19 adopted a curved α-helix structure, possibly due to the electrostatic attraction between the OD1 atom from Asp9 and the atom NH2 from Arg5. Structural statistics revealed that 100% of possible amino acid residues are located in the most favorable region in the Ramachandran Map (Supplementary Material – Figure 1B). Moreover, the three-dimensional model for KWI-19 also exhibited a *z-score* (-0.91), like those reported for peptides of similar size and determined by nuclear magnetic

resonance (NMR), thus reinforcing the fold quality for this peptide structure (Supplementary Material – Figure 1 C).
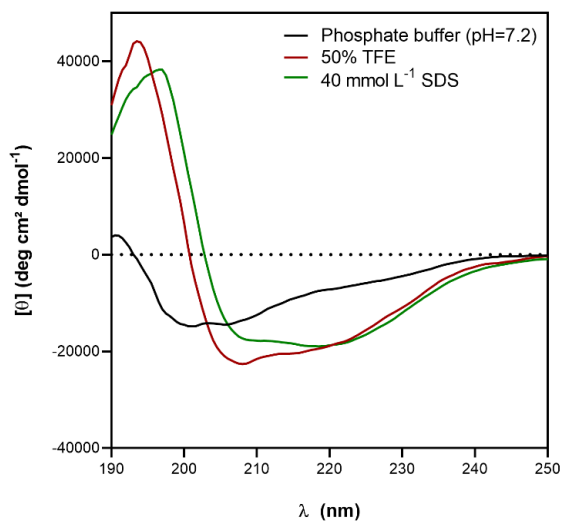
Figure 2 – Circular dichroism spectra of peptide KWI-19 (40 µmol L^{-1}) in phosphate buffer (pH = 7.2), 50% TFE in water (v/v), and in the presence of 40 mmol L^{-1} SDS.
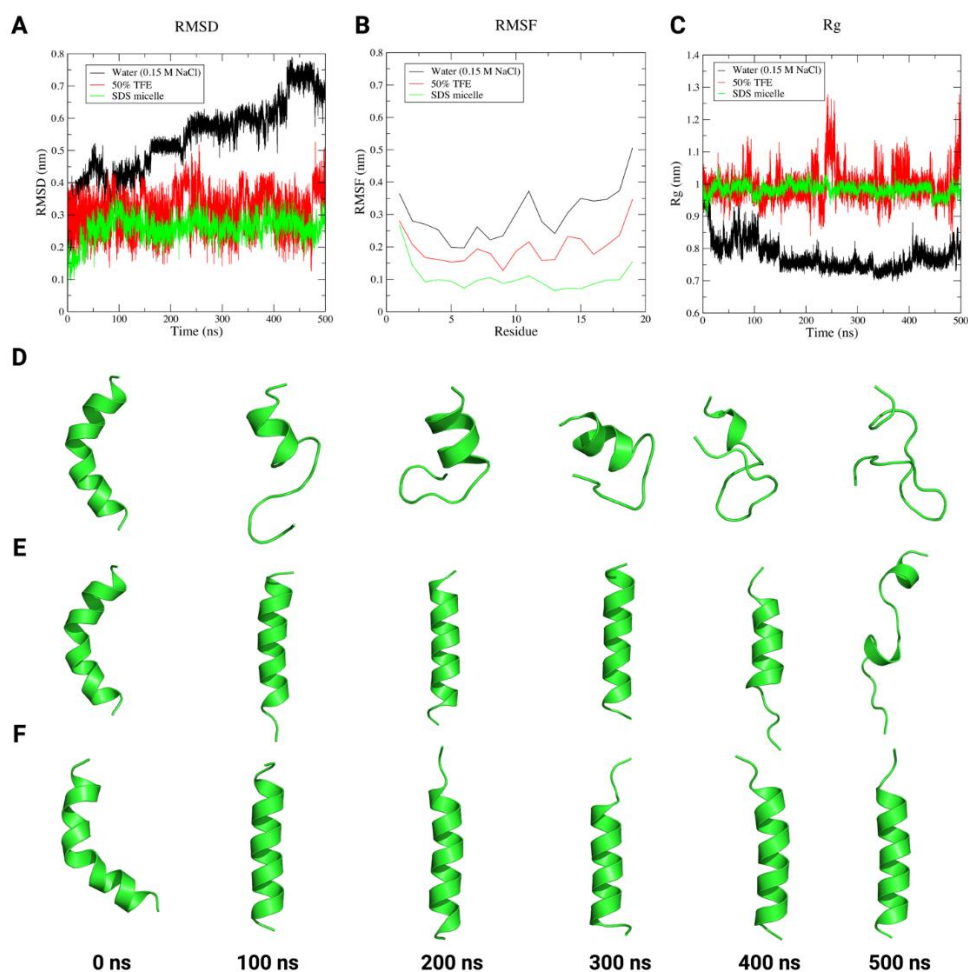
Figure 3 – Molecular dynamics simulations of peptide KWI-19 under similar CD conditions. The simulations were analyzed by means of (A) root mean square deviation (RMSD), (B) root mean square fluctuation (RMSF), and (C) radius of gyration. The theoretical structures of KWI-19 are also shown from 0 to 500 ns, at 100 ns intervals, in water (D), 50% TFE (E) and SDS micelles (F).

KWI-19 was designed aiming at an α-helical secondary structure (Supplementary Material – Figure 1), which was confirmed by molecular modeling and CD studies (Figure 2). To investigate the behavior of peptide KWI-19 in a hydrophilic environment, MD simulations were performed, and the theoretical tridimensional structures obtained were analyzed for 500 ns (Figure 3A-F). Peptide KWI-19 showed a significant loss of its secondary structure in aqueous solution from 100 ns, presenting higher root mean square deviation (RMSD) values (0.8 nm) than the other biological

conditions tested (Figure 3A). At 500 ns, in aqueous solution, the peptide adopts an extended structure with loops, characterizing a random coil arrangement (Figure 3D). By contrast, when evaluated in 50% TFE and in contact with an SDS micelle, peptide KWI-19 preserved its α-helix content (Figure 3E and 3F). It is worth noting that the input structure presented a slight curvature in the α-helix segment, which migrated to a more extended α-helix in 50% TFE and SDS (Figure 3E and F). Interestingly, however, peptide KWI-19 adopts an extended structure in 50% TFE at the end of the simulation, thus suggesting this peptide's structural plasticity when in contact with this co-solvent (Figure 3E). Additionally, in SDS, peptide KWI-19 preserved four α-helical turns throughout the simulations (Figure 3F).

Root mean square fluctuation (RMSF) analysis were also performed. As shown in Figure 3B, peptide KWI-19 is more flexible when in contact with aqueous solution and 50% TFE. In SDS, low RMSF values were recorded, indicating this peptide's preference for membrane-like environments (Figure 3B). Finally, through radius of gyration (Rg) analysis we observed that peptide KWI-19 tends to compact its structure in water, whereas a stable Rg was recorded for the simulation in 50% TFE and SDS.

Hemolytic assay, cell viability and acute toxicity

In addition to our structural studies, a suite of biological experiments was carried out to investigate the potential of KWI-19 as a new AMP, with a core focus on antifungal activities. The primary sequence of KWI-19 has many non-polar amino acid residues, resulting in a hydrophobicity of 52% (Table 2). This characteristic is related to the cytotoxicity of molecules, including AMPs, since the greater the number of hydrophobic residues, the greater the penetrability of cell membranes, which can cause cell death without specificity. Therefore, biological assays were performed to evaluate *in vitro* and

in vivo the possible toxic effects of KWI-19 on erythrocytes, murine macrophages, and *Galleria mellonella* larvae. The hemolytic assay with KWI-19 revealed a HC_{50} of 6.5 µmol L^{-1} (Figure 4A). Moreover, RAW 264.7 cells (murine macrophage) were submitted to cell viability assays, resulting in an IC_{50} of 64 µmol L^{-1} (Figure 4B). Finally, the acute toxicity of KWI-19 was also evaluated in *G. mellonella* larvae. We verified that, at the highest concentrations tested (25 and 50 µmol L^{-1}), all larvae treated with KWI-19 remained alive at the end of 72 h, except for one larva that was found dead after 12 h of treatment with KWI-19 at 12.5 µmol L^{-1}, evidencing the non-toxicity of KWI-19 *in vivo* (Figure 4C).
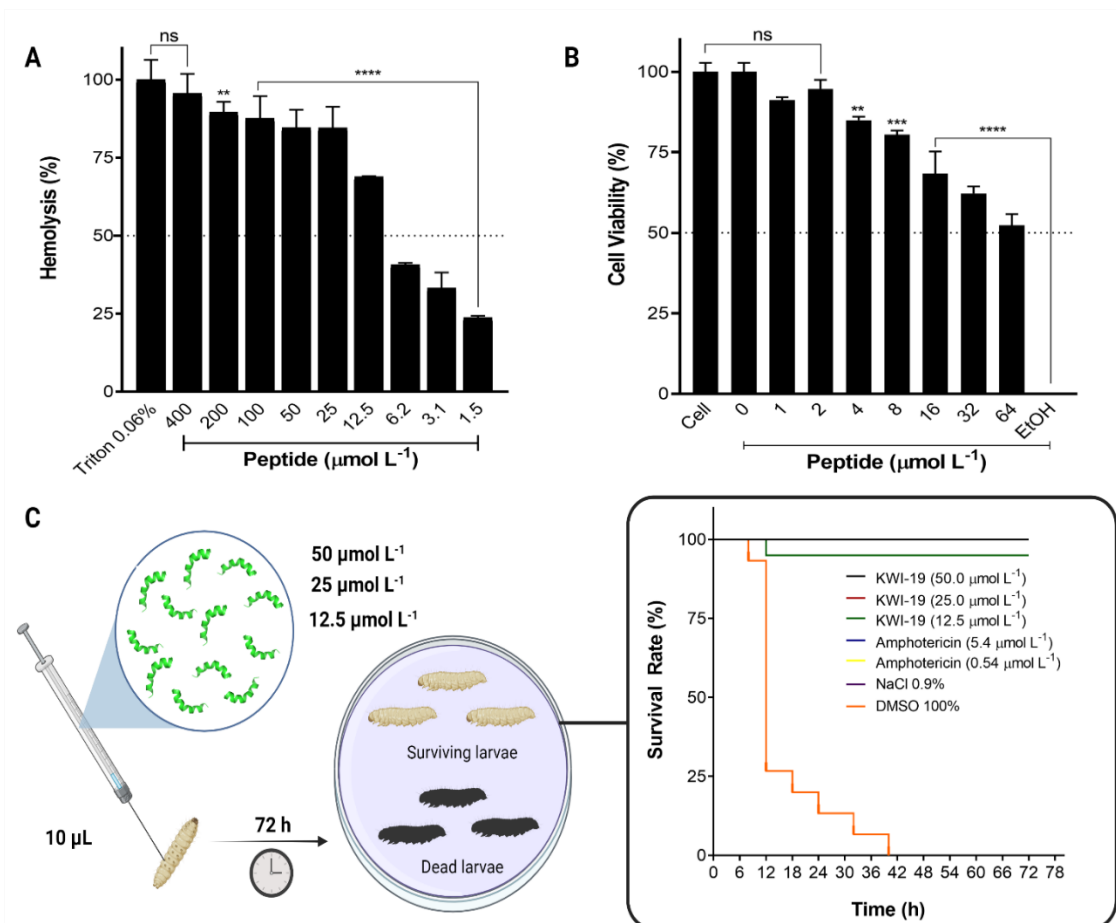
Figure 4 – Toxic profile of KWI-19 on erythrocytes, murine macrophages and *G. mellonella* larvae. (A) Percentage of hemolysis for peptide KWI-19 from 400 µmol L^{-1} to 1.5 µmol L^{-1} toward erythrocytes (Dunnett analysis, with 95% confidence. $p < 0.05$ =*; $p < 0.002$ = **; $p < 0.0002$ = *** and $p < 0.0001$ = ****). (B) Percentage of RAW 264.7 cell viability when treated with KWI-19 at concentrations ranging from 64 µmol L^{-1} to 0.25 µmol L^{-1} (*$p=0.05$; **$p=0.01$; ***$p= 0.001$; ****$p=0.0001$, ANOVA). (C)

Survival percentage of *G. mellonella* larvae treated with KWI-19, amphotericin B, 0.9% saline and DMSO (p<0.0001, Log-rank test).

KWI-19 antifungal activity and mechanisms of action

The antifungal activity assays (Table 3) revealed that the MIC and MFC of KWI-19 ranged from 2.5 to 20 μmol L^{-1}. The occurrence of damage to the cell wall was investigated with antifungal assays carried out in the presence of 0.8 mol L^{-1} sorbitol. The MIC of KWI-19 in presence of sorbitol was unaltered, indicating that the peptide has no direct action on the fungal cell wall, once it does not interact with free sorbitol in the medium (Table 3). The addition of ergosterol in media increased the MIC of KWI-19 significantly, indicating possible interactions with the plasma membrane, since the peptide interacts more with free ergosterol present in the medium and, therefore, decreasing the peptide's molar concentration around the candida cells (Table 3).

Table 3 – Determination of the minimum inhibitory concentrations (MICs), minimum fungicidal concentration (MFC) and MIC in the presence of 0.8 mol L^{-1} sorbitol and ergosterol at 1.01 mmol L^{-1} for KWI-19 against *Candida* yeasts.

Yeast	ATCC	KWI-19 (μmol L^{-1})		Amphotericin B (μmol L^{-1})		Mode of action	
		MIC	MFC	MIC	MFC	Sorbitol	Ergosterol
Candida albicans	90028	5.0	10	0.135	1.08	5.0	>20.0
Candida glabrata	90030	>20.0	>20.0	0.135	0.54	-	-
Candida krusei	6258	20.0	>20.0	0.27	0.54	20.0	>20.0
Candida parapsilosis	2209	10.0	20.0	0.27	0.54	10.0	>20.0
Candida tropicalis	750	5.0	5.0	0.54	0.54	5.0	20.0
Candida guillermondii	6260	2.5	2.5	0.067	0.135	2.5	>20.0

Additionally, the combination of KWI-19 and amphotericin B showed synergistic effects against *C. tropicalis* (Table 4). The synergistic activity against *C. tropicalis* ATCC 750 using the combination of KWI-19 and the clinically used antifungal amphotericin B was quantified by the Checkerboard test at subinhibitory

concentrations. This synergistic combination reduced the MIC of both KWI-19 and amphotericin B five-fold.

Table 4 – Individual minimum inhibitory concentration (MIC) values for peptide KWI-19 and amphotericin B, and their synergistic activities.

Microorganism	Association	MIC individual		MIC association		Σ FIC	Activity
		a*	b*	a*	b*	FIC_A+FIC_B	
C. tropicalis	KWI-19 (a) + amphotericin B (b)	5.0	0.54	0.15	0.017	0.06	synergistic

*Concentration in µmol L^{-1}.

The time required for KWI-19 to show fungicidal activity was also determined, aiming at defining the kinetics of action for this peptide. Complete reduction in colony forming units (CFUs) occurred within 60 min (Figure 5A) in non-supplemented medium. In ergosterol supplemented medium there was no reduction in CFUs at MFC (Figure 5 B). By contrast, in sorbitol supplemented medium, there was a total reduction of CFUs in 30 min (Figure 5 C), suggesting a mechanism of action that involves plasma membrane damage. To confirm the action on the membrane, a membrane permeabilization assay with emitted fluorescence reading was performed. In the 1.01 mmol L^{-1} ergosterol supplemented medium (Figure 5E), we verified that the peptide did not compromise the viability of *C. tropicalis* cells in the same way that it acted in the cells when the medium was not supplemented (Figure 5D).

The SYTOX^{TM} green reagent was also used to detect membrane damage induced by KWI-19 incubated with *C. tropicalis* at 2.5 µmol L^{-1}. As a result, no fluorescence signal was recorded in the control group, whereas *C. tropicalis* incubated with KWI-19 for 24 h showed a fluorescence signal, indicating that the integrity of the plasma membrane was compromised, and supporting our above-mentioned hypothesis (Figure 5G).

The antibiofilm properties of KWI-19 was investigated against *C. tropicalis*. The peptide inhibited 81.8% of *C. tropicalis* biofilm formation at MIC (Figure 6A). In the biofilm eradication assay, a reduction of 87.3% in the biofilm biomass was observed at MIC (Figure 6B). Moreover, we evaluated the viability of biofilm-constituting cells. We observed that, at MIC/MFC, the cells lost their viability (Figures 6C and D), suggesting that under these conditions the effect of KWI-19 is related to the rupture of biofilms and that they also affect biofilm cells. This hypothesis was further supported by fluorescence microscopy assays, confirming the effects of KWI-19 and amphotericin B on *C. tropicalis* (Figure 6E).
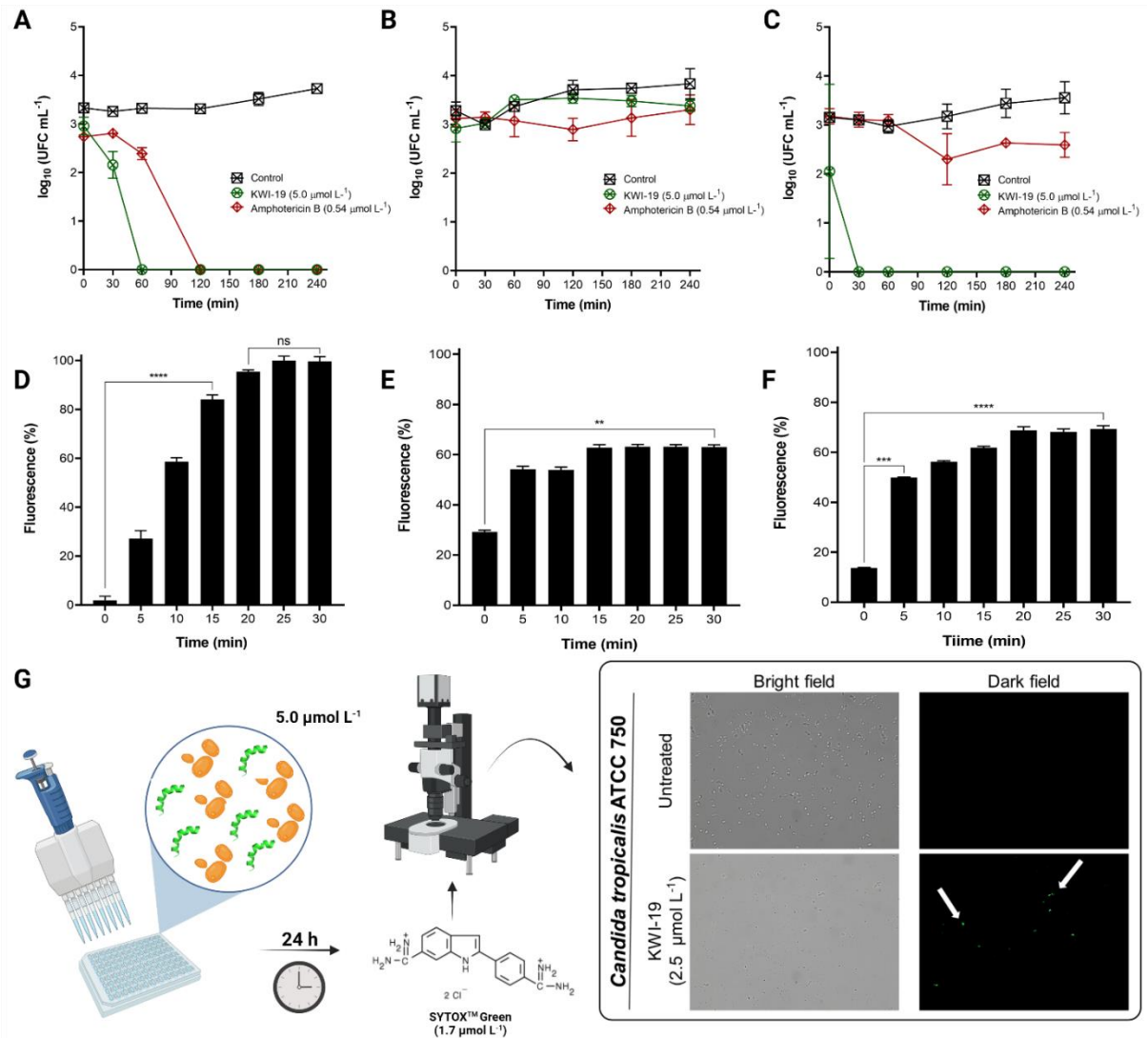
Figure 5 – (A) Time of action for peptide KWI-19 against *C. tropicalis* at MFC in non-supplemented RPMI 1640 medium; (B) RPMI 1640 medium supplemented with 1.01 mmol L^{-1} ergosterol; and (C) RPMI 1640 medium supplemented with 0.8 mol L^{-1} sorbitol. Percentage of fluorescence emitted by SYTOX™ green in the KWI-19 membrane permeability assay against *C. tropicalis* ATCC 750 was measured with reading at wavelengths of 485 nm and 520 nm, excitation and emission, respectively, in (D) non-supplemented RPMI 1640 medium; (E) RPMI 1640 medium supplemented with 1.01 mmol L^{-1} ergosterol; and (F) RPMI 1640 medium supplemented with 0.8 mol L^{-1} sorbitol. (G) Images of *C. tropicalis* cells after membrane permeabilization assays using fluorescence microscopy with the fluorescent agent SYTOX™ green. Cells were treated with 2.5 µmol L^{-1} of KWI-19 and then tested for membrane permeabilization. 40x magnification. Non-viable cells stained green.
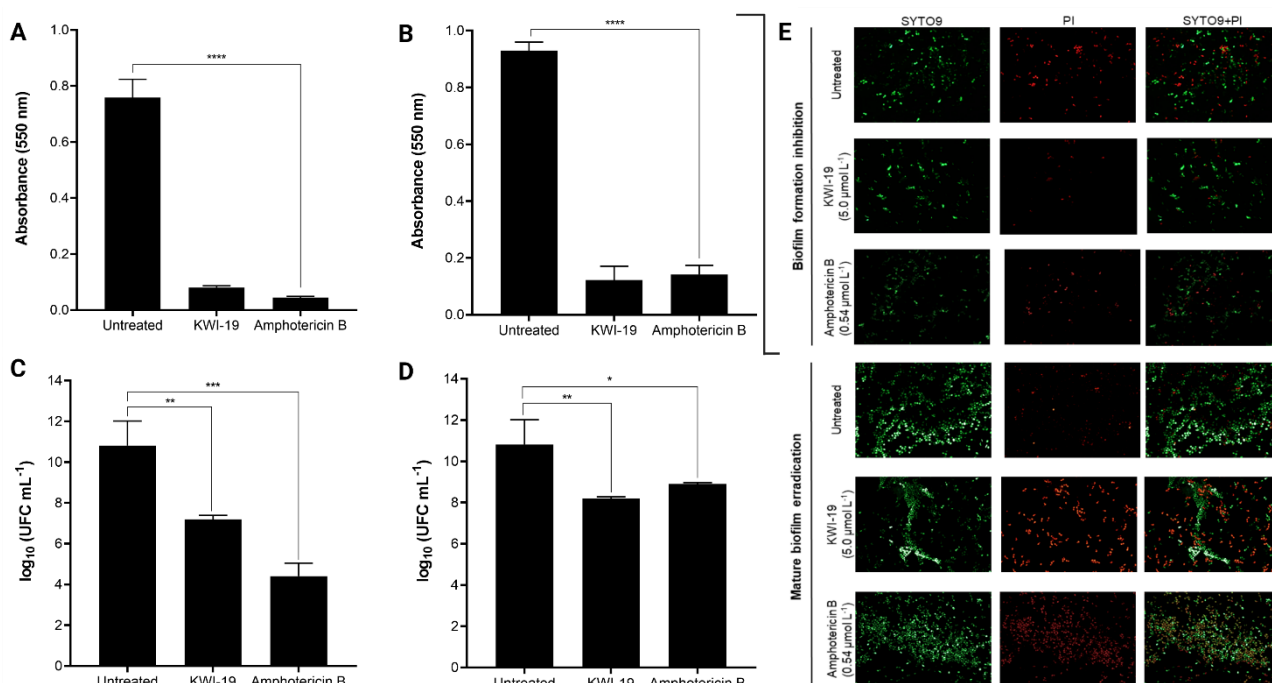
Figure 6 – Antibiofilm potential of KWI-19. (A) Quantitative analysis of the effects of KWI-19 and amphotericin B on *C. tropicalis* ATCC 750 biofilm formation inhibition, and (B) eradication of mature *C. tropicalis* ATCC 750 pre-formed biofilm. The quantitative analysis of the effects of KWI-19 on the viability of *C. tropicalis* ATCC 750 biofilm-constituting cells is also shown (C) in terms of inhibition of biofilm formation and (D) biofilm eradication. Fluorescence assays showing the potential of KWI-19 in inhibiting biofilm formation and eradicating pre-formed biofilms are also shown in comparison with amphotericin B (E). biofilms were stained and visualized using SYTO-9 to stain live biofilm cells (green, live cells) and propidium iodide (PI) (red, dead cells) p<0.0001, ANOVA with Tukey's post-test.

By analyzing the images, we noticed differences between the control biofilm and

the treatments with KWI-19 and amphotericin B. The differences were observed both

in the biofilm mass and in the number of viable cells, mainly in the mature biofilms, after the treatments. Therefore, the activity of KWI-19 against the biofilm is related to the impairment of the biofilm structure, at the level of the extracellular polymeric matrix, and in the cells inserted in the matrix.

4. DISCUSSION

The primary sequence and its spatial arrangement (secondary structure) are directly related to the biological activity of AMPs and their mechanisms of action. Most α-helical AMPs are rich in arginine and/or lysine residues, which contributes to the electrostatic interaction between AMPs and the microorganisms' cell membranes. The first interactions with the plasma membrane allow further structural rearrangement, favoring the adoption of an active secondary structure [44, 45]. The lipid bilayer of most microorganisms exhibits an overall negative charge. Therefore, the design of cationic AMPs contributes to electrostatic interactions, causing disturbances in the membrane integrity, which is a mechanism of action commonly reported for AMPs [44, 46].

A study carried out by Zhang *et al*. [47] showed that several cationic peptides, natural and synthetic, can interact and penetrate membrane models composed of a monolayer of negatively charged phospholipids, including gramicidin S, polymyxin B, indolicidin and polypemusin I, which present net charges of +2, +6, +4 and +8, respectively [19]. We recently described the biological properties of adevonin, a synthetic AMP bioinspired by a plant protein from *Adenanthera pavovina* seeds [48]. Adevonin is a cationic AMP (net charge +6), which causes damage to cell membranes. Through molecular dynamics (MD) simulations we showed that adenovin presents a disordered secondary structure in aqueous solution. In membrane-like environments,

adevonin adopts an α-helix conformation, projecting more positive side chains to facilitate interactions with the target cell membrane [48].

A characteristic observed in natural AMPs and reproduced in most synthetic AMPs is amphipathicity. Part of the peptide sequence is composed of polar (Ser, Thr, Cys, Tyr, Asn, Gln) and non-polar (Gly, Leu, Trp, Ala, Ile, Met, Val, Phe and Pro) residues [45, 49, 50, 51]. This amphipathic character assists in the interaction of the peptide with membrane phospholipids, and facilitates the preparation of compound formulas for administration, since hydrophilic residues contribute to solubility in aqueous media [44, 45, 49, 50, 51]. KWI-19 contains 11 non-polar amino acid residues, including six Ile, which have a short, branched, saturated side chain. The eight polar residues in KWI-19 include seven positively charged residues and one negatively charged residue (Asp). The composition of the residues that constitute the primary sequence of KWI-19 comprises a key step to elucidate its mode of action, as it provides us with information that the peptide can easily interact with target membranes, which was observed in *in vitro* assays carried out and reported in the present study and described below.

A peptide called RsAFP2, obtained from a plant (*Raphanus sativus*), showed activity against different species of *Candida*, with greatest effectiveness against *C. albicans, C. parapsilosis, C. krusei* and *C. tropicalis* [52, 53]. For these species, it was found that RsAFP2 present MIC values in the range of 5-10 µmol L^{-1}. And when compared to the positive control, the peptide was found to be as potent as fluconazole. The MIC values found for RsAFP2 are in the same range as the KWI-19 peptide. However, an advantage of the peptide described in the present work is the size of its peptide chain, since RsAFP2 has 51 amino acid residues in length, which may make it difficult to obtain it on a large scale.

Another peptide called Histatin-5, a peptide belonging to the class of histatins, is a histidine-rich cationic peptide that is secreted by the human salivary gland and is widely known to have potent antifungal activity [53]. This peptide consists of 24 amino acid residues and has MICs ranging from 1.6 – 50 µmol L^{-1} against *C. albicans, C. auris, C. parapsilosis, C. krusei, C. tropicalis, C. guilliermondii* species. When compared to the KWI-19 peptide, we verified similar antifungal activity. However, the Histatin-5 peptide presents a hemolysis with HC$_{50}$ > 100 µmol L^{-1}, proving its safety for diverse treatment applications, whereas KWI-19 is restricted to topical use due to its HC$_{50}$ < 10 µmol L^{-1}.

In addition to these, other peptides also have antifungal activity, including Jelleine-I (MIC: 2.5 – 64 µmol L^{-1}), Lasioglossin III (MIC: 0.2- 11.5 µmol L^{-1}), Lycosin-I (MIC: 8 -256 µmol L^{-1}), and bovine cateslytin (MIC: 1.2 - 8 µmol L^{-1}) [53]. These peptides are obtained from different sources (plants, animals, and insects), have different MIC and different modes of action, which demonstrates the versatility of antifungal peptides.

One of the major problems in the clinical use of peptides is their toxicity, such as their predominantly hemolytic activity, if the concentration needed to kill the target microorganisms is close to the hemolytic concentration [54]. However, this effect can be overcome by combining the peptide with another drug, such as amphotericin B. Thus, it is assumed that by significantly reducing the concentrations of the analyzed compounds, there may also be a reduction in their toxicity [54].

Amphotericin B acts as a fungistatic or fungicidal agent depending on the concentration used, but its mechanism of action does not depend on the concentration. This substance targets the sterols present in the fungal membrane. In the case of the tested yeast (*C. tropicalis*), amphotericin B binds directly to ergosterol, causing a

change in the permeability of the yeast membrane, thus causing the leakage of intracellular components, leading the cells to the death process [55]. A suggested mechanism of action for the KWI-19 peptide is that it acts directly on the membrane of *C. tropicalis*. That is, it causes a rupture in the membrane, leading to cell death. However, it is known that AMPs can have more than one type of mechanism of action for the same microorganism, which difficult the emergence of microbial resistance [56]. Moreover, thinking through this bias and verifying the high affinity of the peptide for ergosterol, two hypotheses can be assumed. The first is that the peptide acts on the membrane by binding to ergosterol together with amphotericin B. The second is that while the cell undergoes the action of amphotericin B by binding to cell membrane sterols, the KWI-19 peptide also acts in the cell causing the rupture of its membrane and leading the cell to death. Therefore, in any of the hypotheses there is a reduction in the concentration of both substances.

Regarding the mode of action of KWI-19 against yeast cells, it was possible to observe that it acts directly on the cell membrane, interacting with one of the main constituents of the membrane, ergosterol. [57]. Comparing the peptide activity under the conditions tested (non-supplemented medium and medium supplemented with ergosterol and csorbitol), we observed that KWI-19 was able to cause the death of 100% of the cells in non-supplemented RPMI medium in 30 min. In medium supplemented with ergosterol, the peptide compromised only about 65% after 30 min of incubation. This indicates that KWI-19 may be interacting with exogenous ergosterol, interfering with the amount of peptide available (less peptide) to interact with fungal cells. On the other hand, we cannot rule out the fact that the effect with ergosterol could be due to a much more non-specific response to having a relatively hydrophobic molecule in solution, or a macromolecular clumping effect. Therefore, to

provide more information on KWI-19's mechanisms of action, we performed further fluorescence microscopy analysis, where we found that there was membrane damage and extravasation of intracellular material (Figure 5G).

Biofilms can cause systemic infections and are a resistance mechanism of microorganisms against common drugs in clinical use [58]. The new classes of antimicrobials under development, in addition to being tested against planktonic cells, are also tested against biofilm. PEP-IA18, a synthetic AMP, was recently investigated for its antibiofilm properties [54]. PEP-IA18 showed antibiofilm activity against *C. tropicalis* at 2.5 µmol L^{-1}, whereas the highest activity was achieved at 25 µmol L^{-1}. Since KWI-19 exhibited antibiofilm properties against *C. tropicalis* at 5 µmol L^{-1}, we performed further assays using fluorescence microscopy (Figure 6E).

5. CONCLUSION

KWI-19, a synthetic AMP obtained from the sequence of a peptide encoded in the sequence of a protein of plant origin, exhibited potent antifungal properties. In view of the enormous difficulty in developing new antifungal agents, especially due to the rapid emergence of antimicrobial resistance, antifungal peptides are an alternative, since they may present more than one mode of action. In the case of KWI-19, it appears that, initially, there is an interaction with the fungal membranes followed by disturbances in its structure, which causes cell lysis. Furthermore, *in vitro* and *in vivo* assays have shown the possible use of KWI-19 as a candidacidal agent.

PATENT APPLICATION

The application of KWI-19 is protected by a patent request, deposited at the National Institute of Industrial Property (INPI), under number BR 10 2021 024849 1.

CRediT AUTHORSHIP CONTRIBUTION STATEMENT

Luís Henrique de Oliveira Almeida: Writing – original draft, Methodology, Investigation, Formal analysis, Data curation, Conceptualization. **Suellen Rodrigues Ramalho:** Methodology, Investigation, Formal analysis, Conceptualization. **Claudiane Vilharroel Almeida:** Methodology, Investigation, Formal analysis. **Camila de Oliveira Gutierrez:** Methodology, Investigation. **Janaina de Cassia Orlandi Sardi:** Methodology, Investigation, Formal analysis. **Antonio de Miranda:** Methodology, Investigation. **Ricardo Abreu de Oliveira:** Methodology, Investigation. **Beatriz de Rezende:** Methodology, Investigation. **Edson Crusca:** Methodology, Investigation, Formal analysis. **Octávio Luiz Franco:** Writing – reviewing and editing, Supervision. **Caio Fernando Ramalho de Oliveira**: Methodology, Investigation, Formal analysis, Conceptualization. **Marlon Henrique Cardoso:** Writing – reviewing and editing, Supervision, Methodology, Investigation, Formal analysis, Conceptualization. **Maria Ligia Rodrigues Macedo:** Writing – reviewing and editing, Supervision, Project administration, Funding acquisition.

DECLARATION OF COMPETING INTEREST

The authors declare no competing interests or personal relationships that could have appeared to influence the work reported in this paper.

ACKNOWLEDGMENT

SUPPORTING INFORMATION

Antimicrobial activity prediction of the 160 fragments obtained from the *in silico* cleavage of the *Inga laurina* trypsin inhibitor (ILTI) protein sequence using the CAMPR$_3$ server (Table S1). Secondary structure of the KWI-19 peptide (Figure S1).

REFERENCES

[1] ROCA, I.; AKOVA, M.; BAQUERO, F.; CARLET, J.; CAVALERI, M.; COENEN, S.; COHEN, J.; FINDLAY, D.; GYSSES, I.; HEURE, O. E.; KAHLMETER, G.; KRUSE, H.; LAXMINARAYAN, R.; LIÉBANA, F.; LÓPEZ-CERERO, L.; MACGOWAN, A.; MARTINS, M.; RODRÍGUEZ-BAÑO, J.; ROLAIN, J. M.; SEGOVIA, C.; VILA, J. The Global threat of antimicrobial resistance: science for intervention. *New Microbes and New Infections*, v. 6, 2015. DOI: 10.1016/j.nmni.2015.02.007

[2] BONGOMIN, F.; GAGO, S.; OLADELE, R. O.; DENNING, D. W. Global and multi-national prevalence of fungal diseases-estimate precision. *Journal of Fungi*, 2017. DOI: 10.3390/jof3040057

[3] MCGRATH, B.; BROADHURST, M.; ROMAN, C. Infectious disease considerations in immunocompromised patients. *JAAPA*, 2020. DOI: 10.1097/01.JAA.0000694948.01963.f4

[4] OSHIRO, K. G. N.; RODRIGUES, G.; MONGES, B. E. D.; CARDOSO, M. H.; FRANCO, O. L. Bioactive Peptides Against Fungal Biofilms. *Frontiers in Microbiology*, v. 10, 2019. DOI: 10.3389/fmicb.2019.02169

[5] CATALANO, A.; IACOPETTA, D.; CARAMELLA, J.; SCUMACI, D.; GIUZIO, F.; SATURNINO, C.; AQUARO, S.; ROSANO, C.; SINICROPI, M. S. Multidrug Resistance (MDR): A Widespread Phenomenon in Pharmacological Therapies. *Molecules*, 2022. DOI: 10.3390/molecules27030616

[6] BHADRA, P.; YAN, J.; LI, J.; FONG, S.; SIU, S.W.I. AmPEP: Sequence-based prediction of antimicrobial peptides using distribution patterns of amino acid properties and random forest. *Nature*, v. 8, n. 1697, 2018. DOI: 10.1038/s41598-018-19752-w

[7] PETERS, B. M.; SHIRTLIFF, M. E.; JABRA-RIZK, M. A. Antimicrobial Peptides: Primeval Molecules or Future Drugs? *PLoS Pathogens*, v. 6, 2010. DOI: 10.1371/journal.ppat.1001067

[8] PORTO, W. F.; IRAZAZABAL, L.; ALVES, E. S. F.; RIBEIRO, S. M.; MATOS, C. O.; PIRES, A. S.; FENSTERSEIFER, I. C. M.; MIRANDA, V. J.; HANEY, E. F.; HUMBLOT, V.; TORRES, M. D .T.; HANCOCK, R. E. W., LIAO, L. M.; LADRAM, A.; LU, T. K.; FUENTE-NUNEZ, C.; FRANCO, O. L. *In silico* optimization of a guava antimicrobial peptide enables combinatorial exploration for peptide design. *Nature*, v. 9, n. 1490, 2018. DOI: 10.1038/s41467-018-03746-3

[9] IAVARONE, F.; DESIDERIO, C.; VITALI, A.; MESSANA, I.; MARTELLI, C.; CASTAGNOLA, M. Cryptides: latent peptides everywhere. *Critical Reviews in Biochemistry and Molecular Biology*, v. 3, 2018. DOI: 10.1080/10409238.2018.1447543

[10] MACEDO, M. L. R.; GARCIA V. A.; FREIRE, M. G. M.; RICHARDSON, M. Characterization of a Kunitz trypsin inhibitor with a single disulfide bridge from seeds of *Inga laurina* (SW.) Willd. *Phytochemistry*, v.68, n. 8, p.1104-1111, 2007. DOI: 10.1016/j.phytochem.2007.01.024

[11] MACEDO, M. L. R.; FREIRE, M. G. M.; FRANCO, O. L.; MIGLIOLO, L.; OLIVEIRA, C. F. R. Practical and theorical characterization of *Inga laurina* Kunitz inhibitor on the control of *Homalinotus coriaceus*. *B: Biochemistry and Molecular Biology*, v. 158, n. 2, p. 164-172, 2011. DOI: 10.1016/j.cbpb.2010.11.005

[12] RAMOS, V. S.; CABRERA, O. G.; CAMARGO, E. L. O.; AMBRÓSIO, A. B.; VIDAL, R. O.; SILVA, D. S., GUIMARÃES, L. C.; MARANGONI, S.; PARRA, J. R. P.; PEREIRA, A. G.; MACEDO, M. L. R. Molecular cloning and insecticidal effect of *Inga laurina* trypsin inhibitor on *Diatrae saccharalis* and *Heliothis virescens*. *C: Toxicology & Pharmacology*, v. 156, n. 3-4, p. 148-158, **2012**. DOI: 10.1016/j.cbpc.2012.07.007

[13] MACEDO, M. L. R.; RIBEIRO, S. F. F.; TAVEIRA, G. B.; GOMES, V. M.; BARROS, K. M. C. A.; NETO, S. M. Antimicrobial activity of ILTI, a Kunitz-type trypsin inhibitor from *Inga laurina* (SW.) Willd. *Current Microbiology*, v. 72, p. 538-544, 2016. DOI: 10.1007/s00284-015-0970-z

[14] CARNEIRO, F. C.; WEBER, S. S.; SILVA, O. N.; JACOBOWAKI, A. C.; RAMADA, M. H. S.; MACEDO, M. L. R.; FRANCO, O. L.; PARACHIN, N. S. Recombinant *Inga laurina* trypsin inhibitor (ILTI) production in *Komagataella phaffii* confirms its potential anti-biofilm effect and reveals an anti-tumoral activity. *Microorganisms*, 2018. DOI: 10.3390/microorganisms6020037

[15] KÄLL, L.; KROGH, A.; SONNHAMMER, E. L. L.. Advantages of combined transmembrane topology and signal peptide prediction – the Phobius web server. Nucleic Acids Research, v. 35, p. W429-W429-2, 2007. DOI: 10.1093/nar/gkm256

[16] WAGHU, F. H.; BARAI, R. S.; GURUNG, P.; IDICULA-THOMAS, S. CAMPR3: a database on sequences, structures and signatures of antimicrobial peptides. *Nucleic Acids Research*, v. 44, 2015. DOI: 10.1093/nar/gkv1051

[17] PIRTSKHALAVA, M.; AMSTRONG, A. A.;GRIGOLAVA, M.; CHUBINIDZE, M.; ALIMBARASHVILI, E.; VISHNEPOLSKY, B.; GABRIELIAN, A.; ROSENTHAL, A.; HURT, D. E.; TARTAKOWSKY, M. DBAASP v3: database of antimicrobial/cytotoxic activity and structure of peptides as a resource for development of new therapeutics. *Nucleic Acids* Research, v. 49 p. D288-D297, 2020. DOI: 10.1093/nar/gkaa991

[18] PORTO, W. F.; FERREIRA, K. C. V.; RIBEIRO, S. M.; FRANCO, O. L. Sense the Moment: a highly sensitive antimicrobial activity predicor based on hydrophobic moment. *bioRxiv*, 2021. DOI: 10.1101/2020.07.15.205419

[19] GAUTIER, R.; DOUGUET, D.; ANTONNY, B.; DRIN, G. HELIQUEST: a web server to screen sequences with specific α-helical properties. *Bioinformatics*, 2008. DOI: 10.1093/bioinformatics/btn392

[20] WEBB, B.; SALI, A. Comparative Protein Structure Modeling Using Modeller. *Current Protocols in Bioinformatics*, 2016. DOI: 10.1002/cpbi.3

[21] WIEDERSTEIN, M.; SIPPL, M. J. ProSA-web: interactive web service for the recognition of errors in three-dimensional structures of proteins. *Nucleic Acids Research*, v. 35, 2007. DOI: 10.1093/nar/gkm290

[22] LASKOWSKI, R. A.; JABLONSKA, J.; PRAVDA, L.; VAREKOVÁ, R. S.; THORNTON, J. M. PDBsum: Structural summaries of PDB entries. *Protein Sci.*, v. 27, n. 1, p. 129–134, 2018. DOI: 10.1002/pro.3289.

[23] ABRAHAM, M.J.; MURTOLA, T.; SCHULZ, R.; PÁIL, S.; SMITH, J. C.; HESS, B.; LINDAHL, E. GROMACS: High performance molecular simulations through multi-level parallelism from laptops to supercomputers. *SoftwareX*, v. 1-2, paa. 19-25, set 2015. DOI: 10.1016/j.softx.2015.06.001.

[24] CARDOSO, M. H.; RIBEIRO, S. M.; NOLASCO, D. O.; FUENTE-NUÑEZ, C.; FELÍCIO, M. R.; GOPNÇALVES, S.; MATOS, C. O.; LIAO, L. M.; SANTOS, N. C.; HANCOK, R. E. W.; FRANCO, O. L.; MIGLIOLO, L. A polyalanine peptide derived from polar fish with anti-infections activities. *Scientific Reports*, 2016. DOI: 10.1038/srep21385

[25] WANG, G., LI, X.; WANG, Z. APD3: the antimicrobial peptide database as a tool for research and education. *Nucleic Acids Research*, v. 44, 2016. DOI: 10.1093/nar/gkv1278.

[26] SHARMA, A.; GUPTA, P.; KUMAR, R. *et al.* dPABBs: A Novel *in silico* Approach for Predicting and Designing Anti-biofilm Peptides. *Sci Rep***. ,** 2016. DOI: 10.1038/srep21839

[27] MILES, A. J.; RAMALLI, S. G.; WALLACE, B. A. DichroWeb, a website for calculating protein secondary structure from circular dichroism spectroscopic data. *Protein Science*, 2021. DOI: https://doi.org/10.1002/pro.4153

[28] SREEREMA, N.; VENYAMINOV, S. Y.; WOODY, R. W. Estimation of the number of helical and strand segments in proteins using CD spectroscopy. *Protein Sci.*, 1999. DOI: 10.1110/ps.8.2.370.

[29] SREERAMA, N.; WOODY, R. W. Estimation of protein secondary structure from CD spectra: Comparison of CONTIN, SELCON and CDSSTR methods with an expanded reference set. *Anal. Biochem.*, 2000. DOI: https://doi.org/10.1006/abio.2000.4880

[30] JO, S.; KIM, T.; IYER, V. G.; IM, W. CHARMM-GUI: A Web-based Graphical User Interface for CHARMM. *J. Comput. Chem.* v. 29, p.1859-1865, 2008. DOI: 10.1002/jcc.20945

[31] MIYAMOTO, S.; KOLLMAN, P.A. Settle - an Analytical Version of the Shake and Rattle Algorithm for Rigid Water Models. *J Comput Chem* v. 13, n.9, p. 952-962, 1992. DOI: 10.1002/jcc.540130805

[32] UGGERHØJ, L. E.; POULSEN, T. J.; MUNK, J. K.; FREDBORG, M.; SONDERGAARD, T. E.; FRIMODT-MOLLER, N. HANSEN. P. R.; WIMMER, R. Rational Design of Alpha-Helical Antimicrobial Peptides: Do's and Don'ts, 2015. DOI: 10.1002/cbic.201402581

[33] MOSMANN, T. Rapid colorimetric assay for cellular growth and survival: application to proliferation and cytotoxicity assays**. *J Immunol Methods*, 1983. DOI: 10.1016/0022-1759(83)90303-4

[34] MEGAW J, THOMPSON TP, LAFFERTY RA, GILMORE BF. Galleria mellonella as a novel in vivo model for assessment of the toxicity of 1-alkyl-3-methylimidazolium chloride ionic liquids. *Chemosphere.*, 2015. DOI: 10.1016/j.chemosphere.2015.06.026

[35] Clinical and Laboratory Standards Institute (CLSI). **2002**. Protocol M27-A2. Reference method for broth dilution antifungal susceptibility testing of yeasts. 2nd ed. Pennsylvania: NCCLS, 51p.

[36] FROST, D. J.; BRANDT, K. D.; CUGIER, D.; GOLDMAN, R. A. A whole-cell Candida albicans assay for the detection of inhibitors towards fungal cell wall synthesis and assembly. *J Antibiot.*, 1995. DOI:10.7164/antibiotics.48.306

[37] MITIĆ-ĆULAFIĆ, D.; VUKOVIĆ-GAČIĆ, B.; KNEŽEVIĆ-VUKČEVIĆ, J.; STANKOVIĆ, S.. SIMIĆ, D. Comparative study on the antibacterial activity of volatiles from sage (Salvia officinalis L.), *Arch. Biol. S*ci., 2005. DOI: 10.2298/abs0503173m

[38] SHARMA, L.; BISHT, G. S. Synergistic effects of short peptides and antibiotics against bacterial and fungal strains. *Journal of Peptide Science*, 2022. DOI: 10.1002/psc.3446

[39] Alain Filloux and Juan-Luis Ramos (eds.), *Pseudomonas Methods and Protocols*, Methods in Molecular Biology, vol. 1149, Springer Science+Business Media New York **2014**. DOI: 10.1007/978-1-4939-0473-0_48

[40] SARDI, J. C. O.; POLAQUINI, C. R.; FREIRES, I. A.; GALVÃO, L. C. C.; LAZARINI, J. G.; TORREZAN, G. S.; REGASINI, L. O.; ROSALEN, P. L. Antibacterial activity of diacetylcurcumin against *Staphylococcus aureus* results in decreased biofilm and cellular adhesion. *J Med Microbiol.*, 2017. DOI: 10.1099/jmm.0.000494

[41] MOHANRAM, H.; BHATTACHARJYA, S. Salt-resistant short antimicrobial peptides, *Biopolymers,* v. 106, p. 345–356, 2016. DOI:10.1002/bip.22819

[42] ALMEIDA, C. V.; OLIVEIRA, C. F. R.; SANTOS, E. L.; SANTOS, H. F.; JÚNIOR, E. C.; MARCHETTO, R.; CRUZ, L. A.; FERREIRA, A. M. T.; GOMES, V. M.; TAVEIRA, G. B.; COSTA, B. O.; FRANCO, O. L.; CARDOSO, M. H.; MACEDO, M. L. R. Differential interactions of the antimicrobial peptide, RQ18, with phospholipids and cholesterol modulate is selectivity for microorganism membranes. *BBA – General Subjects*, 2021. DOI: 10.1016/j.bbagen.2021.129937.

[43] THEVISSEN, K.; GHAZI, A.; SAMBLANY, G.W.; BROWNLEE, C.; OSBORN, R.W.; BROEKAERT, W.F. Fungal membrane responses induced by plant defensins and thionins, *J. Biol. Chem.*, 1996. DOI: 10.1074/jbc.271.25.15018.

[44] SOWA-JASIŁEK, A.; ZDYBICKA-BARABAS, A.; STACZEK, S.; PAWLIKOWSKA-PAWLEGA, B.; GRYGORCZUK-PŁANETA, K.; SKRZYPIEC, K.; GRUSZECKI, W. I.;

MAK, P.; CYTRYNSKA, M. Antifungal Activity of Anionic Defense Peptides: Insight into the Action of *Galleria mellonella* Anionic Peptide. *Int. J. Mol. Sci.*, 2020. DOI: 10.3390/ijms21061912

[45] AVCI, F. G.; AKBULUT, B. S.; OZKIRIMLI, E. Membrane Active Peptides and Their Biophysical Characterization. *Biomolecules*, 2018. DOI: 10.3390/biom8030077

[46] LAZZARO, B. P.; ZASLOFF, M.; ROLFF, J. Antimicrobial peptides: Application informed by evolution. *Science*, 2020. DOI: 10.1126/science.aau5480

[47] ZHANG, L.; ROZEK, A.; HANCOCK, R. E. W. Interaction of Cationic Antimicrobial Peptides with Model Membranes. *The Journal of Biological Chemistry*, v. 28, n. 38, p. 35714-35722, 2001. DOI: 10.1074/jbc.M104925200

[48] RODRIGUES, M. S.; OLIVEIRA, C. F. R.; ALMEIDA, L. H. O.; NETO, S. M.; BOLETI, A. P. A.; SANTOS, E. L.; CARDOSO, M. H.; RIBEIRO, S. M.; FRANCO, O. L.; RODRIGUES, F. S. MACEDO, A. J.; BRUST, F. R.; MACEDO, M. L. R. Adevonin, a novel synthetic antimicrobial peptide designed from the *Adenanthera pavonina* trypsin inhibitor (ApTI) sequence. *Pathogens and Global Health*, 2018. DOI: 10.1080/20477724.2018.1559489

[49] POWERS, J.-P.S.; HANCOCK, R.E. The relationship between peptide structure and antibacterial activity. *Peptides*, 2003. DOI: 10.1016/j.peptides.2003.08.023

[50] BAHAR, A. A.; REN, D. Antimicrobial peptides. *Pharmaceuticals*, 2013. DOI: 10.3390/ph6121543

[51] DI SOMMA, A.; MORETTA, A.; CANÈ, C.; CIRILLO, A.; DUILIO, A. Antimicrobial and Antibiofilm Peptides. *Biomolecules*, 2020. DOI: 10.3390/biom10040652

[52] THEVISSEN, K.; KRISTENSEN, H.-H.; THOMMA, B. P. H. J.; CAMMUE, B. P. A. FRANÇOIS, I. E. J. A. Therapeutic potential os antifungal plant and insect defensins. *Drug Discovery Today*, 2007. DOI: 10.1016/j.drudis.2007.07.016

[53] PEREZ-RODRIGUEZ, A.; ERASO, E.; QUINDÓIS, G.; MATEO, E. Antimicrobial Peptides with Anti-*Candida* Activity. *International Journal of Molecular Scienses*, 2022. DOI: 10.3390/ijms23169264

[54] LIMA, H. V. D.; CAVALCANTE, C. S. P.; RÁDIS-BAPTISTA. Antifungal In Vitro Activity of Pilosulin- and Ponericin-Like Peptides from the Giant Ant Dinoponera quadriceps an Synergistc Effects with Antimycotic Drugs. *Antibiotics*, 2020. DOI: doi.org/10.3390/antibiotics9060354

[55] CAROLUS, H.; PIERSON, S.; LAGROU, K.; VAN DIJCK, P. Amphotericin B and Other Polyenes – Discovery, Clinical Use, Mode of Action and Drug Resistance. *Journal of Fungi*, 2020. DOI: 10.3390/jof6040321

[56] TALAPKO, J.; MESTROVIC, T.; JUZBASIC, M.; TOMAS, M.; ERIC, S.; ALEKSIJEVIC, L. H.; BEKIC, S.; SCHWARZ, D.; MATIC, S.; NEUBERG, M.; SKRLEC,

I. Antimicrobial Peptides – Mechanisms os Action, Antimicrobial Effects and Clinical Applications. *Antibiotics*, 2022. DOI: 10.3390/antibiotics11101417

[56] LIMA, H. V. D.; CAVALCANTE, C. S. P.; RÁDIS-BAPTISTA. Antifungal In Vitro Activity of Pilosulin- and Ponericin-Like Peptides from the Giant Ant Dinoponera quadriceps an Synergistc Effects with Antimycotic Drugs. *Antibiotics*, 2020. DOI: doi.org/10.3390/antibiotics9060354

[57] GOMEZ-LOPEZ, A.; BUITRAGO, M. J.; RODRIGUEZ-TUDELA, J. L.; CUENCA-ESTRELLA, M. *In vitro* antifungal susceptibility pattern and ergosterol content in clinical yeats strains. *Revista Iberoamericana de Micología*, 2011. DOI: 10.1016/j.riam.2010.12.003.

[58] SILVA, A. C. B.; SARDI, J. C. O.; OLIVEIRA, D. G. L.; OLIVEIRA, C. F. R.; SANTOS, H. F.; SANTOS, E. L.; JÚNIOR, E. C.; CARDOSO, M. H.; FRANCO, O. L.; MACEDO, M. L. R. Development of a novel anti-biofilm peptide derived from profilin of *Spodoptera frugiperda*. *Biofouling*, 2020. DOI:: 10.1080/08927014.2020.1776857.

SUPPORTING INFORMATION

A potent candicidal peptide designed based on an encrypted peptide from a proteinase inhibitor

Luís Henrique de Oliveira Almeida[a*], Suellen Rodrigues Ramalho[a], Claudiane Vilharroel Almeida[a], Camila de Oliveira Gutierrez[a], Janaína de Cassia Orlandi Sardi[a], Antonio de Miranda[b], Ricardo Abreu de Oliveira[a], Samilla Beatriz de Rezende[c], Edson Crusca[d], Octávio Luiz Franco[c,e], Caio Fernando Ramalho de Oliveira[a], Marlon Henrique Cardoso[a,c,e] and Maria Lígia Rodrigues Macedo[a]

[a]Laboratório de Purificação de Proteínas e suas Funções Biológicas, FACFAN, Universidade Federal de Mato Grosso do Sul, Campo Grande, Brazil;

[b]Departamento de Biofísica da Universidade Federal de São Paulo – SP, Brazil;

[c]S-Inova Biotech, Programa de Pós-Graduação em Biotecnologia, Universidade Católica Dom Bosco, MS, Brazil;

[d] Instituto de Química, Departamento de Bioquímica e Química Tecnológica, Universidade Estadual Paulista Júlio de Mesquita Filho, Araraquara, São Paulo, Brazil.

[d]Centro de Análises Proteômicas e Bioquímicas, Programa de Pós-Graduação em Ciências Genômicas e Biotecnologia, Universidade Católica de Brasília, DF, Brazil.

* Correspondence:

Prof. Maria Lígia Rodrigues Macedo

Email: ligiamacedo18@gmail.com

Table S1 – Antimicrobial activity prediction of the 160 fragments obtained from the *in silico* cleavage of the *Inga laurina* trypsin inhibitor (ILTI) protein sequence using the CAMP$_{R3}$ server (http://www.camp.bicnirrh.res.in/index.php). Each fragment obtained contains 19 amino acid residues, and the one that presented the most promising prediction for antimicrobial activity was the fragment 54-72 (GWAVTISSPYKAAFIKTSW), with a probability of 88.6% of being antimicrobial.

Position	Sequence	ANN	SVM	RF	DA	Average
1-19	EVVVDSDGEMLRNGGKYYL	NAMP	0.337	0.087	0.003	0.142333333
2-20	VVVDSDGEMLRNGGKYYLS	NAMP	0.177	0.212	0.028	0.139
3-21	VVDSDGEMLRNGGKYYLSP	NAMP	0.126	0.158	0.019	0.101
4-22	VDSDGEMLRNGGKYYLSPA	NAMP	0.107	0.155	0.032	0.098
5-23	DSDGEMLRNGGKYYLSPAN	NAMP	0.286	0.094	0.012	0.130666667
6-24	SDGEMLRNGGKYYLSPANP	NAMP	0.218	0.113	0.034	0.121666667
7-25	DGEMLRNGGKYYLSPANPI	NAMP	0.244	0.100	0.078	0.140666667
8-26	GEMLRNGGKYYLSPANPIG	NAMP	0.336	0.488	0.274	0.366
9-27	EMLRNGGKYYLSPANPIGG	NAMP	0.185	0.397	0.073	0.218333333
10-28	MLRNGGKYYLSPANPIGGG	NAMP	0.181	0.481	0.204	0.288666667
11-29	LRNGGKYYLSPANPIGGGA	AMP	0.676	0.814	0.595	0.695
12-30	RNGGKYYLSPANPIGGGAI	AMP	0.829	0.660	0.621	0.703333333
13-31	NGGKYYLSPANPIGGGAII	AMP	0.785	0.662	0.949	0.798666667
14-32	GGKYYLSPANPIGGGAIIS	AMP	0.874	0.744	0.967	0.861666667
15-33	GKYYLSPANPIGGGAIISA	AMP	0.853	0.756	0.945	0.851333333
16-34	KYYLSPANPIGGGAIISAA	NAMP	0.744	0.583	0.832	0.719666667
17-35	YYLSPANPIGGGAIISAAI	NAMP	0.571	0.681	0.868	0.706666667
18-36	YLSPANPIGGGAIISAAIR	AMP	0.652	0.694	0.714	0.686666667
19-37	LSPANPIGGGAIISAAIRH	AMP	0.861	0.756	0.897	0.838
20-38	SPANPIGGGAIISAAIRHG	AMP	0.645	0.477	0.775	0.632333333
21-39	PANPIGGGAIISAAIRHGD	AMP	0.153	0.354	0.618	0.375
22-40	ANPIGGGAIISAAIRHGDH	AMP	0.531	0.496	0.708	0.578333333
23-41	NPIGGGAIISAAIRHGDHL	AMP	0.145	0.318	0.668	0.377
24-42	PIGGGAIISAAIRHGDHLC	AMP	0.276	0.444	0.563	0.427666667
25-43	IGGGAIISAAIRHGDHLCS	AMP	0.523	0.684	0.789	0.665333333
26-44	GGGAIISAAIRHGDHLCSL	AMP	0.362	0.533	0.786	0.560333333
27-45	GGAIISAAIRHGDHLCSLA	AMP	0.443	0.582	0.834	0.619666667
28-46	GAIISAAIRHGDHLCSLAV	AMP	0.536	0.657	0.836	0.676333333
29-47	AIISAAIRHGDHLCSLAVV	AMP	0.553	0.700	0.658	0.637

30-48	IISAAIRHGDHLCSLAVVS	AMP	0.560	0.698	0.682	0.646666667
31-49	ISAAIRHGDHLCSLAVVSA	NAMP	0.495	0.642	0.561	0.566
32-50	SAAIRHGDHLCSLAVVSAR	NAMP	0.207	0.353	0.354	0.304666667
33-51	AAIRHGDHLCSLAVVSARY	AMP	0.413	0.539	0.530	0.494
34-52	AIRHGDHLCSLAVVSARYT	NAMP	0.347	0.346	0.356	0.349666667
35-53	IRHGDHLCSLAVVSARYTN	NAMP	0.203	0.180	0.271	0.218
36-54	RHGDHLCSLAVVSARYTNG	NAMP	0.368	0.102	0.068	0.179333333
37-55	HGDHLCSLAVVSARYTNGW	NAMP	0.184	0.236	0.027	0.149
38-56	GDHLCSLAVVSARYTNGWA	NAMP	0.419	0.414	0.329	0.387333333
39-57	DHLCSLAVVSARYTNGWAV	NAMP	0.292	0.282	0.118	0.230666667
40-58	HLCSLAVVSARYTNGWAVT	NAMP	0.453	0.314	0.142	0.303
41-59	LCSLAVVSARYTNGWAVTI	NAMP	0.739	0.521	0.393	0.551
42-60	CSLAVVSARYTNGWAVTIS	NAMP	0.694	0.550	0.431	0.558333333
43-61	SLAVVSARYTNGWAVTISS	NAMP	0.497	0.416	0.323	0.412
44-62	LAVVSARYTNGWAVTISSP	NAMP	0.604	0.507	0.634	0.581666667
45-63	AVVSARYTNGWAVTISSPY	NAMP	0.477	0.388	0.269	0.378
46-64	VVSARYTNGWAVTISSPYK	NAMP	0.263	0.539	0.294	0.365333333
47-65	VSARYTNGWAVTISSPYKA	NAMP	0.314	0.537	0.326	0.392333333
48-66	SARYTNGWAVTISSPYKAA	NAMP	0.556	0.487	0.199	0.414
49-67	ARYTNGWAVTISSPYKAAF	NAMP	0.685	0.592	0.410	0.562333333
50-68	RYTNGWAVTISSPYKAAFI	NAMP	0.538	0.483	0.132	0.384333333
51-69	YTNGWAVTISSPYKAAFIK	NAMP	0.277	0.511	0.529	0.439
52-70	TNGWAVTISSPYKAAFIKT	AMP	0.513	0.538	0.643	0.564666667
53-71	NGWAVTISSPYKAAFIKTS	AMP	0.818	0.768	0.912	0.832666667
54-72	GWAVTISSPYKAAFIKTSW	AMP	0.863	0.868	0.927	0.886
55-73	WAVTISSPYKAAFIKTSWP	NAMP	0.699	0.738	0.884	0.773666667
56-74	AVTISSPYKAAFIKTSWPL	AMP	0.908	0.766	0.946	0.873333333
57-75	VTISSPYKAAFIKTSWPLN	AMP	0.631	0.584	0.856	0.690333333
58-76	TISSPYKAAFIKTSWPLNL	AMP	0.566	0.473	0.780	0.606333333
59-77	ISSPYKAAFIKTSWPLNLR	AMP	0.597	0.829	0.848	0.758
60-78	SSPYKAAFIKTSWPLNLRF	AMP	0.411	0.510	0.179	0.366666667
61-79	SPYKAAFIKTSWPLNLRFA	AMP	0.573	0.540	0.268	0.460333333
62-80	PYKAAFIKTSWPLNLRFAY	AMP	0.465	0.489	0.273	0.409
63-81	YKAAFIKTSWPLNLRFAYL	AMP	0.393	0.621	0.234	0.416
64-82	KAAFIKTSWPLNLRFAYLA	AMP	0.868	0.906	0.764	0.846

65-83	AAFIKTSWPLNLRFAYLAP	AMP	0.801	0.870	0.500	0.723666667
66-84	AFIKTSWPLNLRFAYLAPN	AMP	0.679	0.823	0.382	0.628
67-85	FIKTSWPLNLRFAYLAPNV	AMP	0.605	0.797	0.515	0.639
68-86	IKTSWPLNLRFAYLAPNVC	AMP	0.534	0.742	0.371	0.549
69-87	KTSWPLNLRFAYLAPNVCT	NAMP	0.378	0.487	0.045	0.303333333
70-88	TSWPLNLRFAYLAPNVCTN	NAMP	0.125	0.170	0.035	0.11
71-89	SWPLNLRFAYLAPNVCTNS	NAMP	0.198	0.198	0.060	0.152
72-90	WPLNLRFAYLAPNVCTNSP	NAMP	0.276	0.172	0.061	0.169666667
73-91	PLNLRFAYLAPNVCTNSPN	NAMP	0.241	0.119	0.052	0.137333333
74-92	LNLRFAYLAPNVCTNSPNW	AMP	0.341	0.284	0.088	0.237666667
75-93	NLRFAYLAPNVCTNSPNWV	NAMP	0.298	0.195	0.112	0.201666667
76-94	LRFAYLAPNVCTNSPNWVV	NAMP	0.375	0.346	0.062	0.261
77-95	RFAYLAPNVCTNSPNWVVV	NAMP	0.449	0.258	0.067	0.258
78-96	FAYLAPNVCTNSPNWVVVK	NAMP	0.384	0.419	0.272	0.358333333
79-97	AYLAPNVCTNSPNWVVVKS	NAMP	0.585	0.467	0.373	0.475
80-98	YLAPNVCTNSPNWVVVKSR	NAMP	0.227	0.278	0.078	0.194333333
81-99	LAPNVCTNSPNWVVVKSRS	NAMP	0.758	0.445	0.295	0.499333333
82-100	APNVCTNSPNWVVVKSRSL	NAMP	0.865	0.418	0.217	0.5
83-101	PNVCTNSPNWVVVKSRSLG	AMP	0.005	0.300	0.130	0.145
84-102	NVCTNSPNWVVVKSRSLGE	NAMP	0.017	0.248	0.035	0.1
85-103	VCTNSPNWVVVKSRSLGEA	NAMP	0.041	0.493	0.085	0.206333333
86-104	CTNSPNWVVVKSRSLGEAV	NAMP	0.063	0.486	0.055	0.201333333
87-105	TNSPNWVVVKSRSLGEAVM	NAMP	0.095	0.222	0.003	0.106666667
88-106	NSPNWVVVKSRSLGEAVML	NAMP	0.144	0.248	0.014	0.135333333
89-107	SPNWVVVKSRSLGEAVMLG	NAMP	0.198	0.233	0.012	0.147666667
90-108	PNWVVVKSRSLGEAVMLGD	NAMP	0.168	0.185	0.007	0.12
91-109	NWVVVKSRSLGEAVMLGDK	NAMP	0.635	0.394	0.077	0.368666667
92-110	WVVVKSRSLGEAVMLGDKQ	NAMP	0.746	0.582	0.085	0.471
93-111	VVVKSRSLGEAVMLGDKQE	NAMP	0.458	0.276	0.012	0.248666667
94-112	VVKSRSLGEAVMLGDKQEF	NAMP	0.349	0.132	0.022	0.167666667
95-113	VKSRSLGEAVMLGDKQEFG	NAMP	0.252	0.140	0.008	0.133333333
96-114	KSRSLGEAVMLGDKQEFGN	NAMP	0.142	0.065	0.001	0.069333333
97-115	SRSLGEAVMLGDKQEFGNA	NAMP	0.143	0.082	0.001	0.075333333
98-116	RSLGEAVMLGDKQEFGNAF	NAMP	0.178	0.048	0.008	0.078
99-117	SLGEAVMLGDKQEFGNAFV	NAMP	0.396	0.076	0.032	0.168

100-118	LGEAVMLGDKQEFGNAFVS	NAMP	0.432	0.148	0.063	0.214333333
101-119	GEAVMLGDKQEFGNAFVSG	NAMP	0.523	0.171	0.130	0.274666667
102-120	EAVMLGDKQEFGNAFVSGS	NAMP	0.308	0.083	0.028	0.139666667
103-121	AVMLGDKQEFGNAFVSGSF	NAMP	0.412	0.172	0.147	0.243666667
104-122	VMLGDKQEFGNAFVSGSFS	NAMP	0.294	0.090	0.115	0.166333333
105-123	MLGDKQEFGNAFVSGSFSI	NAMP	0.214	0.050	0.043	0.102333333
106-124	LGDKQEFGNAFVSGSFSIE	NAMP	0.288	0.327	0.139	0.251333333
107-125	GDKQEFGNAFVSGSFSIET	NAMP	0.243	0.223	0.222	0.229333333
108-126	DKQEFGNAFVSGSFSIETH	NAMP	0.116	0.075	0.026	0.072333333
109-127	KQEFGNAFVSGSFSIETHD	NAMP	0.133	0.078	0.020	0.077
110-128	QEFGNAFVSGSFSIETHDT	NAMP	0.067	0.112	0.022	0.067
111-129	EFGNAFVSGSFSIETHDTE	NAMP	0.090	0.086	0.053	0.076333333
112-130	FGNAFVSGSFSIETHDTEK	NAMP	0.132	0.071	0.131	0.111333333
113-131	GNAFVSGSFSIETHDTEKH	NAMP	0.208	0.044	0.351	0.201
114-132	NAFVSGSFSIETHDTEKHH	NAMP	0.138	0.017	0.340	0.165
115-133	AFVSGSFSIETHDTEKHHY	NAMP	0.137	0.029	0.134	0.1
116-134	FVSGSFSIETHDTEKHHYK	NAMP	0.177	0.078	0.387	0.214
117-135	VSGSFSIETHDTEKHHYKL	NAMP	0.185	0.065	0.330	0.193333333
118-136	SGSFSIETHDTEKHHYKLV	NAMP	0.225	0.051	0.197	0.157666667
119-137	GSFSIETHDTEKHHYKLVF	NAMP	0.208	0.049	0.360	0.205666667
120-138	SFSIETHDTEKHHYKLVFR	NAMP	0.082	0.034	0.091	0.069
121-139	FSIETHDTEKHHYKLVFRQ	NAMP	0.081	0.055	0.318	0.151333333
122-140	SIETHDTEKHHYKLVFRQQ	NAMP	0.064	0.068	0.157	0.096333333
123-141	IETHDTEKHHYKLVFRQQG	NAMP	0.085	0.071	0.354	0.17
124-142	ETHDTEKHHYKLVFRQQGQ	NAMP	0.368	0.155	0.138	0.220333333
125-143	THDTEKHHYKLVFRQQGQD	NAMP	0.064	0.127	0.045	0.078666667
126-144	HDTEKHHYKLVFRQQGQDE	NAMP	0.083	0.159	0.032	0.091333333
127-145	DTEKHHYKLVFRQQGQDES	NAMP	0.084	0.121	0.038	0.081
128-146	TEKHHYKLVFRQQGQDESA	NAMP	0.070	0.052	0.003	0.041666667
129-147	EKHHYKLVFRQQGQDESAN	NAMP	0.052	0.055	0.010	0.039
130-148	KHHYKLVFRQQGQDESANI	NAMP	0.082	0.039	0.011	0.044
131-149	HHYKLVFRQQGQDESANIG	NAMP	0.087	0.022	0.004	0.037666667
132-150	HYKLVFRQQGQDESANIGV	NAMP	0.126	0.111	0.010	0.082333333
133-151	YKLVFRQQGQDESANIGVK	NAMP	0.156	0.330	0.062	0.182666667
134-152	KLVFRQQGQDESANIGVKL	AMP	0.668	0.413	0.471	0.517333333

135-153	LVFRQQGQDESANIGVKLD	NAMP	0.606	0.287	0.187	0.36
136-154	VFRQQGQDESANIGVKLDS	NAMP	0.528	0.209	0.143	0.293333333
137-155	FRQQGQDESANIGVKLDSE	NAMP	0.557	0.210	0.113	0.293333333
138-156	RQQGQDESANIGVKLDSED	NAMP	0.142	0.208	0.019	0.123
139-157	QQGQDESANIGVKLDSEDR	NAMP	0.119	0.312	0.020	0.150333333
140-158	QGQDESANIGVKLDSEDRR	NAMP	0.261	0.287	0.030	0.192666667
141-159	GQDESANIGVKLDSEDRRR	NAMP	0.450	0.257	0.011	0.239333333
142-160	QDESANIGVKLDSEDRRRL	NAMP	0.363	0.168	0.003	0.178
143-161	DESANIGVKLDSEDRRRLV	NAMP	0.138	0.156	0.008	0.100666667
144-162	ESANIGVKLDSEDRRRLVV	NAMP	0.463	0.207	0.013	0.227666667
145-163	SANIGVKLDSEDRRRLVVT	NAMP	0.435	0.254	0.104	0.264333333
146-164	ANIGVKLDSEDRRRLVVTD	NAMP	0.509	0.234	0.031	0.258
147-165	NIGVKLDSEDRRRLVVTDK	NAMP	0.539	0.278	0.078	0.298333333
148-166	IGVKLDSEDRRRLVVTDKE	NAMP	0.497	0.283	0.063	0.281
149-167	GVKLDSEDRRRLVVTDKEA	NAMP	0.471	0.195	0.039	0.235
150-168	VKLDSEDRRRLVVTDKEAL	NAMP	0.527	0.235	0.031	0.264333333
151-169	KLDSEDRRRLVVTDKEALI	NAMP	0.512	0.220	0.030	0.254
152-170	LDSEDRRRLVVTDKEALIF	NAMP	0.465	0.241	0.088	0.264666667
153-171	DSEDRRRLVVTDKEALIFK	NAMP	0.101	0.141	0.045	0.095666667
154-172	SEDRRRLVVTDKEALIFKF	NAMP	0.153	0.135	0.103	0.130333333
155-173	EDRRRLVVTDKEALIFKFD	NAMP	0.003	0.205	0.116	0.108
156-174	DRRRLVVTDKEALIFKFDK	NAMP	0.041	0.352	0.589	0.327333333
157-175	RRRLVVTDKEALIFKFDKV	AMP	0.293	0.547	0.714	0.518
158-176	RRLVVTDKEALIFKFDKVK	NAMP	0.395	0.580	0.586	0.520333333
159-177	RLVVTDKEALIFKFDKVKD	NAMP	0.390	0.240	0.511	0.380333333
160-178	LVVTDKEALIFKFDKVKDN	NAMP	0.772	0.281	0.733	0.595333333

SVM = Support Vector Machine
RF = Random Forest
ANN = Artificial Neural Network
DA = Discriminant Analysis
AMP = Antimicrobial Peptide
NAMP = Non Antimicrobial Peptide
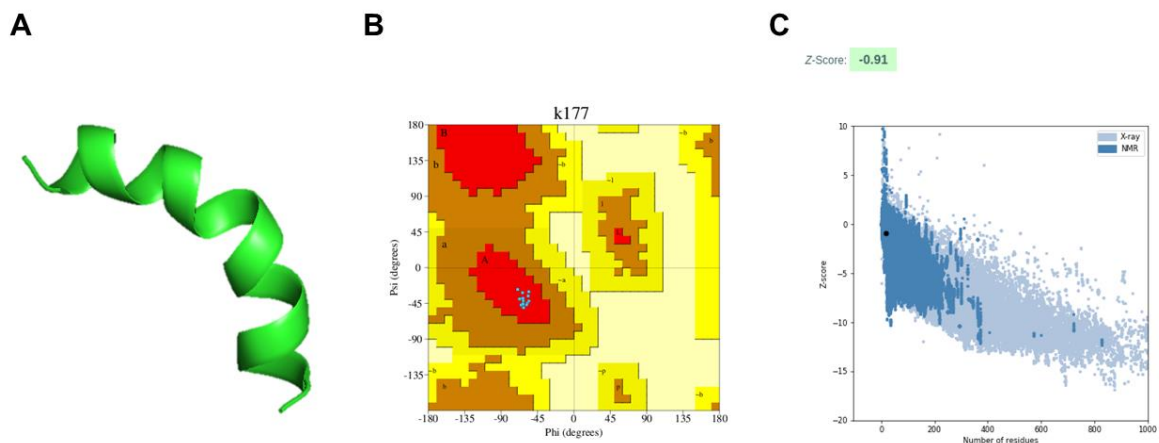
Figure S1 – (A) Secondary structure of the KWI-19 peptide obtained by the I-TASSER server by the homology modeling method and image generated by the PyMOL program; (B) Ramachandran diagram generated by PROCHECK software using the lowest energy model. where the KWI-19 peptide has 100% of the amino acid residues in the most favorable allowed regions; (C) Validation graph generated by the ProSA-web software for the KWI-19 peptide. which showed a Z-score of -0.91.

CAPÍTULO II – AVALIAÇÃO DA ATIVIDADE ANTIBACTERIANA DE KWI-19

KWI-19: a new broad-spectrum antibacterial peptide with direct action on the cell membrane of *Pseudomonas aeruginosa* and *Staphylococcus saprophyticus*

Luís Henrique de Oliveira Almeida[a*], Suellen Rodrigues Ramalho[a], Claudiane Vilharroel Almeida[a], Camila de Oliveira Gutierrez[a], Janaína de Cassia Orlandi Sardi[a], Edson Crusca[b], Octávio Luiz Franco[c,d], Caio Fernando Ramalho de Oliveira[a], Marlon Henrique Cardoso[a,c,d] and Maria Lígia Rodrigues Macedo[a*]

[a]*Laboratório de Purificação de Proteínas e suas Funções Biológicas, FACFAN, Universidade Federal de Mato Grosso do Sul, Campo Grande, Brazil;*
[b]*Departamento de Biofísica da Universidade Federal de São Paulo – SP, Brazil;*
[c]*S-Inova Biotech, Programa de Pós-Graduação em Biotecnologia, Universidade Católica Dom Bosco, MS, Brazil;*
[d]*Centro de Análises Proteômicas e Bioquímicas, Programa de Pós-Graduação em Ciências Genômicas e Biotecnologia, Universidade Católica de Brasília, DF, Brazil.*

* Correspondence:

Prof. Maria Lígia Rodrigues Macedo

Email: ligiamacedo18@gmail.com

ABSTRACT

Antimicrobial resistance (AMR) acquired by bacteria, either naturally or due to the indiscriminate use of antibiotics, has become a serious public health problem worldwide. Especially, for a select group of bacteria (ESKAPE), the problem is even more alarming, since the antibiotics available for clinical use are not effective in combating these microorganisms. In addition to microorganisms capable of overcoming the effects of antibiotics, one of their resistance mechanisms is the formation of biofilms, which has made the treatment of bacterial infections more difficult. In this context, there is an urgency to discover new compounds that have antibacterial and antibiofilm activities. A class of bioactive compounds in which microorganisms have difficulty acquiring AMR, when compared to conventional antibiotics, are antimicrobial peptides (AMP). AMPs may have more than one biological activity (antifungal, antibacterial, antiviral, antiparasitic, among others). Based on this, an AMP, called KWI-19, was chosen to evaluate its antibacterial activity, as it already has proven antifungal activity. KWI-19 showed *in silico* and *in vitro* antibacterial potential. Minimal inhibitory concentration values were between 1.25 and 10 µmol L^{-1}. Moreover, KWI-19 was found to also inhibit and eradicate *P. aeruginosa* biofilm and inhibit *S. saprophyticus* biofilm formation. Furthermore, KWI-19 showed rapid bactericidal action through membrane-associated mechanisms, as most AMP described in the literature. Therefore, KWI-19 is a peptide with a broad spectrum of biological activities with the potential to become a novel antimicrobial agent.

Key words: drug resistance; antibiotics; biofilm; antimicrobial peptide; membrane permeability

1. INTRODUCTION

Bacteria acquire antimicrobial resistance (AMR) naturally; however, this has become a serious public health problem due to the indiscriminate use of antibiotics [1]. The AMR phenomenon is one of the main threats to human health in the 21st century and it is estimated that 10 million people will die from these infections by 2050 [2]. In 2017, the World Health Organization (WHO) published a list of the "superbugs" that present the greatest risk to human health, categorizing these bacteria into three groups according to their priority (medium, high and critical) [1]. These bacteria pose a greater risk to hospitalized, immunosuppressed and elderly patients. The bacteria belonging to the critical priority group include *Acinetobacter baumannii*, *Pseudomonas aeruginosa*, some *Enterobacteriaceae* and *Enterobacter spp.* [1]. In the high priority group are the microorganisms *Enterococcus faecium* and *Staphylococcus aureus* [1]. And in the medium priority category are *Streptococcus pneumoniae* and *Shigella spp.* [1].

Among the species mentioned above, *P. aeruginosa* stands out for being an opportunistic pathogen, causing a series of nosocomial infections and resistant to antibiotics. *P. aeruginosa* is a Gram-negative aerobic bacterium that is present in most environments and can survive on different surfaces and in water [3]. This bacterial species causes ventilator-associated pneumonia (VAP), intensive care unit infections, central line-related bloodstream infections, surgical site infections, urinary tract infections, burn infections, keratitis, and otitis media. [3]. In addition to infections caused by planktonic cells, *P. aeruginosa* also forms biofilms, which causes serious damage to the host's health due to the enormous difficulty in treating this type of infection [3].

Another species of bacteria that we should pay attention to, despite not being on the "superbacteria" list, is *Staphylococcus saprophyticus*. *S. saprophyticus* is a Gram-positive bacterium classified as uropathogen, present in 10 – 20% of urinary tract infections (UTIs) and can lead to the development of complications such as acute pyelonephritis, urethritis and endocarditis [4]. This bacterium is present in the gastrointestinal tract, cervix, urethra, vagina, perineum, and rectum in humans, and in food-producing animals it colonizes the intestine and skin [4]. As reported for *P. aeruginosa*, *S. saprophyticus* also forms biofilms, generating more serious infection in the host.

One of the forms of resistance that bacteria acquire is the formation of biofilms. Biofilms are 10 to 1,000 times more resistant to the action of antibiotics than planktonic cells, which makes treatment more difficult and expensive [5]. Biofilms are clusters of bacterial cells that are united by a matrix composed of proteins, polysaccharides, and DNA, offering protection to cells that can develop different strategies to overcome the defense and escape the host's immune system [6]. Due to this protection provided by the matrix, biofilm-related diseases are persistent infections that are difficult to eradicate by the immune system itself, and treatments with antimicrobial agents are not very effective [6].

Considering all the above, there is an urgent need to develop promising alternative antimicrobial therapies to reduce the burden of drug-resistant bacterial infections caused by planktonic cells and biofilms. One class of bioactive compounds with a broad spectrum of biological activity and promising drug candidates are antimicrobial peptides (AMPs). AMPs are a diverse class of molecules, with more than 3,000 reported peptides (APD3, http://aps.unmc.edu/AP/), being obtained from natural, semi-synthetic or synthetic sources [7]. AMPs are low molecular weight

compounds (< 10KDa) made up of amino acid residues (10 – 50 aa), which generally have a net positive charge (+2 to +13), are amphipathic and classified according to their secondary structure into α-helix, β-sheet, or random coil peptides [7].

Antimicrobial peptides can act directly on microorganisms, damaging the membrane or acting on intracellular targets; but they can also act indirectly, recruiting immune system cells to combat invading microorganisms (Fig. 1 A) [7]. Cationic AMPs can interact with the membrane due to an initial electrostatic attraction. Thus, when AMPs interact with the bacterial membrane, they act in different ways, as they cause destabilization of the phospholipid bilayer. Due to the initial electrostatic interaction of the AMPs with the bacterial membrane, pores may be formed, which causes to leakage of intracellular material, leading to cell death (Fig. 1 B) [7]. Furthermore, they can penetrate the membrane and act on intracellular targets, preventing DNA replication, RNA synthesis, protein synthesis, cell wall synthesis, inhibiting the action of enzymes essential for maintaining the life of the microorganism (Fig. 1 B) [7].
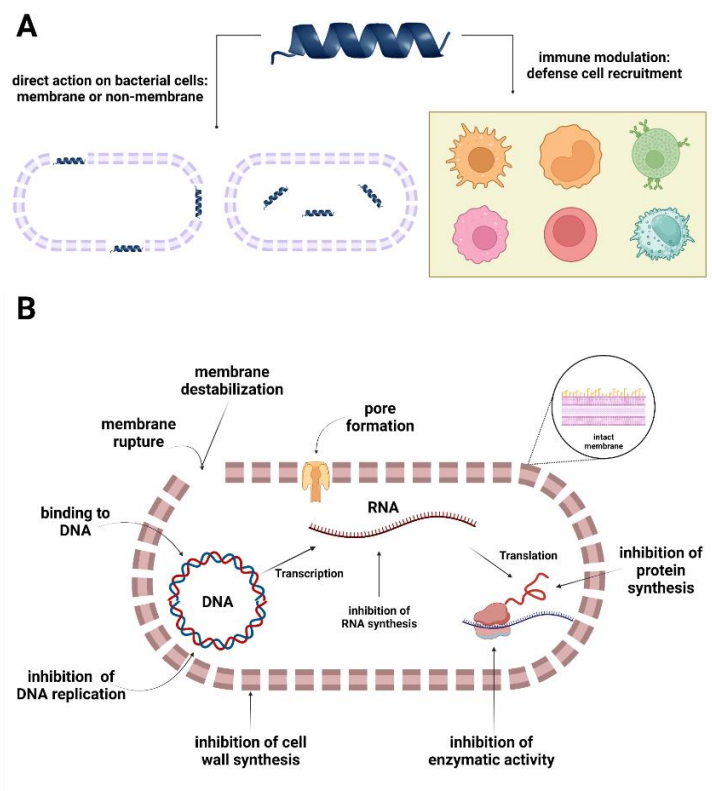
Figure 1 – AMPs modes of action. (A) AMPs can act directly on microorganisms or they can promote the recruitment of host immune system cells to combat invading cells. (B) AMPs that act directly on the cells of microorganisms can cause rupture or damage of the pathogens' membranes, thus releasing the intracellular content. Moreover, they can also act on intracellular targets, permeating the membrane, and inhibiting protein synthesis, inhibiting the action of enzymes, inhibiting cell wall synthesis, inhibiting DNA replication, among other activities essential for cell survival.

Due to the urgent threat of antibiotic resistance reported by the WHO and considering that antibiotics under development are ineffective against infections caused by "superbugs", we decided to explore the antibacterial potential of KWI-19. KWI-19 is a 19-amino acid peptide sequence designed using computational tools and modeled after a multifunctional plant-derived protein known as the *Inga laurina* trypsin inhibitor (ILTI) [8]. Computational modeling made it possible to obtain a peptide with the desired *in silico* physicochemical characteristics in relation to antimicrobial and stability properties. In addition, it has characteristics such as net charge of +6 and adopting an α-helix secondary structure. In studies previously carried out by our group,

we proved the antimicrobial potential of the peptide *in vitro* with the inhibition of the growth of eight (08) bacterial species (Gram-negative and Gram-positive) with MIC < 10.0 µmol L-1 and, also against the genus *Candida* spp.. Additionally, we also confirmed its antibiofilm potential against *Pseudomonas aeruginosa* and *Staphylococcus saprophyticus*, acting through the fungal cell membrane. Furthermore, KWI-19 did not show toxicity against *Galleria mellonela* larvae. In this context, the objective of the present work was to describe in more detail the antibacterial potential of the KWI-19 peptide.

2. MATERIALS AND METHODS

2.1. Access to genetic heritage

Access to the genetic heritage was registered in the National System for the Management of Genetic Heritage and Associated Traditional Knowledge (SISGEN), under number A315278.

2.2. In silico analyzes of biological activities

First, *in silico* analyzes of the potential biological activities of the KWI-19 peptide (H_2N–KWIRRIIRDYKKFFIKFII–COOH) were carried out through free online servers, with main emphasis on the antibacterial properties. To predict the antimicrobial activity and classify it, the ClassAMP server was used (http://www.bicnirrh.res.in/classamp/) [9, 10]; to predict the antibiofilm activity, the dPABBs server (http://ab-openlab.csir.res.in/abp/antibiofilm/protein.php) was used [11]; to predict the ability or not to penetrate cell membranes, the CellPPD server (http://crdd.osdd.net/raghava/cellppd/submission.php) was used [12, 13]; and to identify whether the peptide has activity against Gram-positive and/or Gram-negative bacterial species, the DBAASP server (https://dbaasp.org/tools?page=linear-amp-prediction) was used [14].

2.3. Engineered peptide synthesis

The KWI-19 peptide (sequence: H2N–KWIRRIIRDYKKFFIKFII–COOH) was synthesized through a chemical synthesis protocol according to the Fmoc solid phase methodology by the company AminoTech Research and Development. Verification of the molecular weights and the degree of purity (>95%) of the synthesized peptide was

performed using high performance liquid chromatography (HPLC) and matrix-assisted laser ionization and desorption mass spectrometry - time of flight (MALDI-TOF /MS).

2.4. Cultivation of bacterial cells

The bacterial species used were *Klebsiella pneumoniae* ATCC 13883, *Klebsiella aerogenes* ATCC 13048, *Escherichia coli* ATCC 35218, *Pseudomonas aeruginosa* ATCC 27853, Klebsiella oxytoca ATCC 13182, *Salmonella enterica* ATCC 51741, *Enterobacter cloacae* ATCC 13047 , *Acinetobacter baumani* ATCC 19606, *Proteus mirabilis* ATCC 12453 , *Serratia marcescens* ATCC 13880, *Staphylococcus saprophyticus* ATCC 49453, *Staphylococcus epidermidis* ATCC 12228, *Staphylococcus aureus* ATCC 29213, *Staphylococcus haemolyticus* ATCC 29970, and the resistant species was Methicillin Resistant *Staphylococcus aureus* (MRSA) ATCC 43300. Bacteria were kept as frozen stocks at –80 °C until use. For the assays, the bacterial species were inoculated in Mueller Hinton broth and incubated at 37 °C for 24 h. In sequence, the inoculation was performed in Mueller Hinton agar and incubated at 37 °C for 24 h and then the inoculum was prepared.

2.5. Tests for determination of MIC and CBM

The minimum inhibitory concentrations (MIC) of the KWI-19 peptide against bacteria were determined using the broth microdilution technique, according to the Clinical and Laboratory Standards Institute (CLSI) protocols [15]. KWI-19 was dissolved in sterile 0.9% sodium chloride solution and tested at concentrations ranging from 0.02 µmol L^{-1} to 10 µmol L^{-1}. Ciprofloxacin and vancomycin were used as positive controls in the assays. Muller Hinton broth culture medium, without the addition of any other agent, was used to check sterility. Bacterial inocula were prepared by suspending

colony forming units (CFU) of the tested species in sterile 0.9% saline solution and adjusting their optical density in the range of 0.08 to 0.1 at a wavelength of 595 nm. After that, 20 µL of this previously prepared suspension were diluted in 9,980 µL of Muller Hinton broth and 100 µL were transferred to the wells of a 96-well microplate (~1.5 x 10^5 cells mL^1). Then, 100 µL of culture medium containing KWI-19 were added. For positive controls, 100 µL of medium containing ciprofloxacin or vancomycin were added. For growth controls, 100 µL of culture medium alone were added. Untreated culture medium was used as sterility control. The 96-well microplate was then incubated for 24 h at 37 °C. After 24 h, the results were read visually, where the MIC was determined in the wells in which there was no growth of the microorganisms tested and the medium remained translucent. To determine the minimum bactericidal concentration (MBC), 10 µL aliquots from the wells where the MIC were determined were cultured on Muller Hinton agar plates, and incubated for 24 h at 37 °C. MBC was determined as the lowest concentration of the peptide and antibiotics where there was no visible growth in the solid medium.

2.6.   Determination of the Selectivity Index (I.S.) against bacterial cells

The Selectivity Index (S.I.) was calculated using the equation below, to verify whether the KWI-19 peptide is toxic at minimum inhibition concentrations against bacterial species. The higher the numerical value of the I.S., the more selective it is, that is, less toxic to healthy cells and more active against the target microorganism cell.

$$I.S. = \frac{HC_{50}}{CIM}$$

where,

HC_{50} = Hemolytic Concentration at 50%

MIC = Minimum Inhibitory Concentration

2.7. Time-dependent bactericidal activity

The bactericidal activity was evaluated in relation to the time of death of *P. aeruginosa* ATCC 27853 and *S. saprophyticus* ATCC 49453 species at their respective CBM [16]. Muller Hinton broth culture medium, without the addition of any other agent, was used to check sterility. Bacterial inocula were prepared by suspending CFU of bacterial species in sterile 0.9% saline solution and adjusting their optical density in the range of 0.08 to 0.1 at a wavelength of 595 nm. After that, 20 µL of the prepared suspensions of microorganisms were diluted in 9,980 µL of Muller Hinton broth, and then 100 µL were transferred to a microtube. In this same microtube, 100 µL of culture medium containing the KWI-19 peptide were added. Microtubes containing only the medium and the suspension of microorganisms were prepared for growth control. A 10 µL aliquot of each culture microtube was collected and transferred to Mueller Hinton agar plates at time intervals of 0, 30, 60, 90 and 120 min. After transferring the aliquots, they were spread using a Drigalski loop and then the plates were incubated for 24 h at 37 °C. After the incubation period, CFU were counted.

2.8. Crystal Violet Capture Assay

The change in permeability of the bacterial membrane was evaluated by the crystal violet test [17]. The bacterial strains of *P. aeruginosa* ATCC 27853 and *S. saprophyticus* ATCC 49453 had their inoculum prepared from CFU in sterile 0.9% saline solution and their optical density was adjusted in the range of 0.08 to 0, 1 at a wavelength of 595 nm. From this suspension, a 5 mL aliquot was centrifuged at 4,500 × g for 5 min at 4 °C. The bacterial pellet was washed twice, resuspended in PBS (pH 7.4) and adjusted to obtain 5×10^5 CFU mL^{-1}, and then 180 µL were transferred to a

96-well microplate. 20 µL of the peptide at MIC were added to each well. The bacterial growth control was prepared in a similar way, but without addition of the peptide. After incubation at 37 °C for 240 min, cells were collected by centrifugation at 9,300 × g for 5 min, resuspended in 180 µL of PBS containing 10 µg mL^{-1} of crystal violet and incubated for 10 min at 37 °C. The suspension was then centrifuged at 13,400 × g for 15 min and the pellet was discarded. The collected supernatant had its OD$_{570nm}$ reading performed in the microplate reader Varioskan Lux Microplate Reader (Thermo Scientific).

2.9. Nucleic acid release assay

The release of nucleic acids (DNA and RNA) into the extracellular medium was measured through the absorbance of the supernatant at OD$_{260nm}$ [18]. A bacterial inoculum of *P. aeruginosa* ATCC 27853 and *S. saprophyticus* ATCC 49453 was prepared with an OD$_{595nm}$ of 2.0. Cells were collected by centrifugation at 400 × g for 15 min, the supernatant discarded, and the pellet washed twice and resuspended in 0.9% saline. 20 µL of the peptide at MIC were added to cell suspensions (180 µL). The well without peptide was used as a growth control. After incubation at 37 °C for 240 min, centrifugation was performed at 13,400 × g for 15 min, cells were discarded and the OD$_{260nm}$ of the supernatant was determined using the microplate reader Varioskan Lux Microplate Reader (Thermo Scientific).

2.10. Bacterial plasma membrane permeability by fluorescence emission

Membrane permeability was investigated using the SYTOX^{TM} Green dye capture assay, as described by Mohanram & Bhattacharjya (2016), with modifications proposed by Almeida *et al.* (2021) [19, 20]. In the assay, suspensions of *P. aeruginosa*

ATCC 27853 and *S. saprophyticus* ATCC 49453 were cultivated in Muller Hinton broth for 18 h at 37°C and prepared at 0.5 (OD$_{595nm}$) in 10 mmol L^{-1} sodium phosphate buffer, pH 7.0. Then, 280 µL of the bacterial suspension were transferred to 96-well black microplates, where 10 µL of SYTOX^{TM} Green at 30 µmol L^{-1} were added and the plate was incubated for 10 min at 37 °C. Subsequently, 10 µL of the peptide, at a concentration 30 times greater than the MIC, were added to each well, and the kinetic assay was performed for 120 min, with readings every 5 min. The assay was performed with fluorescence reading, excitation at 485 nm and emission at 520 nm in a microplate reader Varioskan Lux microplate reader (Thermo Scientific). Negative control of membrane damage was performed with bacterial suspensions incubated with 10 µL of 10 mM sodium phosphate buffer, pH 7.0.

2.11. Synergistic effect of KWI-19 peptide with ciprofloxacin and vancomycin

To reduce the amount of peptide and antibiotics used, and enhance the action of these substances, synergism tests using the Checkerboard method were performed [21]. The activities of KWI-19+ciprofloxacin and KWI-19 + vancomycin were evaluated against *P. aeruginosa* ATCC 27853 and *S. saprophyticus* ATCC 49453, respectively. 96-well microplates were prepared with serial dilution, starting from MIC (KWI-19 horizontally and antibiotics vertically). After that, a new 96-well microplate was prepared with 50 µL of the KWI-19 dilution and another 50 µL of the antibiotic dilution. Afterwards, 100 µL of the bacterial suspension prepared above were added as described in the MIC determination assay. After 24 h at 37 °C, a visual reading was performed and the wells in which there was total inhibition of fungal growth were determined. After obtaining the data, calculations were made to determine the FIC$_{(KWI-19)}$ and FIC$_{(antibiotic)}$, and then the determination of the $\sum$FIC, using the equations below:

$$FIC_{(KWI-19)} = \frac{MIC_{combination}}{MIC_{individual}}$$

$$FIC_{(antibiotic)} = \frac{MIC_{combination}}{MIC_{individual}}$$

$$\sum FIC = FIC_{(KWI-19)} + FIC_{(antibiotic)}$$

2.12. Inhibition and eradication of bacterial biofilms

The effects of KWI-19 on bacterial biofilms were evaluated against *P. aeruginosa* ATCC 27853 and *S. saprophyticus* ATCC 49453, according to Coffey and Anderson (2014) [25]. The KWI-19 peptide was dissolved in a sterile 0.9% NaCl solution at 1.25 µmol L^{-1}. Ciprofloxacin and vancomycin were used as positive controls. BHI broth culture medium supplemented with 1% glucose was used as a sterility control. Bacterial inocula were prepared by suspending microorganisms in sterile 0.9% saline and adjusting their OD from 0.08 to 0.1 at 595 nm. A 1:10 dilution (inoculum: culture medium) was prepared. For the biofilm formation inhibition assay, 170 µL of BHI broth medium supplemented with 1% glucose, 20 µL of bacterial cell suspension (1:100 dilution), and 10 µL of peptide solution were placed in a well from a 96-well microplate and incubated for 24 h at 37 ° C. For the mature biofilm eradication assay, 180 µL of BHI broth supplemented with 1% glucose and 20 µL of bacterial suspension were added and then incubated for 24 h at 37 °C. After incubation, the supernatant was removed and 190 µL of BHI broth supplemented with 1% glucose and 10 µL of peptide were added. After 24 h at 37 °C, the supernatant was removed, the wells were washed and 125 µL of 0.1% crystal violet solution were added and incubated for 10 min. The supernatant was aspirated, the wells were washed twice with distilled water

125

and the microplate was allowed to dry at room temperature for 2 h. The biofilm was dissolved in 150 µL of a 30% acetic acid solution and the OD was determined at 550 nm in a Varioskan Lux microplate reader (Thermo Scientific).

2.13. Viability test of cells present in bacterial biofilm

To analyze the viability of cells from the biofilms of *P. aeruginosa* ATCC 27853 and *S. saprophyticus* ATCC 49453, an assay was performed in which, after treatment of the biofilm with peptide, plating and CFU mL^{-1} counts were performed. Initially, 200 µL of the bacterial suspension was added to the wells of a 96-wells microplate. The bacterial suspension was prepared as described in the MIC determination assay. The microplate was then incubated at 37°C statically for 2 h. After that time, the supernatant was carefully removed and the respective treatments (KWI-19 peptide or vancomycin or ciprofloxacin) were added to BHI broth supplemented with 1% glucose at MIC, for each substance tested. Then, the microplate was incubated for 24 h at 37 °C. After the treatment time, the supernatant was carefully removed, and the wells were washed twice with 0.9% saline solution. After washing, 50 µL of 0.9% saline solution were added and the biofilms adhered to the wells were scraped off using the tip of a micropipette. This 50 µL volume was then transferred to a microtube containing 450 µL of saline solution and a 10-fold serial dilution was performed, after which 10 µL of each new suspension was cultured in BHI agar and the plates were incubated for 24 h at 37 °C. After the incubation time, the CFU were counted, and the percentage of biofilm survival was quantified, based on the amount of CFU mL^{-1}. For the biofilm eradication assay, the process was similar, differing only in the first period of static incubation, which lasted 24 hours and used BHI broth supplemented with 1% glucose.

2.14. Effects of the KWI-19 peptide on bacterial biofilms using fluorescence microscopy

The assay was performed in a sterile 24-well microplate containing a removable circular coverslip at the bottom. Initially, 500 µL of bacterial suspension in 0.9% saline solution with optical density of 0.1 at 595 nm, were added and incubated for 2 h at 37 °C for pre-adhesion (in the eradication assay, the suspension was prepared in BHI broth supplemented with 1% glucose for a period of 24h). Then, the supernatant was removed and 500 µL of BHI broth supplemented with 1% glucose was added and used as a biofilm growth control. Other wells were treated with 500 µL of BHI broth, supplemented with 1% glucose and the KWI-19 peptide or ciprofloxacin or vancomycin. The microplate was incubated for 24 hours at 37 °C. Non-adherent cells were washed off the coverslip using 500 µL of sterile 0.9% saline. The Live/DEAD BacLight kit (InvitrogenTM) was used to investigate the viability of the biofilm, where the manufacturer's instructions were followed. Coverslips were incubated with 500 µL of SYTO9/Propidium Iodide (PI) for 10 min at 37 ºC, under low light. The excess dye was washed in 0.9% saline solution and the cover slip was analyzed in a Leica DM 2000 LED microscope, equipped with a Leica DFC 7000 camera (SYTO9: excitation at 490 nm and emission at 520 nm; PI: excitation at 490 nm and emission at 635 nm). Images were analyzed using the LAS V4.12 software.

2.15. Preparation of vesicles for circular dichroism studies

To carry out the peptide-membrane interaction studies, vesicles (LUVs – large unilamellar vesicles) of different lipid compositions were used. In the present work, the following lipids were used: 1-palmitoyl-2-oleoyl-sn-glycero-3-phosphocholine (POPC), 1-palmitoyl-2-oleoyl-sn-glycero-3-phospho(1-rac-glycerol)   (POPG),   2-oleoyl-1-

palmitoyl-sn-glycero-3-phospho-L-serine (POPS) and cholesterol, which were duly weighed and dissolved in 1 mL of chloroform/methanol (1:4) and evaporated under N_2 flow until the complete drying of the solution, allowing the formation of a thin lipid film on the tube wall. Subsequently, the residual solvent was eliminated under vacuum for 12 hours, and resuspended (with phosphate buffer) until the formation of a homogeneous suspension of multilamellar vesicles. The solution was subjected to 6 freeze-thaw cycles, and then subjected to the extrusion technique through polycarbonate membranes with a pore size of 100 nm for 15 cycles. The homogeneity and size of the LUVs were verified by DLS - Dynamic light scattering (Malvern instruments).

2.16. Studies of Circular Dichroism (CD)

CD analyzes were performed on a Jasco J-815 spectropolarimeter (Jasco Inc., Japan), using a quartz cuvette with a 0.1 cm optical path [22, 23, 24]. Spectra were collected over a wavelength range of 190-280 nm, with 0.5 nm step resolution at 100 nm/s, at 30°C, and an average was obtained from 12 scans for each spectrum. The KWI-19 peptide was prepared in a 40 µmol L^{-1} aqueous solution and subjected to analysis in the presence of LUVs, which were used as a membrane models in four different systems: POPG/POPC (3:1), POPC, POPS/POPC (3:1) and POPC/Chol (3:1) in the peptide:lipid ratio of 1:10. The data obtained in were converted into residual molar ellipticity [θ] according to the equation:

$$[\theta] = \frac{\theta}{10 * C * l * n_r}$$

2.17. Statistical analysis

The results were expressed as the mean ± standard deviation (SD). The analysis of variance were performed by One way-ANOVA, followed by Dunnett's or

Tukey's multiple comparison posttest, to compare the groups. Results were performed with the software GraphPad Prism version 8.0.0 for Windows, GraphPad Software, San Diego, California, USA.

3. RESULTS

In silico analysis

From the primary sequence of KWI-19 and using free online servers, it was possible to predict biological activities. Through the analyzes we verified that the peptide has potential antibacterial and antibiofilm activity (both Gram-positive and Gram-negative) and is also capable of penetrating cell membranes (Table 1).

Table 1 – *In silico* prediction of the biological activities of the KWI-19 peptide.

Properties	Server	Prediction	Score Prediction
Antimicrobial	ClassAMP	Antibacterial	0,934
Antibiofilm	dPABBs	Biofilm-active	0,71
Probability of cell penetration	CellPPD	CPP	0,03
Antimicrobial (strain type: *Pseudomonas aeruginosa* ATCC 27853)	DBAASP	Active	0,91
Antimicrobial (strain type: *Staphylococcus aureus* ATCC 25923)	DBAASP	Active	0,76

Antibacterial activity on planktonic cells

The antibacterial activity assays revealed that the antibacterial action of KWI-19 peptide was against 13 bacteria, out of 15 tested (Table 2). MIC and MBC concentrations ranged from 1.25 µmol L^{-1} to 10 µmol L^{-1}. The maximum concentration evaluated against bacteria was 10.0 µmol L^{-1}. The hemolytic activity assay was performed as reported by Almeida and collaborators [8]. The HC$_{50}$ of KWI-19 was shown to compromise 50% of erythrocytes at a concentration of 6.5 µmol L^{-1}.

From the HC$_{50}$ value and the determined MIC values, it was possible to calculate the Selectivity Index (S.I.) for each of the tested species. It was possible to observe

that KWI-19 presents greater selectivity for bacterial cells than for erythrocyte cells (Table 2).

Table 2 – Minimum Inhibitory Concentration (MIC), and Minimum Bactericidal Concentration (MBC) values for the KWI-19 peptide, ciprofloxacin, and vancomycin, as well as their selective indexes (S.I.) against Gram-negative and Gram-positive bacteria.

Gram-negative bactéria

Species	ATCC	Peptideo KWI-19 (μmol L^{-1})		Ciprofloxacin (μmol L^{-1})		S.I.
		MIC	MBC	MIC	MBC	(MIC/HC$_{50}$)
Klebsiella pneumoniae	13883	5.0	5.0	0.0625	0.0625	1.3
Klebsiella aerogenes	13048	2.5	2.5	0.0625	0.125	2.6
Escherichia coli	35218	1.25	2.5	< 0.0156	0.125	5.2
Pseudomonas aeruginosa	27853	1.25	2.5	0.5	1.0	5.2
Klebsiella oxytoca	13182	2.5	2.5	0.0625	0.0625	2.6
Salmonella enterica	51741	1.25	1.25	0.0625	0.0625	5.2
Enterobacter cloacae	13047	2.5	2.5	0.0625	0.125	2.6
Acinetobacter baumani	19606	2.5	5.0	1.0	8.0	2.6
Proteus mirabilis	12453	>10.0	>10.0	4.0	8.0	-
Serratia marcescens	13880	>10.0	>10.0	0.5	4.0	-

Gram-positive bactéria

Species	ATCC	Peptide KWI-19 (μmol L^{-1})		Vancomycin (μmol L^{-1})		S.I.
		MIC	MBC	MIC	MBC	(MIC/HC$_{50}$)
Staphylococcus saprophyticus	49453	1.25	2.5	0.68	0.68	5.2
Staphylococcus epidermidis	12228	2.5	2.5	1.36	1.36	2.6
Staphylococcus aureus	29213	5.0	5.0	0.68	0.68	1.3
Staphylococcus haemolyticus	29970	>10.0	>10.0	> 43.5	–	-
MRSA	43300	5.0	5.0	> 43.5	–	1.2

Due to the results obtained and the importance in the emergence of new compounds with effective antibacterial potential, whe chose the species *P. aeruginosa* ATCC 27853 and *S. saprophyticus* ATCC 49453 to continue investigating the action of the KWI-19 peptide. For these species, time-dependent assays were carried out, which allows identifying the kinetics of action of the peptide, that is, how long it takes to act against these microorganisms. As result, the counted CFU proved that KWI-19 inhibits bacterial growth within 30 min for *S. saprophyticus* and 120 minutes for *P. aeruginosa* (Table 3), compared to the control group.

Table 3 – Time-dependent bactericidal activity of the KWI-19 peptide at a concentration of 2.5 µmol L^{-1} against *P. aeruginosa* ATCC 27853 and *S. saprophyticus* ATCC 49453.

Time	*P. aeruginosa* ATCC 27853		*S. saprophyticus* ATCC 49453	
	Growth Control	Treatment with KWI-19	Growth Control	Treatment with KWI-19
0	>2.10^4 CFU.ml^{-1}	>2.10^4 CFU.ml^{-1}	>2.10^4 CFU.ml^{-1}	7.8 .10^3 CFU.ml^{-1}
30	>2.10^4 CFU.ml^{-1}	5.7 .10^3 CFU.ml^{-1}	>2.10^4 CFU.ml^{-1}	0 CFU.ml^{-1}
60	>3.10^4 CFU.ml^{-1}	1.5 .10^3 CFU.ml^{-1}	>3.10^4 CFU.ml^{-1}	0 CFU.ml^{-1}
90	>3.10^4 CFU.ml^{-1}	1.2 .10^3 CFU.ml^{-1}	>3.10^4 CFU.ml^{-1}	0 CFU.ml^{-1}
120	>3.10^4 CFU.ml^{-1}	0 CFU.ml^{-1}	>3.10^4 CFU.ml^{-1}	0 CFU.ml^{-1}

The action of the KWI-19 peptide in inhibiting the formation and eradication of monospecies biofilms of *P. aeruginosa* and *S. saprophyticus* was also carried out. In this assay, we found that the KWI-19 peptide inhibited the formation of *P. aeruginosa* and *S. saprophyticus* biofilms by 84.3% and 62.1%, respectively, at 1 x MIC (Figure 2A and Figure 3A). The treatment with the antibiotic used as a positive control presented inhibition of 40.5% and 55.2% for *P. aeruginosa* and *S. saprophyticus*, respectively. In the mature biofilm eradication assay, it was found that the KWI-19 peptide caused the disruption of *P. aeruginosa* and *S. saprophyticus* biofilms by 85.3% and 6.1%, respectively, at a concentration of 1 x MIC (Figure 2B and Figure 3B), while the antibiotic showed eradication of 44.6% and 16.3% for *P. aeruginosa* and *S. saprophyticus*, respectively.

When determining the biofilm cell viability, it was found that KWI-19 compromised *P. aeruginosa* and *S. saprophyticus* biofilm constituting cell viability by 40.5% and 40.6%, respectively (Figure 2C and Figure 3C), when compared to the control, which showed impaired viability in 33.3% and 12.2% of *P. aeruginosa* and *S. saprophyticus* cells, respectively. In the eradication test, KWI-19 eliminated mature biofilm by 23.28% and 48.0% for the same species, respectively (Figure 2D and Figure 3D). Ciprofloxacin was able to reduce the viability of *P. aeruginosa* cells 22.2%, and Vancomycin compromised 48.5% of *S. saprophyticus* cells.

In addition, previously data are corroborated by the qualitative tests carried out with fluorescence microscopy. In all the concentrations tested, for both, inhibition of biofilm formation and eradication of mature biofilm, there is a difference between the KWI-19 treatment compared to the growth control (Figures 2E and F; Figures 3E and F).
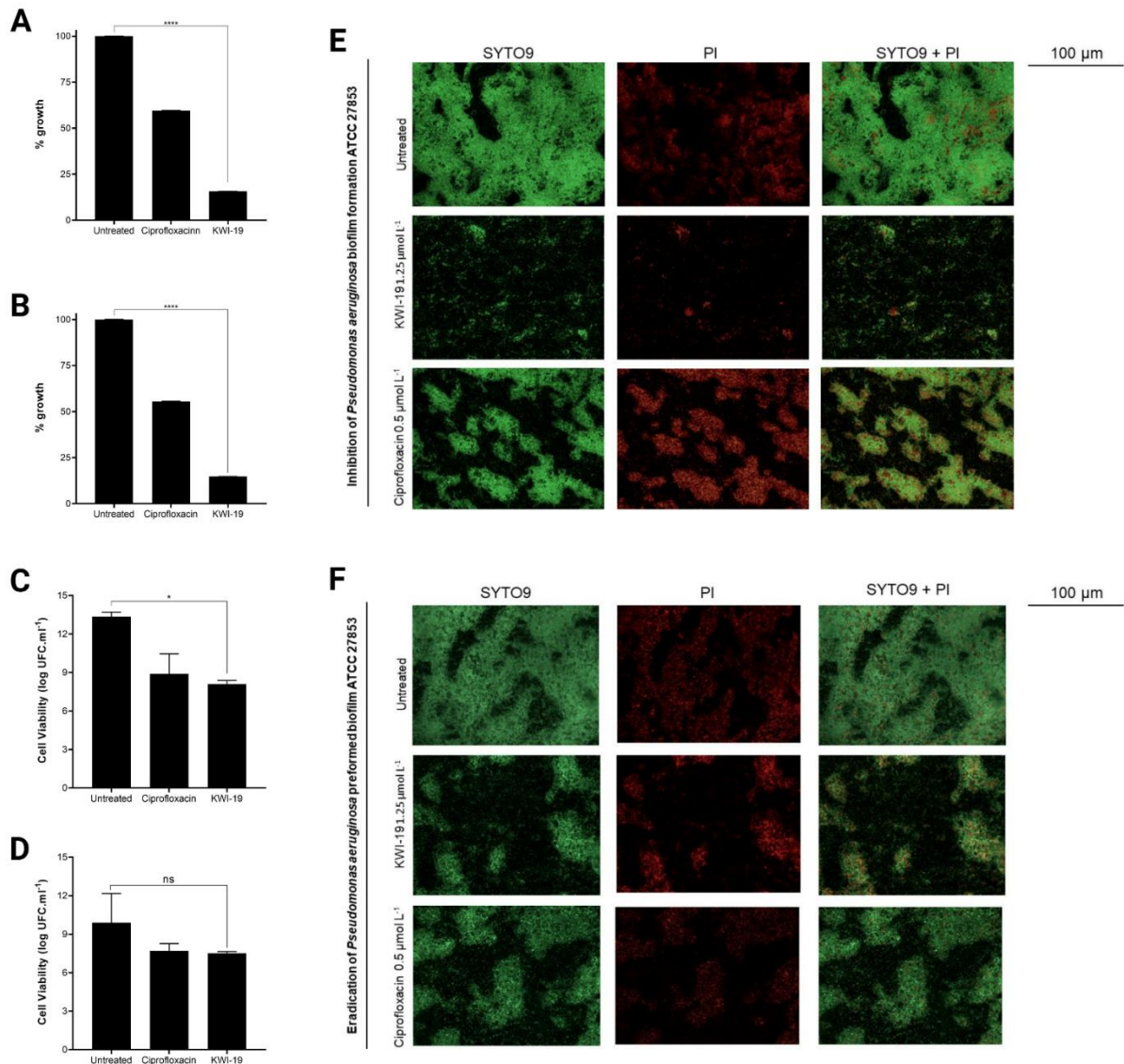

Figure 2 – Qualitative and quantitative analysis of the *P. aeruginosa* biofilm. (A) Quantitative analysis of the inhibitory effects of KWI-19 on biofilm formation; (B) Effects of KWI-19 on mature biofilm eradication; (C) Quantitative analysis of the effects of KWI-19 on cell viability in biofilm formation; (D) Quantitative analysis of the effects of KWI-19 on cell viability in biofilm eradication; (E) Qualitative analysis by fluorescence microscopy of inhibition of biofilm formation; (F) Qualitative fluorescence microscopy analysis of mature biofilm eradication. 40x magnification. Viable cells stain green and

non-viable cells stain red. (Common one-way ANOVA analysis, with 95% confidence. $p < 0.05 = *$; $p < 0.002 = **$; $p < 0.0002 = ***$ and $p < 0.0001 = ****$).
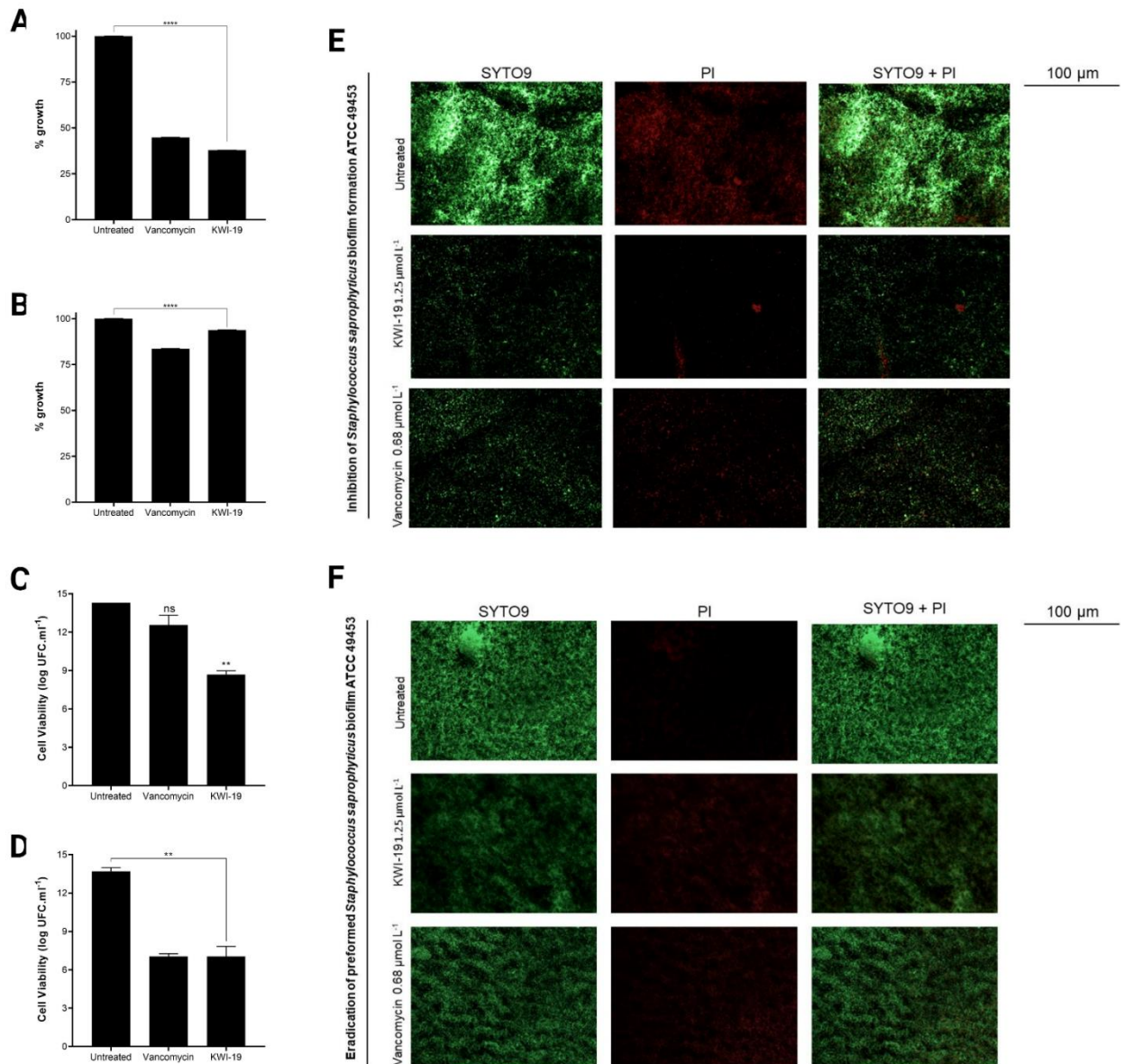

Figure 3 – Qualitative and quantitative analysis of the *S. saprophyticus* biofilm. (A) Quantitative analysis of the inhibitory effects of KWI-19 on biofilm formation; (B) Effects of KWI-19 on mature biofilm eradication; (C) Quantitative analysis of the effects of KWI-19 on cell viability in biofilm formation; (D) Quantitative analysis of the effects of KWI-19 on cell viability in biofilm eradication; (E) Qualitative analysis by fluorescence microscopy of inhibition of biofilm formation; (F) Qualitative fluorescence microscopy analysis of mature biofilm eradication. 40x magnification. Viable cells stain green and non-viable cells stain red. (Common one-way ANOVA analysis, with 95% confidence. $p < 0.05 = *$; $p < 0.002 = **$; $p < 0.0002 = ***$ and $p < 0.0001 = ****$).

The synergistic effect of KWI-19 with ciprofloxacin and vancomycin against *P. aeruginosa* and *S. saprophyticus* was performed. As a result, it can be seen in Table 4 that the association of the peptide with the antibiotics resulted in a synergistic action.

Table 4 – Values of the individual MIC and the combination of the KWI-19 peptide with ciprofloxacin and vancomycin and their respective activities.

Bacteria	Combination	Individual MIC (μmol L^{-1})		Combination MIC (μmol L^{-1})		Σ FIC	Activity
		A	b	A	B	FIC$_A$+FIC$_B$	
S. saprophyticus	KWI-19 (a) + vancomycin (b)	1,25	0,68	0,15	0,08	0,23	Synergistic
P. aeruginosa	KWI-19 (a) + ciprofloxacin (b)	1,25	0,5	0,31	0,12	0,5	Synergistic

Mechanism of action assays

We also investigated whether the KWI-19 peptide has a direct action on the cell membrane. For this, crystal violet uptake, nucleic acid release and membrane permeability assays with SYTOX^{TM} Green were performed. In the crystal violet uptake assay, we observed that when treated with KWI-19 a higher percentage of crystal violet remained present in the medium, that is, there are more cells with membrane damage that did not allow the uptake of crystal violet (Figure 4 A and D). In the nucleic acid release assay, it was observed that there is a greater amount of DNA and RNA in the extracellular environment (Figure 4 B and E), corroborating the results obtained in the crystal violet uptake assay. In the membrane permeability assay, we verified at what point there was 100% of cell death and whether it could have been caused by disturbances in the bacterial membranes. KWI-19 was found to be a peptide that interacts with the membrane of *P. aeruginosa* and *S. saprophyticus*, causing extravasation of intracellular material in 120 min and 30 min, respectively (Figure 4 C and F). These time intervals support the findings in the time-dependent test and the action corresponding to what was verified in the tests described previously.

With the purpose of seeking additional information about the mode of interaction of peptides with membranes, CD experiments were performed using LUVs as membrane models in four different systems: POPC, POPG/POPC (3:1), POPS/POPC (3 :1) and POPC/Chol (3:1). According to the results presented in Figure 4G, it can be observed that the peptide has the ability to adopt a well-defined structure in the presence of LUVs containing POPG and POPS, in which the spectra show well-defined bands at 190, 208 and 222 nm, characteristic of α-helix. However, the spectra indicate that there is a tendency for the peptide to reduce its ability to adopt a secondary helical structure when in the presence of LUVs containing only POPC or POPC/cholesterol in its composition. This behavior could be correlated with the peptide interaction dynamics and by the nature of the phospholipids and their charges, as well as the curvature angle of the different membrane models.
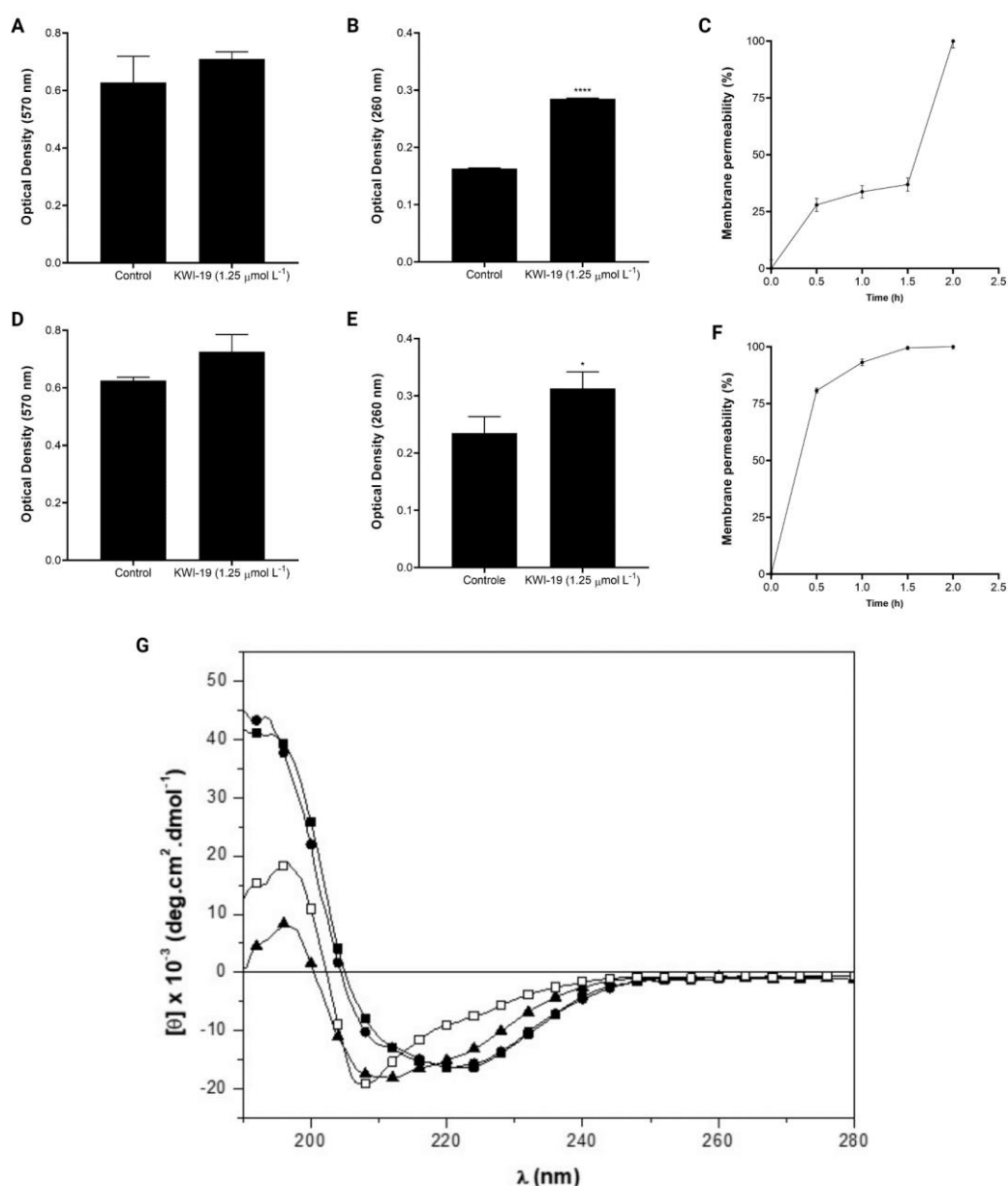
Figure 4 – KWI-19 peptide modes of action. (A) *P. aeruginosa* violet crystal uptake; (B) Release of nucleic acids from *P. aeruginosa*; (C) Membrane permeability of *P. aeruginosa* with SYTOX green; (D) Crystal violet capture from *S. saprophyticus*; (E) Release of nucleic acids from *S. saprophyticus*; (F) Membrane permeability of *S. saprophyticus* with SYTOX green; (G) Circular dichroism spectra of the LWI-19 peptide at 40 µmol L^{-1} in the presence of POPG/POPC (3:1) (■), POPS/POPC (3:1) (●), POPC (▲) and POPC:Chol (3:1) (□) pH 7,2 the 30 °C.

4. DISCUSSION

Due to the inappropriate, prolonged, and abusive use of traditional antibiotics, bacterial resistance to drugs available for clinical use has become a serious public health problem worldwide, and one of the greatest current difficulties is to find new agents that fight these microorganisms with efficiency and safety [27]. An AMP called KWI-9, which has previously described antifungal activity, was evaluated for antibacterial activity against planktonic cells and biofilm. In this work, we evaluate and describe the mode of action of this peptide against Gram-negative and Gram-positive bacteria. AMPs are a very advantageous option for new antibacterial agents due to their broad-spectrum activity, acting on Gram-negative and Gram-positive bacteria. Its effect is also described against infections caused by biofilms, which is one of the most difficult defense mechanisms for antibacterial agents to overcome [7]. Numerous peptides are currently in various stages of development and analysis within clinical trials. Regarding infections caused by bacteria from the *Staphylococcus* genus, several noteworthy peptides are in the process of development. These include Nisin, which is being explored for the treatment of ventilation-associated pneumonia; LL-37, being investigated for venous ulcers that are challenging to heal; OP-145, aimed at chronic suppurative otitis media; PMX-30063, targeted at acute bacterial skin infections caused by Staphylococcus aureus MRSA; LTX-109, focusing on persistent carriers of nasal *S. aureus*; and PLG0206, designed for periprosthetic joint infections, among other antimicrobial peptides [28].

In addition to these, other peptides are being studied with a wide diversity of biological activities and distinct modes of action. For example, the LL-37 peptide, which is already undergoing clinical trials in infections caused by bacteria of the genus *Staphylococcus*, has also been studied against Gram-negative bacteria, among other species of *P. aeruginosa*, one of the most difficult opportunistic bacteria [29]. The LL-

37 peptide, in the study carried out by Han and collaborators, was tested with two species of *P. aeruginosa*, ATCC 15962 and ATCC 29260, and presented a MIC of 64 and 32 µg mL^{-1}, respectively [29]. Furthermore, it was found that LL-37 when combined with the antibiotics vancomycin, azithromycin, polymyxin B and colistin, presented a synpergic effect and caused strong permeabilization of the outer membrane, as demonstrated by measuring an increased uptake of the fluorescent probe N-phenyl-1 -naphthylamine [29]. Acting against *P. aeruginosa* species, we also found that other peptides have already had their antibacterial activity described. We highlight Sp-LECin and adepamycin, as they presented low MIC values, 12 – 24 µmol L^{-1} and 2.8 µmol L^{-1}, respectively [30, 31].

Comparing the values of these peptides described in the previous paragraph, KWI-19 showed a superior antibacterial activity, since its MIC was 1.25 µmol L^{-1} for *S. saprophyticus*. However, regarding our knowledge about research in the literature, we did not find peptides that showed activity against this bacterial species, therefore, it is not possible to establish a direct comparison. But, when comparing the MIC of *Staphylococcus spp.,* KWI-19 had activity with those found in the literature, we can see that KWI-19 has a potent antibacterial activity, since its MIC range was between 1.25 - 5.0 µmol L^{-1}, whereas the peptides described in this article, that are already in the clinical test phase, presented MIC in the range of 0.62 – 128 µmol L^{-1}. To make this new antibacterial agent a future medicine for clinical use, safety studies are still needed. This potent antibacterial agent was tested and it was found that KWI-19 has a greater affinity for bacterial cells than for healthy cells. For *P. aeruginosa* and S. *saprophyticus* species, the peptide had a selectivity index of 5.2 for both species.

In addition to exhibiting antibacterial activity alone, it was found that when combined with the antibiotics ciprofloxacin and vancomycin, KWI-19 showed

synergistic effect in its activity against *P. aeruginosa* and *S. saprophyticus* species. For *P. aeruginosa*, KWI-119 was tested with ciprofloxacin and showed a 2X reduction in the MIC of both KWI-19 and ciprofloxacin. For *S. saprophyticus*, KWI-19 was tested in combination with vancomycin and there was a 3x reduction in the KWI-19 MIC of vancomycin. The strategy of combining peptides and antibiotics aims to reduce the amount of substances to be used, and this becomes beneficial, as it is capable of reducing the hemolytic and/or cytotoxic activity that most AMPs present [21]. As an example, the LL-37 peptide demonstrated synergistic effects when used in combination with several antibiotics commonly used in clinical practice. These antibiotics, which are peptides, include gentamicin, colistin, vancomycin, azithromycin and polymyxin-B. This synergy not only reduces the required dosage of both the peptide and antibiotics, but also minimizes potential toxic side effects. Furthermore, it contributes to the conservation of resources in the production of substances, preserving the biological activity of these agents [29]. The synergistic effect can be of the peptide with another antibiotic or with some type of biomaterial, not restricted only to infections caused by planktonic cells, but the combination resource can be used to act against bacterial biofilms [32]. Among the combinations found in the literature to combat the *P. aeruginosa* biofilm, we found the AMPs Nisin with colistin, tridecaptin B with rifamcipin, lactoferricin with ciprofloxacin or ceftazidime, among other combinations [32].

Regarding antibiofilm activity, KWI-19 was highly effective in combating the formation and eradication of the P. aeruginosa biofilm, which we can verify qualitatively in the fluorescence microscopy images, as well as quantitatively in the test with crystal violet, inhibiting the formation of biofilm. With the species *S. saprophyticus*, KWI-19 showed the same activity as the antibiotic vancomycin and was not as effective in

inhibiting the formation or eradication of *S. saprophyticus* biofilms. In the study carried out by Wang and collaborators, a new AMP, called PEW300, had its antibiofilm properties analyzed against *P. aeruginosa*, where it was verified that this peptide showed strong antibiofilm activity against *P. aeruginosa*, inhibiting biofilm formation by 98% when treated with 20 µg ml-1 (5.01 µmol L-1) of PEW300 [33]. Regarding the eradication of *P. aeruginosa* biofilm, PEW300 eradicated 95% of the biofilm at a concentration of 50 µg ml-1 (12.52 µmol L-1) [33]. Comparing these results with those described in this study, we found that KWI-19 had significant antibiofilm potential, as it inhibited and eradicated 84.3% and 85.3% of *P. aeruginosa* biofilm, with a concentration of 1.25 µmol L-1. In planktonic cells, the likely mechanism of action for the KWI-19 peptide involves membrane damage. This is strongly supported by evidence from crystal violet uptake, nucleic acid release, and membrane permeability assays. Furthermore, the circular dichroism technique revealed that KWI-19 adopts its most stable conformation, the α-helix. AMPs adopt their most stable conformation when they are in an environment that favors this (hydrophobic-membrane environment) and this was possible after the peptide (charge +6) had an initial electrostatic attraction with the bacterial cell membrane, which is negatively charged [27].

5. CONCLUSION

AMPs offer an efficient alternative in the fight against bacterial infections, particularly those caused by resistant microorganisms. In the present work, we demonstrated the efficacy of a peptide derived from a peptidase inhibitor found in *Inga laurina* seeds (ILTI). This peptide has previously shown anti-*Candida* activity (*in vitro*), and our data proved it to be a potent antibacterial and antibiofilm agent against *P.*

aeruginosa. Its mechanism of action, like most AMPs described in the literature, is directly on the membrane, causing the leakage of intracellular material, which leads to bacterial cell death. Therefore, KWI-19 is a promising agent in combating bacterial infections, and studies must be carried out in order to prove the same potential *in vivo.*

COMPETING INTERESTS

The authors declare that there are no conflicting interests or personal relationships that could influence the work described in this article.

ETHICAL APPROVAL

Not required.

6. REFERENCES

1 - MANCUSO, G.; MIDIRI, A.; GERACE, E.; BIONDO, C. Bacterial Antibiotic Resistance: The Most Critical Pathogens. *Pathogens,* 2021. DOI: doi.org/10.3390/pathogens10101310

2 - Antimicrobial Resistance Collaborators. **Global burden of bacterial antimicrobial resistance in 2019: a systematic analysis.** *Lancet*, 399: 629-655; 2022.

3- TUON, F.F.; DANTAS, L.R.; SUSS, P.H.; TASCA RIBEIRO, V.S. Pathogenesis of the *Pseudomonas aeruginosa* Biofilm: A Review. *Pathogens,* 2022, *11*, 300. DOI: https://doi.org/10.3390/pathogens11030300

4 – LAWAL, O. U.; BARATA, M.; FRAQUEZA, M. J.; WORNING, P.; BARTELS, M. D.; GONCALVES. L.; PAIXÃO, P.; GONCALVES, E.; TOSCANO, C.; EMPEL, J.; URBAŚ, M.; DOMIÌNGUEZ, M. A.; WESTH, H.; DE LENCASTRE, H.; MIRAGAIA, M. *Staphylococcus saprophyticus* From Clinical and Environmental Origins Have Distinct Biofilm Composition. *Front. Microbiol.,* 2021. DOI: 10.3389/fmicb.2021.663768

5 - LIU, S.; LU, H.; ZHANG, S.; SHI, Y.; CHEN, Q. Phages against Pathogenic Bacterial Biofilms and Biofilm-Based Infections: A Review. *Pharmaceutics, 2022*. DOI: https://doi.org/10.3390/pharmaceutics14020427

6 - VESTBY, L.K.; GRØNSETH, T.; SIMM, R.; NESSE, L.L. Bacterial Biofilm and its Role in the Pathogenesis of Disease. *Antibiotics,* 2020. DOI: https://doi.org/10.3390/antibiotics9020059

7 - CHEN N, JIANG C. Antimicrobial peptides: Structure, mechanism, and modification. *Eur J Med Chem.* 2023. DOI: 10.1016/j.ejmech.2023.115377. Epub 2023 Apr 20. PMID: 37099837.

8 – ALMEIDA, L. H. O.; RAMALHO, S. R.; ALMEIDA, C. V.; GUTIERREZ, C. O.; SARDI, J. C. O.; MIRANDA, A.; OLIVEIRA, R. A.; REZENDE, S. B.; CRUSCA, E.; FRANCO, O. L.; OLIVEIRA, C. F. R.; CARDOSO, M. H.; MACEDO, M. L. R. A potent candicidal peptide designed based on an encrypted peptide from a proteinase inhibitor. *BBA - General Subjects*, 2023.

9 - JOSEPH, S; KARNIK, S; NILAWE, P; VALADI, J; IDICULA-THOMAS, S. ClassAMP: A Prediction Tool for Classification of Antimicrobial Peptides. *IEEE/ACM transactions on computational biology and bioinformatics*, 2012. DOI: 10.1109/TCBB.2012.89.

10 - WAGHU, F. H.; IDICULA-THOMAS, S. Collection of antimicrobial peptides database and its derivatives: Applications and beyond. *Protein Science*, 2019. DOI: 10.1002/pro.371436

11 - SHARMA, A.; GUPTA, P.; KUMAR, R. *et al.* dPABBs: A Novel *in silico* Approach for Predicting and Designing Anti-biofilm Peptides. *Sci Rep*. **,** 2016. DOI: 10.1038/srep21839

12 - GAUTAM, A.; CHAUDHARY, K.; KUMAR, R. *et al. In silico* approaches for designing highly effective cell penetrating peptides. *J Transl Med*. 2013. DOI: 10.1186/1479-5876-11-74

13 - GAUTAM, A.; CHAUDHARY, K.; KUMAR, R.; RAGHAVA, G. P. S. Computer-Aided Virtual Screening and Designing of Cell-Penetrating Peptides. In: Langel, Ü. (eds) Cell-Penetrating Peptides. *Methods in Molecular Biology*. Humana Press, 2015. DOI: 10.1007/978-1-4939-2806-4_4

14 - PIRTSKHALAVA, M.; AMSTRONG, A. A.;GRIGOLAVA, M.; CHUBINIDZE, M.; ALIMBARASHVILI, E.; VISHNEPOLSKY, B.; GABRIELIAN, A.; ROSENTHAL, A.; HURT, D. E.; TARTAKOWSKY, M. DBAASP v3: database of antimicrobial/cytotoxic activity and structure of peptides as a resource for development of new therapeutics. *Nucleic Acids* Research, v. 49 p. D288-D297, 2020. DOI: 10.1093/nar/gkaa991

15 - **Clinical and Laboratory Standards Institute** (CLSI). 2012. Protocol M27-A9. Reference method for broth dilution antifungal susceptibility testing of bacteria. 2nd ed. Pennsylvania: NCCLS, 70p.

16 - MITIĆ-ĆULAFIĆ, D.; VUKOVIĆ-GAČIĆ, B.; KNEŽEVIĆ-VUKČEVIĆ, J.; STANKOVIĆ, 900 S.. SIMIĆ, D. Comparative study on the antibacterial activity of

volatiles from sage (Salvia 901 officinalis L.). *Arch. Biol. Sci.*, 2005. DOI: 10.2298/abs0503173m

17 - VAARA, M., VAARA, T. Outer membrane permeability barrier disruption by polymyxin in polymyxin-sesceptible and –resistant *Salmonella typhimurium*. *Antimicrob Agents Chemther*, v. 19, n. 4, p. 578-83, 1981. doi: 10.1128/AAC.19.4.578.

18 - ZHOU, K. *et al*. Mode of action pentocin 31-1: An antilisteria bacteriocina produced by Lactobacillus pentosus from Chinese traditional ham. *Food Control*, v. 19, n. 8, p. 817 – 822, 2008. doi: 10.1016/j.foodcont.2007.08.008.

19 – MOHANRAM, H.; BHATTACHARJYA, S. Salt-resistant short antimicrobial peptides, *Biopolymers*, 2016. https://doi.org/10.1002/bip.22819.

20 - ALMEIDA, C. V.; OLIVEIRA, C. F. R.; SANTOS, E. L.; SANTOS, H. F.; JÚNIOR, E. C.; MARCHETTO, R.; CRUZ, L. A.; FERREIRA, A. M. T.; GOMES, V. M.; TAVEIRA, G. B.; COSTA, B. O.; FRANCO, O. L.; CARDOSO, M. H.; MACEDO, M. L. R. Differential interactions of the antimicrobial peptide, RQ18, with phospholipids and cholesterol modulate is selectivity for microorganism membranes. *BBA – General Subjects*, 2021. doi: https://doi.org/10.1016/j.bbagen.2021.129937.

21 - SHARMA, L.; BISHT, G. S. Synergistic effects of short peptides and antibiotics against 904 bacterial and fungal strains. *Journal of Peptide Science*, 2022. DOI: 10.1002/psc.3446

22 - MILES, A. J.; RAMALLI, S. G.; WALLACE, B. A. DichroWeb, a website for calculating protein secondary structure from circular dichroism spectroscopic data. *Protein Science*, 2021. DOI: https://doi.org/10.1002/pro.4153

23 - SREEREMA, N.; VENYAMINOV, S. Y.; WOODY, R. W. Estimation of the number of helical and strand segments in proteins using CD spectroscopy. *Protein Sci.*, 1999. DOI: 10.1110/ps.8.2.370.

24 - SREERAMA, N.; WOODY, R. W. Estimation of protein secondary structure from CD spectra: Comparison of CONTIN, SELCON and CDSSTR methods with an expanded. *Anal. Biochem.,* 2000. DOI: https://doi.org/10.1006/abio.2000.4880

25 - Alain Filloux and Juan-Luis Ramos (eds.), Pseudomonas Methods and Protocols, Methods in Molecular Biology, vol. 1149, Springer Science+Business Media New York 2014. DOI: 10.1007/978-1-4939-0473-0_48

26 - SARDI, J. C. O.; POLAQUINI, C. R.; FREIRES, I. A.; GALVÃO, L. C. C.; LAZARINI, J. G.; TORREZAN, G. S.; REGASINI, L. O.; ROSALEN, P. L. Antibacterial activity of diacetylcurcumin against *Staphylococcus aureus* results in decreased biofilm and cellular adhesion. *J Med Microbiol.,* 2017. DOI: 10.1099/jmm.0.000494.

27 – LEI, J.; SUN, L.; HUANG, S.; ZHU, C.; LI, P.; HE, J.; MACKEY, V.; COY, D. H.; HE, Q. The antimicrobial peptides and their potential clinical applications. *Am J Transl Res.* 2019,11(7):3919-3931. PMID: 31396309; PMCID: PMC6684887.

28 – LE, M. N. T.; KAWADA-MATSUO, M.; KOMATSUZAWA, H. Efficiency of antimicrobial peptides against multidrug-resistant Staphylococcal pathogens. *Frontiers in Microbiology*, 2022. DOI: 10.3389/fmicb.2022.930629

29 – HAN, W.; WEI, Z.; CAMESANO, T. A. New antimicrobial peptide-antibiotic combination strategy for *Pseudomonas aeruginosa* inactivation. *Biointerphases*, 2022. DOI: 0.1116/6.0001981

30 – CHEN, Y. C.; QIU, W.; ZHANG, W.; ZHANG, J.; CHEN, R.; CHEN, F.; WANG, K. J. A novel antimicrobial peptide Sp-LECinwith broad-spectrum antimicrobial activity and anti-*Pseudomonas aeruginosa* infection in Zebrafish. *Molecular Scienses*, 2022. DOI: 10.3390/ijms24010267

31 – ALMEIDA, L. H. O.; OLIVEIRA, C. F. R.; RODRIGUES, M. S.; NETO, S. M.; BOLETI, A. P. A.; TAVEIRA, G. B.; MELLO, E. O.; GOMES, V. M.; SANTOS, E. L.; JUNIOR, E. C.; FRANCO, O. L.; CARDOSO, M. H. S.; MACEDO, M. L. R. Apemaycin: design, synthesis and biological porperties of a new peptide with antimicrobial properties. *Archives of Biochemistry and Biophysisc*, 2020. DOI: 10.1016/j.abb.2020.108487

32 – MBA, I. E.; NWEZE, E. I. Antimicrobial peptides therapy: na emerging alternative for treating drug-resistant bactéria. *Yale Journal of Biology and Medicine*, 2022. PMID: 36568838; PMCID: PMC9765339.

33 – WANG, M.; DENG, Z.; LI, Y.; XU, K.; MA, Y.; YANG, S. T.; WANG, J. Antibiofilm property and multiple action of peptide PEW300 against *Pseudomonas aeruginosa*. *Front Microbiol*. 2022, 29;13:963292. DOI: 10.3389/fmicb.2022.963292.

CAPÍTULO III – ATIVIDADE ANTICÂNCER DE KWI-19 FRENTE A LINHAGEM DE MELANOMA MURINO (B16F10-Nex2)

Exploring the Potente Dual Action of na Antimicrobial Peptide: Inhibiting Proliferation and Inducing Necrosis in Murine Melanoma Cells (B16F10-Nex2)

Luís Henrique de Oliveira Almeida[a], Suellen Rodrigues Ramalho[a], Caio Fernando Ramalho de Oliveira[a], Claudiane Vilharroel Almeida[a], Camila de Oliveira Gutierrez[a], Tamaeh Monteiro-Alfredo[a], Kamylla Fernanda Souza de Souza[b], Breno Fernandes Barreto Sampaio[c], Bianca Acacio[c], Kely de Picoli Souza[d], Octávio Luiz Franco[e,f], Marlon Henrique Cardoso[a,e,f] and Maria Lígia Rodrigues Macedo[a]*

[a]Laboratório de Purificação de Proteínas e suas Funções Biológicas (LPPFB), FACFAN, Universidade Federal de Mato Grosso do Sul, Campo Grande, Brazil;

[b]Laboratório de Biologia Molecular, INBIO, Universidade Federal de Mato Grosso do Sul, Campo Grande, Brazil;

[c]Laboratório Multiuso da FAMEZ, Universidade Federal de Mato Grosso do Sul, Campo Grande, Brazil;

[d]Grupo de Apoio aos Estudos da Biodiversidade (GAEB), Universidade da Grande Dourados, Dourados, Brazil;

[e]S-Inova Biotech, Programa de Pós-Graduação em Biotecnologia, Universidade Católica Dom Bosco, MS, Brazil;

[f]Centro de Análises Proteômicas e Bioquímicas, Programa de Pós-Graduação em Ciências Genômicas e Biotecnologia, Universidade Católica de Brasília, DF, Brazil.

* Correspondence:

Prof. Maria Lígia Rodrigues Macedo

Email: ligiamacedo18@gmail.com

ABSTRACT

Malignant melanoma is classified as the most aggressive and fatal type of skin cancer. It has become a serious global health problem due to the significant increase in cases in recent years and to the resistance to the available treatments. In this way, the importance of discovering and/or developing new anticancer agents stands out. Among the classes of biomolecules available for treatment, peptides have stood out due to their broad spectrum of biological activities. Several cationic peptides have promising antineoplastic effects. In this work, we describe the antiproliferative activity of KWI-19, a cationic peptide composed by 19 amino acid residues that adopts α-helix structure in membrane-like environments and that has been characterized by its candicidal, antibacterial, antibiofilm and non-toxic activities. KWI-19 showed antiproliferative activity in murine melanoma cells (B16F10-Nex2) with an IC_{50} of 22.14 $\mu mol\ L^{-1}$. Furthermore, this peptide affected mitochondrial membrane potential, caused nuclear swelling, induced caspase activation, caused cell death through necrosis, and promoted the release of DAMPs, signaling the recruitment of the immune system to combat neoplastic cells. Due to the promising results of KWI-19 with murine melanoma cells, new tests, including with other types of cells, must be carried out to determine its mechanism of action to reinforce the anticancer potential of this peptide.

Keywords: melanoma; anticancer; anticancer peptide; fluorescence microscopy.

1. INTRODUCTION

Melanoma is a type of cancer that affects melanocytes, pigment-producing cells, found in the basal layer of the epidermis [1]. This malignancy originates from genetic mutations in melanocytes and is predominantly found in the skin, eyes, inner ear, and leptomeninges [2]. Melanoma is the most aggressive and deadly form of skin cancer, affecting mainly the Caucasian population [2]. According to data from the Surveillance, Epidemiology, and End Results Program (SEER), melanoma was the fifth most common cancer diagnosis in the United States in 2021, with an estimated 106 thousand new cases, accounting for 5.6% of all cancer diagnoses in the country [1]. Furthermore, according to GLOBOCAN, in 2020, melanoma represented 1.7% of global cancer diagnoses, with estimated 325 thousand new cases [3].

While cancer primarily results from a series of genetic and/or epigenetic changes (intrinsic factors), affecting irregular cell growth, extrinsic factors such as diet, smoking, radiation, and infectious pathogens also play a significant role [4]. These extrinsic factors encompass various influences such as radiation exposure, diet, smoking, and infections, caused by pathogens. Infectious pathogens, including bacteria and fungi, cause approximately 20% of all human cancers [5]. Various types of cancer can occur due to the contribution of persistent infections, lack of immune system response, and chronic inflammation [4]. These events can lead to disordered cell proliferation and an increased risk of oncogenic transformation, even in immunocompetent individuals [4].

Cancer treatment can be performed through surgical procedures, chemotherapy, radiotherapy, photodynamic therapy, immunotherapy, targeted therapy, and combination of two of these treatments, but the most appropriate type of therapy depends largely on the characteristics of the tumor, such as stage, location

and genetic profile [2]. Among the available treatments, chemotherapy was the first option for the treatment of advanced melanoma, but the drug combinations studied to improve clinical response did not improve overall survival, and one of the hypotheses is due to resistance to apoptosis, which is the main cause of resistance to chemotherapy in melanoma [2]. Among the available drugs are dacarbazine (1974), interferon α-2b (1995), interleukin-2 (1998), ontak (1999), penginterferon α-2b (2011), vemurafenib (2011), ipilimumab (2011), dabrafenib (2013), trametinib (2013), nivolumab (2014), pembrolizumab (2014), dabrafenib+trametinib (2014), talimogene laherparepvec (2015) and cobimetinib+vermurafenib (2015) [2].

However, in the treatment of melanoma, some limitations are important for carrying out the most appropriate therapy, such as adverse effects, which can lead to toxicity and reduced efficiency, due to the acquired resistance mechanism [2]. In this context, there is a need for the discovery and development of new drugs with anticancer activity, such as antimicrobial peptides (AMP). Many of the antimicrobial peptides (AMPs) have shown a broad spectrum of biological activities, including antibacterial, antifungal, antiparasitic, and even anticancer (ACP). ACP are cationic, short in-length peptides (5 to 50 amino acid residues), rich in hydrophobic amino acid residues, as well as positively charged residues [6]. The presence of positively charged residues facilitates the action of ACP on neoplastic cells, since these cells have negatively charged membranes, therefore there is electrostatic attraction, causing a cytotoxic effect through the disruption of cell membranes [6].

AMPs can have more than one biological activity, which makes them attractive compounds for the next generation of drugs. One way to explore the potential of these compounds is to carry out different biological assays with those compounds that have already shown some biological activity. Among the AMPs that have been studied, one

that showed significant activity against planktonic bacterial cells, biofilms, and yeast is the KWI-19 peptide [7]. KWI-19 is a bioinspired peptide following the *Inga laurina* trypsin inhibitor (ILIT). It has an amphipatic α-helical secondary structure, determined both theoretically and experimentally. The peptide has a positive net charge of +6 (cationic). In terms of toxic effects on healthy mammalian cells, the KWI-19 peptide showed no cytotoxic effect against murine macrophages (IC_{50} = 64 µmol L^{-1}) and was non-toxic *in vivo* on *Galleria mellonella* larvae. In this context, we aimed to assess the antiproliferative potential of the KWI-19 peptide in murine melanoma cells, investigate its mechanism of action, and evaluate its ability to activate the immune system for the future development of an *in vivo* vaccine.

2. MATERIALS AND METHODS

2.1. In silico analysis of cytotoxic activity

The *in silico* analyzes to predict the cytotoxic and anticancer activity of the peptide KWI-19 (H_2N–KWIRRIIRDYKKFFIKFII–COOH) were performed using free online servers. To evaluate the prediction of anticancer activity, the software ACPred, AntiCP 2.0 and ENNAACT [8, 9 and 10] were used.

2.2. Cell culture

The murine melanoma cell line (B16F10-Nex2) was cultivated in Roswell Park Memorial Institute Medium (RPMI-1640, Sigma, USA), supplemented with 10% fetal bovine serum (FBS, Sigma, USA) and 1% antibiotics (5 mg mL^{-1} penicillin, 5 mg mL^{-1} streptomycin and 10 mg mL-1 of neomycin). Cells were cultivated at 37 °C and 5% CO_2. Experiments conducted in the absence of FBS supplementation in the culture medium were performed with the purpose of preventing the interference of the enzymes present in FBS with the action of the peptide.

2.3. Cell viability assays

Cell viability was evaluated with the 3-(4,5-dimethylthiazol-2-yl)-2,5-diphenyltetrazolium bromide (MTT, Invitrogen, USA) assay. Cells were seeded ($5x10^3$ cells/well, confluence ≥ 80%) in 96-well microplates and treated with different concentrations of KWI-19 peptide (0.25 – 64 µmol L^{-1}), diluted in culture medium without supplementation with FBS (0% FBS). After a period of 24 h, the microplates had the culture medium replaced by 100 µL of MTT (0.5 mg mL^{-1}, prepared in RPMI 1640, 10% FBS), followed by a new incubation of 4 h. Subsequently, the MTT was removed and 100 µL of dimethylsulfoxide (DMSO) was added to the wells, in order to

solubilizy the formazan crystals. Absorbances were determined at 630 nm in a Varioskan Lux microplate reader (Thermo Scientific) and cell viability was calculated using the SkanIt 6.0 software (Thermo Scientific). Data are presented as mean ± standard deviation of the mean. The values of 50% inhibitory concentration (IC_{50}) were calculated with GraphPad Prism 8.0 software.

2.4. Cellular morphological changes

Cells were seeded ($5x10^4$ cells/well, confluence ≥ 80%) in 24-well microplates and treated with the KWI-19 peptide at the IC_{50} concentration (previously determined). The peptide was diluted in RPMI 1640, 0% FBS, and the cells were incubated for 12 h with cell monitoring on the zenCELL 24-channel microscope. The peptide's action time could be determined according to the count of non-viable cells in the evaluated perod and, through the images it was possible to observe alterations in the cellular physical integrity.

2.5. Mitochondrial potential and nuclear morphology

The experiments of mitochondrial potential and nuclear morphology of B16F10-Nex2 cells were performed according to the protocol described by Wodlej *et al*. (2019) [11]. Cells were seeded ($5x10^4$ cells/well, confluence ≥ 80%) in 24-well microplates and treated with the KWI-19 peptide, at the IC_{50} concentration, diluted in RPMI 1640, 0% FBS, and incubated for 120 min. For fixation, cells were washed gently with Dulbecco's phosphate buffered saline without calcium and magnesium (DPBS, Gibco, Thermo Fisher Scientific, USA) and fixed with 1% (w/v) paraformaldehyde for 10 min at room temperature. MitoTracker Deep Red (Molecular Probes Inc., Eugene, OR, USA) (excitation wavelength, 650 nm; emission wavelength ,668 nm) was used for

staining mitochondria in B16F10-Nex2 cells. The stock solution of the probe (1 mmol L^{-1} in DMSO) was diluted 1:20000 in DPBS. Cells were stained with 0.05 μmol L^{-1} of MitoTracker Deep Red for 15 minutes at 37 ˚C. NucBlue Live ReadyProbes reagent (Molecular Probes Inc., Eugene, OR, USA) (excitation wavelength, 359 nm; emission wavelength, 461 nm) was used for co-staining of nucleus with mitochondria. One drop of the ready-to-use kit (~5 μL) was transferred to each well and incubated for 5 minutes before carrying out the microscopic analyses. Images were captured in a Leica DM 2000 LED microscope, equipped with a Leica DFC 7000 T camera.

2.6. Detection of active caspases in cells

B16F10-Nex2 cells were seeded ($1.05x10^6$ cells/well, confluence ≥ 80%) in wells of a 06-well microplate in RPMI 1640, 0% FBS, and incubated for 24 h. After reaching the confluence, the supernatant was replaced by the KWI-19 peptide treatment was added at the IC_{50} concentration for 24 h. As a negative control, RPMI 1640 was used. After the incubation time, the supernatant was removed and 3 mL of CaspACETM FITC- VAD-FMK *In situ* Marker was added to the wells at a concentration of 10 μmol L^{-1}, incubated for 20 minutes, protected from light. Posteriorly, the supernatant was aspirated and the cells washed 2 times with 1X PBS. Cells were fixed with formalin solution and washed 3 times for 5 minutes with 1X PBS. Fluorescence microscopy analyzes were performed using a Leica DM 2000 LED microscope, equipped with a Leica DFC 7000 T camera.

2.7. Flow cytometry

Annexin V binding was assessed by flow cytometry, and cell staining was assessed using FITC-labelled annexin V (green fluorescence) and propidium iodide

(PI) (red fluorescence negative) simultaneously. This test allows the identification of intact cells (An-/PI-), late apoptotic cells (An+/PI+), apoptotic cells (An+/PI-) and necrotic cells (An-/PI+) [12]. B16F10-Nex2 cells were exposed to KWI-19 (IC_{50} - 22.14 μmol L^{-1}) for 2 and 4 hours. Cells were washed with PBS, resuspended in 400 μL binding buffer (10 mmol L^{-1} Hepes/NaOH, pH 7.4, 140 mmol L^{-1} NaCl, 2.5 mmol L^{-1} $CaCl_2$) and incubated with 10 μL of annexin V-FITC (MedSystems Diagnostics, GmbH, Australia) for 10 minutes at room temperature. After incubation, cells were washed with binding buffer and exposed to 1 μg of PI in a final volume of 400 μl. annexin-FITC and PI fluorescence were determined using a CytoFLEX Beckman COULTER flow cytometer, from the Multidisciplinary Laboratory of FAMEZ-UFMS. Data analyzes were carried out in FlowJo.

2.8. Release of DAMPs – calreticulin and HMGB1

ELISA assays were performed for the quantification of calreticulin and HMGB1 (Mouse Calreticulin, CALR ELISA Kit; Mouse High Mobility Group Protein B1, HMGB-1 ELISA Kit; Bioassay Technology Laboratory, Shanghai Korain Biotech Co., Ltd.) in cell culture supernatants according to the manufacturer's instructions.

2.10. Statistical analysis

Statistical analyzes were performed using One way-ANOVA, followed by Dunnett's or Tukey's multiple comparison tests using GraphPad Prism version 8.0. for Windows, GraphPad Software, San Diego, California, USA, www.graphpad. with.

3. RESULTS

In silico analysis of cytotoxic activity

From the primary sequence of the KWI-19 peptide, it was possible to predict its cytotoxic activity using free online servers. In this prediction analysis, the ACPred, AntiCP 2.0 and ENNAACT servers were used (Table 1), in which we verified that the KWI-19 peptide sequence has a high prediction of anticancer activity (> 70%), which was crucial for carrying out *in vitro* and *in vivo* tests.

Table 1 – Anticancer activity predicted *in silico* by the ACPred, AntiCP 2.0 and ENNAACT software of the parental peptide and the KWI-19 peptide.

Server	Prediction	Score
ACPred	ACP	0.99
AntiCP 2.0	AntiCP	0.72
ENNAACT	ACP	0.99

Cell viability assay

Once the *in silico* anticancer activity of the KWI-19 peptide was predicted, the *in vitro* cell viability assay was performed using the MTT assay, where formazan crystals are formed. The test was carried out with murine melanoma cells (B16F10-Nex2), and it was found that the IC_{50} value of the KWI-19 peptide for this cell line was 22.14 µmol L^{-1} (Figure 1). This obtained value is less than half of the value observed for a healthy murine macrophage cell line (RAW 264.7), where the KWI-19 peptide had an IC_{50} of 48.82 µmol L^{-1} [7].
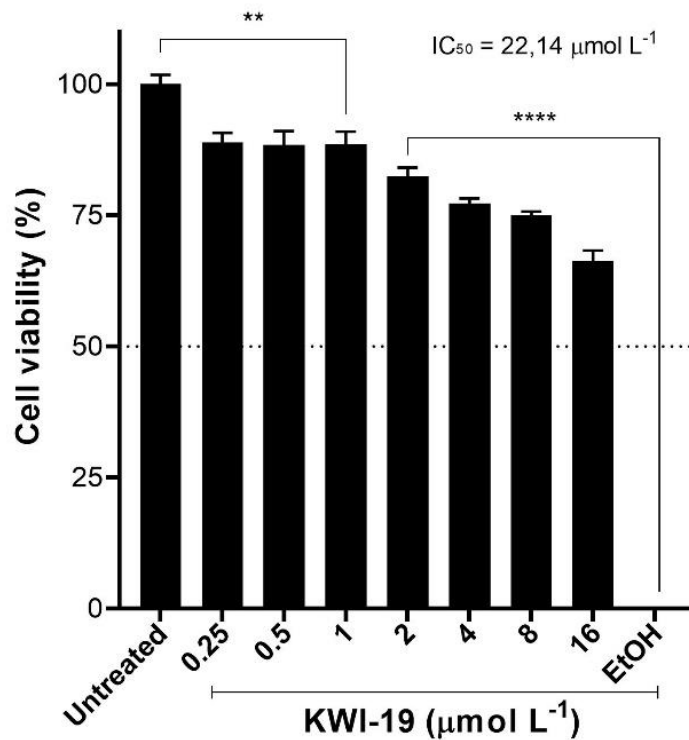
Figure 1 – Percentage of cell viability of the B16F10-Nex2 strain when treated with KWI-19 at different concentrations (* *vs* Untreated cells; *p < 0.05; **p < 0.01; ***p < 0.001; ****p < 0.0001, ANOVA). The IC_{50} was determined from seven increasing concentrations and calculated from the standard dose curve by non-linear regression.

Analysis of morphological and functional changes in cells treated with KWI-19

To assess whether the peptide was able to promote changes in cell morphology after treatment, a viability assay was performed and monitored in real time with the *zenCELL* microscope, where images were captured every 5 min. Through this process, the morphology of cancer cells underwent intense changes within 2 hours after exposure to the KWI-19 peptide. This was detected through intense nuclear staining and changes in cell shape, as the cells were no longer adherent and began to present a circular format (Figure 2).
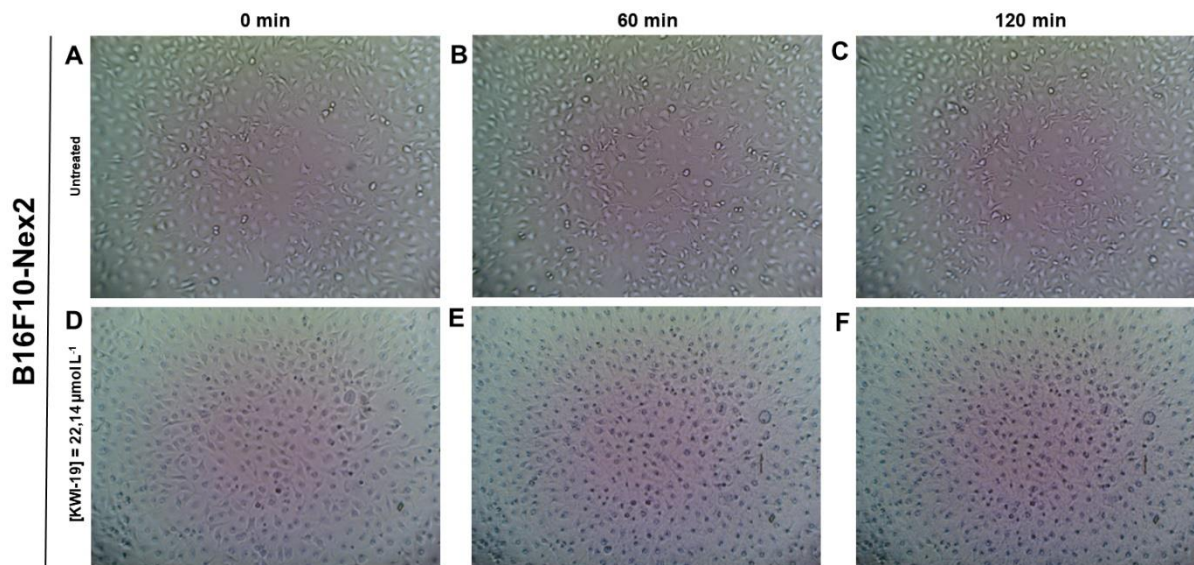
Figure 2 – Analysis of morphological and functional changes in cells B16F10-Nex2 treated and non-treated with KWI-19. Cells without treatment (A) 0min, (B) 60 min, (C) 120 min; and B16F10-Nex 2 cells treated with KWI-19 at 22.14 µmol L^{-1} at times (D) 0 min, (E) 60 min, (E) 120 min.

The staining of mitochondria and cell nuclei with MitoTracker™ and NucBlue probes made it possible to observe significant induction of KWI-19 in swelling of the cell nucleus (blue coloration), and in the mitochondria we verified that the treated cells showed less fluorescence when compared to the control (red coloration). MitoTracker™ is a membrane-permeating dye and its accumulation in mitochondria depends exclusively on the mitochondrial membrane potential. When undamaged cells are treated with MitoTracker™ there is an accumulation of this fluorophore in the mitochondria, which allows its visualization through fluorescence emission. This process shows that there is an active mitochondrial membrane potential. In contrast, when there is damage to cells treated with this fluorophore, there is no fluorescence emission, since there is no active mitochondrial membrane potential, which is an indication of death by apoptosis. We observed that KWI-19 can damage the mitochondrial membranes of melanoma cells, in accordance with the lower fluorescence emitted in treated cells.
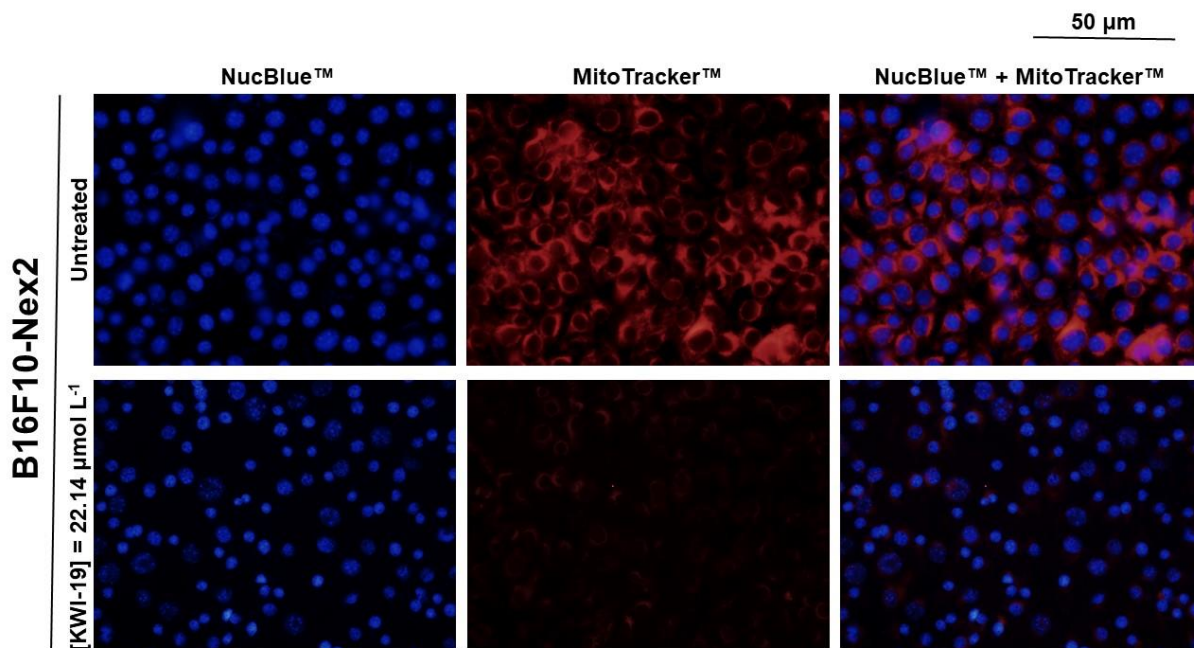
Figure 3 – Changes in the nuclear and mitochondrial morphology of B16F10-Nex2 cells after exposure to the KWI-19 peptide at IC_{50} - 22.14 µmol L^{-1}. Overlay of images of melanoma cells (B16F10-Nex2) with stained mitochondria (red, MitoTracker Deep Red) and nucleus (blue, NucBlue). It is possible to observe that the changes caused by nuclear swelling and reduction of mitochondrial potential are noteworthy.

Determination of the type of cell death

To determine the type of cell death after KWI-19 exposure, two assays were performed. The first was the detection of active caspases in B16F10-Nex2 cells using the FITC-VAD-FMK caspase detection kit. This fluorescent marker is a non-toxic and cell-permeable inhibitor that binds irreversibly to activated caspases in cells dying by apoptosis, and the fluorescence intensity was observed under fluorescence microscopy. When treated with KWI-19, we observed that the fluorescence emitted by the cells was of high intensity (Figure 4). This suggests that apoptosis may be one of the likely mechanisms of action for the KWI-19 peptide against B16F10-Nex2 cells.
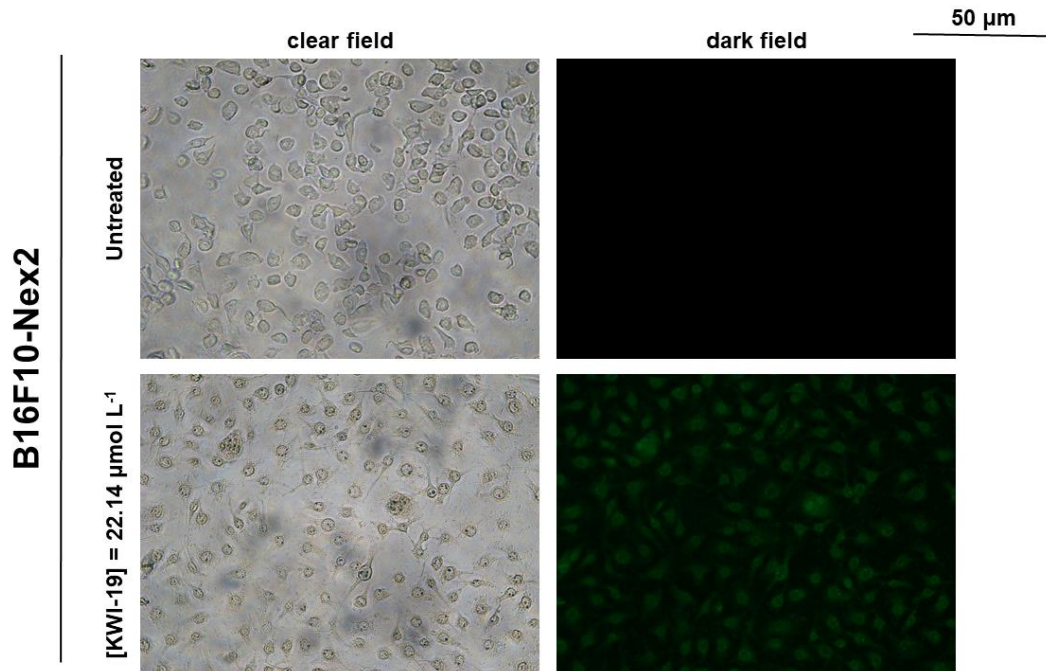
Figure 4 – Detection of active caspases in B16F10-Nex2 cells treated with KWI-19 at 22.14 µmol L^{-1}. Green cells indicate the presence of active caspase pathways.

To detect the death process that occurs with greater predominance in cells treated with the KWI-19 peptide, a flow cytometry assay was performed. As a result, we observed that the KWI-19 peptide induces necrosis in B16F10-Nex2 cells (Annexin V - / PI +), with a percentage of 62.4% after 2h of treatment and 73.1% after 4h of treatment (Figure 5).

Figure 5 – Flow cytometry of treated and untreated cells with KWI-19 at 22.14 µmol L^{-1}. (A) B16F10-Nex2 cells without any treatment. (B) B16F10-Nex2 cells treated with KWI-19 peptide at IC$_{50}$ for 2 h. (C) B16F10-Nex2 cells treated with KWI-19 peptide at

IC$_{50}$ for 4 h. [An+Pi+ late apoptosis; An+Pi- apoptosis; An-Pi- healthy cells; An-Pi+ necrosis].

Evaluation of immunogenic cell death

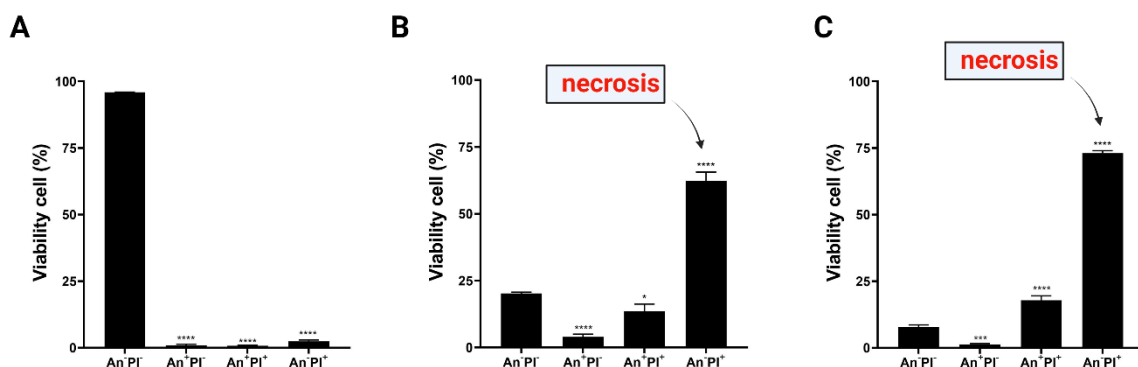To assess whether the KWI-19 peptide can induce immunogenic cell death (ICM) in B16F10-Nex2 murine melanoma cells, our objective was to determine whether the peptide could promote the release of molecular patterns associated with specific damage (DAMPs). The release of DAMPs in a cancer-affected system allows the recruitment of dendritic cells, enhances the uptake of tumor antigens, initiates cross-presentation of antigens, and subsequently triggers an adaptive antitumor response. Peptides with anticancer activity can initiate a series of cascading cellular signaling reactions that may ultimately lead to the development of immunological memory against tumor-related antigens, thus promoting the prevention of neoplasm recurrence. To verify whether KWI-19 could induce the release of DAMPs, we conducted ELISA assays, following the manufacturers' guidelines for the kits used. In this assay, we found that KWI-19 promoted the release of both HMGB1 and calreticulin. Specifically, KWI-19 induced the release of calreticulin at 6.5 nmol mL^{-1} within 1 hour of treatment and 8.7 nmol mL^{-1} within 2 hours (Figure 6A). As for HMGB1, release reached 72.3 nmol mL^{-1} in 1 hour and 95.2 nmol mL^{-1} at 2 hours (Figure 6B).

Figure 6 – Immunogenic cell death in B16F10-Nex2 cells. (A) Quantification of calreticulin released by B16F10-Nex2 cells after exposure to KWI-19; (B) Quantification of HMGB1 released by B16F10-Nex2 cells after exposure to KWI-19.

4. DISCUSSION

Cancer has become a significant public health problem due to the limited effectiveness of conventional drugs. This ineffectiveness is exacerbated by the increasing acquisition of resistance to multiple drugs (MDR) by neoplastic cells, especially after prolonged use of chemotherapy drugs [23]. Furthermore, in recent years, compelling evidence has emerged indicating that an inflammatory response triggered by persistent microbial infections can enhance the metastatic potential of tumor cells [24]. To evaluate the potential of new drugs, we selected a peptide sequence known as KWI-19, which has already demonstrated antimicrobial activity documented in the literature [7]. Our objective was to explore its antiproliferative potential against murine melanoma cells.

The primary sequence of peptides and their spatial arrangement (secondary structure) are directly related to biological activity and their mechanisms of action. Most α-helical AMPs are rich in arginine and/or lysine residues, which contribute to the electrostatic interaction between AMPs and the cell membranes of their targets. The first interactions with the plasma membrane allow a better structural rearrangement, favoring the adoption of an active secondary structure [14, 15]. Furthermore, many AMPs exhibit anticancer activity, due to some characteristics that the cell membranes of microorganisms shares with cancer cell membranes. For example, the electrostatic attraction of peptides to cancer cell membranes is only possible because cancer cells have a lipid bilayer membrane rich in phospholipids, such as phosphatidic acid (PA) and phosphatidylserine (PS), which have a negative charge [16]. Therefore, the design of active biomolecules belonging to the cationic AMP class contributes to electrostatic

interactions, causing disturbances in membrane integrity, which is a commonly reported mechanism of action for AMP [14, 17].

The obtained data in this study align with the findings of the existing literature. The KWI-19 peptide (KWIRRIIRDYKKFFIKFII) has a positive charge (+6) and an α-helix secondary structure defined by circular dichroism (CD) spectroscopy [7]. These characteristics of the KWI-19 peptide are correlated with its anticancer activity and its initial interaction with the cell membrane. AMPs with anticancer activity can lead to cell death through the activation of apoptosis, e.g.,, signaling cascades and caspase activation [18], as seen in Figure 4. Nevertheless, AMPs can also induce cell death through the process of necrosis, where the peptide directly interacts with the membrane, causing substantial damage to the cell membrane [18], as we also observed in Figure 5. Furthermore, a single AMP with anticancer activity can have more than one mechanism of action, reaching up to intracellular targets, which can cause the inhibition of vital processes of cancer cells [18].

As peptides gained notoriety due to their applications in healthcare, research laboratories and pharmaceutical industries engaged in the study and production of medicines based on these compounds. A series of peptides have already been approved and have clinical use in combating different types of cancer, such as carfilzomib, venetoclax, osimertinib, doxorubicin, cisplatin, among others approved by the Food and Drug Administration (FDA) [19]. Compared to other peptides that have anticancer activity on B16F10 cell lineage, it appears that the IC_{50} does not show significant variation. For example, the Figainin 1 peptide has an IC_{50} of 10.5 µmol L^{-1} [20], while the KWI-19 peptide has an IC_{50} of 22.14 µmol L^{-1} (Figure 1). As KWI-19, Figainin 1 presents itself as an hemolytic peptide (HC_{50} = 10.0 µmol L^{-1}), however, the selectivity index of KWI-19 (HC_{50} = 6.54 µmol L^{-1}) [7] is greater than that of Figainin 1,

being 3.39 and 1.05, respectively. Another peptide that showed antiproliferative activity against B16F10 cells was the LVTX-9 peptide, with an IC_{50} of 59.2 µmol L^{-1} [21]. The LVTX-9 peptide was also analyzed for its derivatives, which were obtained through modifications with the inclusion of fatty acids in its structure to increase cytotoxicity against B16F10 cells, but some of the molecules obtained proved to be ineffective, with an IC_{50} greater than 200 µmol L^{-1} [21].

The immunogenic cell death induction activity was also evaluated. In this type of death, the cell, when exposed to the peptide, undergoes a stress process that is initially detectable by the endoplasmic reticulum, through induction of the so-called unfolded protein response (UPR). UPR stimulates the phosphorylation of eIF2α and leads to cell surface exposure of calreticulin (CALR), which is a chaperone protein constitutively abundant in the endoplasmic reticulum. When exposed, this protein signals dendritic cells that begin the phagocytosis process [13]. Another signaling molecule that is released in the extracellular environment is the high mobility group box 1 protein (HMGB1), which can also be detected by dendritic cells through interaction with different receptors, including TLR4, leading to maturation of dendritic cells and, then the same process prescribed previously [13]. KWI-19 was able to induce the release of these DAMPs *in vitro*, which required further experiments to be performed *in vivo*.

In *in vivo* assays, the immunogenic response is common in regard to peptide vaccines, since most of these vaccines have low efficiency and/or moderate therapeutic results. One hypothesis for this to occur is correlated with the delivery of peptides, since they are molecules that have low stability due to the ease of being degraded by several enzymes present in the host's system. One strategy to overcome this difficulty is the encapsulation of the peptide in nanoliposomes, as described in the

work of Zahedipour and collaborators [22]. Zahedipour, using immunoinformatics tools, obtained peptide sequences derived from VEGFR-2, a functional protein linked to neovascularization of newly formed tumors, and selected the three peptides with the highest binding affinities [22]. These peptides were encapsulated in nanopolysomal formulations and administered subcutaneously in mice with melanoma tumors (B16F10), and substantial activation of CD4+ and CD8+ T cells was observed, significantly increasing the production of INF-γ and IL-4, and decreasing the tumor volume [22]. This is a proposal that can be used to evaluate how the KWI-19 peptide would act in recruiting immune system cells for better delivery. With this objetive in mind, further studies will be carried out at a later stage.

5. CONCLUSION

In this study, through *in silico* and *in vitro* analyses, it was possible to confirm that a peptide that has antibacterial, antifungal, and antibiofilm activity also exhibits anticancer properties. KWI-19 showed antiproliferative effects on murine melanoma cells *in vitro*, acting through multiple mechanisms of action. KWI-19 showed evidence of direct interaction with the cell plasma membrane, inducing ecrotic cell death, activating caspase pathways, reducing mitochondrial potential, and initiating processes associated with apoptosis. Additionally, it facilitated the release of Damage-Associated Molecular Patterns (DAMPs). Therefore, KWI-19 is a multifunctional peptide with significant potential for *in* vivo testing for the future development of a new peptide-based therapeutic strategy for the treatment of cancer.

PATENT APPLICATION

The application of KWI-19 is protected by a patent request, deposited at the National Institute of Industrial Property (INPI), under the number BR 10 2021 024849 1.

DECLARATION OF COMPETING INTERESTS

The authors declare no competing interests or personal relationships that could have appeared to influence the work reported in this paper.

SUPPORTING INFORMATION

The certificate issued by the Commission for Ethics in the Use of Animals (CEUA), issued by the Federal University of Grande Dourados Foundation is available in the Supplementary Material section.

6. REFERENCES

1 – SAGINALA, K.; BARSOUK, A.; ALURU, J. S.; RAWLA, P.; BARSOUK, A. Epidemiology of melanoma. *Medical Sciences*, 2021. DOI: 10.3390/medsci9040063

2 – DOMINGUES, B.; LOPES, J. M.; SOARES, P.; PÓPULO, H. Melanoma treatment in review. *Immno Targets and Therapy*, 2018. DOI: 10.2147/ ITT.S134842

3 - FERLAY, J.; ERVIK, M.; LAM, F.; COLOMBET, M.; MERY, L.; PIÑEROS, M.; ZNAOR, A.; SOERJOMATARAM, I.; BRAY, F. Global Cancer Observatory: Cancer Today. International Agency for Research on Cancer: Lyon, France. Available online: https://gco.iarc.fr/today (accessed on 10 May 2021).

4 – YUSUF, K.; SAMPATH, V.; UMAR, S. Bacterial infections and cancer: exploring this association and its implications for cancer patients. *International Journal of Molecular Sciences*, 2023. DOI: 10.3390/ijms24043110

5 – DE MARTEL, C.; GEORGES, D.; BRAY, F.; FERLAY, J.; CLIFFORD, G.M. Global burden of cancer attributable to infections in 2018: A worldwide incidence analysis. *Lancet Glob. Health*, 2020. DOI: 10.1016/S2214-109x(19)30488-7

6 – ZHANG, Y.; WANG, C.; ZHANG, W.; LI, X. Bioactive peptides for anticancer therapies. *Biomaterials Translational*, 2023. DOI: 10.12336/ biomatertransl.2023.01.00

7 – ALMEIDA, L. H. O.; RAMALHO, S. R.; ALMEIDA, C. V.; GUTIERREZ, C. O.; SARDI, J. C. O.; MIRANDA, A.; OLIVEIRA, R. A.; REZENDE, S. B.; CRUSCA, E.;

FRANCO, O. L.; OLIVEIRA, C. F. R.; CARDOSO, M. H.; MACEDO, M. L. R. A potent candicidal peptide designed based on an encrypted peptide from a proteinase inhibitor. *BBA - General Subjects*, 2023.

8 – SCHADUANGRAT, N.; NANTASENAMAT, C.; PRACHAYASITTIKUL, V.; SHOOMBUATONG, W. ACPred: A Computational Tool for the Prediction and Analysis of Anticancer Peptides. *Molecules*, 2019 May 22;24(10):1973. DOI: 10.3390/molecules24101973

9 – AGRAWAL, P.; BHAGAT, D.; MAHALWAL, M.; SHARMA, N.; RAGHAVA, G. P. S. AntiCP 2.0: an updated model for predicting anticancer peptides. *Briefings in Bioinformatics*, 2020. DOI: 10.1093/bib/bbaa153

10 – TIMMONS, P. B. & HEWAGE, C. M. ENNAACT is a novel tool which employs neural networks for anticancer activity classification for therapeutic peptides. *Biomedicine & Pharmacotherapy*, 2021. DOI: 10.1016/j.biopha.2020.111051

11 – WODLEJ, C.; RIEDL, S.; RINNER, B.; LEBER, R.; DRECHSLER, C.; VOELKER, D. R.; CHOI, J. Y.; LOHNER, K.; ZWEYTICK, D. Interaction of two antitumor peptides with membrane lipids – influence os phosphatidylserine and cholesterol on specificity for melanoma cells. *PLOS one*, 2019. DOI: 10.1371/journal. pone.0211187

12 – HAANEN, C.; VERMES, I. Apoptosis and inflammation. *Mediators os Inflammation*, 1995. DOI: doi.org/10.1155/S0962935195000020

13 – HUMEAU, J.; LÉVESQUE, S.; KROEMER, G.; POL, J. G. Gold Standar Assessment of Immunogenic Cell Death in Oncological Mouse Models. In: López-Soto, A., Folgueras, A. (eds) *Cancer Immunosurveillance*. Methods in Molecular Biology, vol 1884. Humana Press, New York, NY. DOI: doi.org/10.1007/978-1-4939-8885-3_21

14 – SOWA-JASIŁEK, A.; ZDYBICKA-BARABAS, A.; STACZEK, S.; PAWLIKOWSKA-PAWLEGA, B.; GRYGORCZUK-PŁANETA, K.; SKRZYPIEC, K.; GRUSZECKI, W. I.; MAK, P.; CYTRYNSKA, M. Antifungal Activity of Anionic Defense Peptides: Insight into the Action of Galleria mellonella Anionic Peptide 2. *Int. J. Mol. Sci.*, v. 21, 2020. doi: 10.3390/ijms21061912

15 – AVCI, F. G.; AKBULUT, B. S.; OZKIRIMLI, E. Membrane Active Peptides and Their Biophysical Characterization. *Biomolecules*, 2018. doi: 10.3390/biom8030077.

16 – SZLASA, W.; ZENDRAN, I.; ZALESINSKA, A.; TAREK, M.; KULBACKA, J. Lipid composition of the cancer cell membrane. *Journal of Bioenergetics and Biomembranes*, 2020. DOI: 10.1007/s10863-020-09846-4

17 – LAZZARO, B. P.; ZASLOFF, M.; ROLFF, J. Antimicrobial peptides: Application informed by evolution. *Science*, 2020. doi: 10.1126/science.aau5480.

18 – GASPAR, D.; VEIGA, A. S.; CASTANHO, M. A. R. B. From antimicrobial to anticancer peptides. A review. *Frontiers in Microbiology*, 2013. DOI: 10.3389/fmicb.2013.00294

19 – LATH, A.; SANTAL, A. R.; KAUR, N.; KUMARI, P.; SINGHN. P. Anti-cancer peptides: their current trends in the development of peptide-based therapy and anti-tumor drugs. *Biotechnology and Genetic Engineering Reviews*, 2022. DOI: 10.1080/02648725.2022.2082157

20 – SANTANA, C. J C.; MAGALHÃES, A. C. M.; SANTOS, A. C. M.; RICART, C. A. O.; LIMA, B. D.; ÁLVARES, A. C. M.; FREITAS, S. M.; PIRES, O. R.; FONTES, W.; CASTRO, M. S. Figainin 1, a novel amphibian skin peptide with antimicrobial and antiproliterative properties. *Antibiotics*, 2020. DOI: 10.3390/antibiotics9090625

21 – LI, F. ; WU, S.; CHEN, N.; ZHU, J.; ZHAO, X.; ZHANG, P.; ZENG, Y.; LIU, Z. Fatty acid modification of the anticancer peptide LVTX-9 to enhance its cytotoxicity aginst malignant melanoma cells. *Toxins*, 2021. DOI: doi.org/10.3390/toxins13120867

22 – ZAHEDIPOUR, F.; ZAMANI, P.; MASHREGHI, M.; ASTANEH, M.;SANKIAN, M.; AMIRI, A.; JAMIALAHMADI, K.; JAAFARI, M. R. Nanopolisomal VEGF-R2 peptide vaccine acts as na effective therapeutic vaccine in a murine B16F10 model of melanoma. *Cancer Nanotechnology*, 2023. DOI: 10.1186/s12645-023-00213-7

23 - WANG, J.; SEEBACHER, N.; SHI, H.; KAN, Q.; DUAN, Z. Novel strategies to prevent the development of multidrug resistance (MDR) in cancer. *Oncotarget*. 2017. DOI: 10.18632/oncotarget.19187.

24 - KOUZU, K.; TSUJIMOTO, H.; KISHI, Y.; UENO, H.; SHINOMIYA, N. Role of Microbial Infection-Induced Inflammation in the Development of Gastrointestinal Cancers. *Medicines* 2021, *8*, 45. DOI: 10.3390/medicines8080045

CONCLUSÃO

- Foi encontrado um peptídeo antimicrobiano encriptado na sequência de ILIT e feito modificações na sequência, as quis deram origem a um novo peptídeo multifuncional denominado KWI-19;

- A estrutura secundária teórica foi determinada, e KWI-19 apresentou estrutura secundária do tipo α-hélice;

- KWI-19 apresentou atividade antibacteriana frente espécies Gram-positivas e Gram-negativas e atividade antifúngica frente espécies leveduras do gênero *Candida*, com CIM variando entre 1,25 µmol L^{-1} a 20 µmol L^{-1};

- KWI-19 apresentou rápida ação frente *P. aeruginosa*, *S. saprophyticus* e *C. tropicalis*, nos tempos de 120 min, 30 min e 240 min, respectivamente;

- KWI-19 inibiu a formação do biofilme de *P. aeruginosa*, *S. saprophyticus* e *C. tropicalis* e e erradicou o biofilme maduro de *P. aeruginosa* e *C. tropicalis*;

- Foi verificado que o modo de ação do peptídeo KWI-19 tanto para as bactérias *P. aeruginosa* e *S. saprophyticus* quanto para *C. tropicalis* envolve danos na membrana celular;

- Quanto aos ensaios de citotoxicidade e toxicidade aguda, foi verificado que KWI-19 apresentou taxa de 50% de hemólise na concentração de 6,54 µmol L^{-}

[1] e não apresentou toxicidade aguda nas concentrações de 50 µmol L^{-1}, 25 µmol L^{-1} e 12,5 µmol L^{-1} quando testado i*n vivo* em larvas de *Galleria mellonella*;

- Quando testado com células saudáveis e de melanoma murino, RAW264.7 e B16F10-Nex2, respectivamente, apresentou IC$_{50}$ de 48,82 µM e 22,14 µM, ou seja, apresentou uma seletividade maior para células cancerígenas do que para células saudáveis;

- Através da citometria de fluxo foi verificado que a principal via de morte ativada por KWI-19 em células de melanoma murino é a necrose;

- KWI-19 foi capaz de liberar DAMPs *in vitro*, indicando uma provável ação imunogênica.

Portanto, KWI-19 é um potencial candidato a novos estudos *in vivo* para verificar a sua eficácia frente infecções microbianas e se apresentar resultados positivos pode vir a se tornar um novo agente antimicrobiano e anticâncer de uso clínico.

ANEXO

29409161937926302

Pedido nacional de Invenção, Modelo de Utilidade, Certificado de Adição de Invenção e entrada na fase nacional do PCT

Número do Processo: BR 10 2021 024849 1

Dados do Depositante (71)

Depositante 1 de 1

Nome ou Razão Social:	UNIVERSIDADE FEDERAL DE MATO GROSSO DO SUL
Tipo de Pessoa:	Pessoa Jurídica
CPF/CNPJ:	15461510000133
Nacionalidade:	Brasileira
Qualificação Jurídica:	Instituição de Ensino e Pesquisa
Endereço:	Av Costa e Silva, s/nº - Cidade Universitária
Cidade:	Campo Grande
Estado:	MS
CEP:	79070-900
País:	Brasil
Telefone:	(67) 3345 7188
Fax:	
Email:	nit.aginova@ufms.br

Dados do Pedido

Natureza Patente: 10 - Patente de Invenção (PI)

Título da Invenção ou Modelo de Utilidade (54): PEPTÍDEO SINTÉTICO BIOINSPIRADO NA SEQUÊNCIA DO INIBIDOR DE TRIPSINA DE Inga laurina

Resumo: A presente invenção se trata de uma nova sequência peptídica bioinspirada no inibidor de tripsina de Inga laurina (ILTI), que foi projetada utilizando ferramentas computacionais, com a finalidade de se obter uma nova sequência peptídica com as características físico-químicas desejáveis para um peptídeo classificado como antimicrobiano e anticâncer. Dessa forma, o peptídeo com a sequência composta por 19 resíduos de aminoácidos, KWIRRIIRDYKKFFIKFII, a qual foi sintetizado e testado in vitro e in vivo, trata-se de um peptídeo antibacteriano com atividade frente bactérias Gram-positivas e Gram-negativas susceptíveis e multirresistentes; antifúngico frente diversas cepas de Candida; antibiofilme frente Staphylococcus saprophyticus, Pseudomonas aeruginosa e Candida tropicalis; com potente atividade anticâncer predita in silico e não se mostrou tóxico em ensaios in vitro e in vivo.

Figura a publicar: 1

Dados do Inventor (72)

Inventor 1 de 5

Nome:	LUÍS HENRIQUE DE OLIVEIRA ALMEIDA
CPF:	04118933195
Nacionalidade:	Brasileira
Qualificação Física:	Pesquisador
Endereço:	Jesus Escalante Ribeiro, n.º146, Pq. Res. Dos Girassóis
Cidade:	Campo Grande
Estado:	MS
CEP:	79091-846
País:	BRASIL
Telefone:	
Fax:	
Email:	

Inventor 2 de 5

Nome:	SUELLEN RODRIGUES RAMALHO
CPF:	02528455100
Nacionalidade:	Brasileira
Qualificação Física:	Pesquisador
Endereço:	Rua Dona Amélia Augusta, n.º 196, Bairro Silvia Regina
Cidade:	Campo Grande
Estado:	MS
CEP:	79103-080
País:	BRASIL
Telefone:	
Fax:	
Email:	

Inventor 3 de 5

Nome: CAIO FERNANDO RAMALHO DE OLIVEIRA

CPF: 35661839898

Nacionalidade: Brasileira

Qualificação Física: Pesquisador

Endereço: Rua dos Jasmins, n.º 1348, Jd. Jóquei Club

Cidade: Campo Grande

Estado: MS

CEP: 79080-640

País: BRASIL

Telefone:

Fax:

Email:

Inventor 4 de 5

Nome: JANAÍNA DE CÁSSIA ORLANDI SARDI

CPF: 19510200816

Nacionalidade: Brasileira

Qualificação Física: Pesquisador

Endereço: Rua Dr. Werneck, n.º 41

Cidade: Campo Grande

Estado: MS

CEP: 79060-300

País: BRASIL

Telefone:

Fax:

Email:

Inventor 5 de 5

PETICIONAMENTO ELETRÔNICO Esta solicitação foi enviada pelo sistema Peticionamento Eletrônico em 09/12/2021 às 10:38, Petição 870210114409

Petição 870210114409, de 09/12/2021, pág. 4/55

Nome:	MARIA LÍGIA RODRIGUES MACEDO
CPF:	22106170300
Nacionalidade:	Brasileira
Qualificação Física:	Pesquisador
Endereço:	Rua das Caldas Aulete, n.ª 635, casa 13, Condomínio Village das Pedras, Coopharadio
Cidade:	Campo Grande
Estado:	MS
CEP:	79052-210
País:	BRASIL
Telefone:	
Fax:	
Email:	

Documentos anexados

Tipo Anexo	Nome
Comprovante de pagamento de GRU 200	00 29409161937926302.pdf
Relatório Descritivo	01 Relatorio Descritivo.pdf
Reivindicação	02 Reivindicação.pdf
Resumo	03 Resumo.pdf
Desenho	04 Desenho.pdf
Cadastro SISGEN	A315278.pdf

Sequências Biológicas

☑ Declaro que a informação contida na 'Listagem de Sequências' apresentada em formato eletrônico está limitada ao conteúdo da matéria revelada pelas sequências de aminoácidos e/ou de nucleotídeos divulgadas no pedido de patente, conforme depositado

Tipos de Sequências Biológicas	Nome
Listagem de Sequências Biológicas em formato TXT	LISTAGEM DA SEQUÊNCIA DE AMINOÁCIDOS DO PEPTÍDEO SINTÉTICO BIOINSPIRADO.txt

Acesso ao Patrimônio Genético

☑ Declaração Positiva de Acesso - Declaro que o objeto do presente pedido de patente de invenção foi obtido em decorrência de acesso à amostra de componente do Patrimônio Genético Brasileiro, realizado a partir de 30 de junho de 2000, e que foram cumpridas as determinações da Lei 13.123 de 20 de maio de 2015, informando ainda:

Número da Autorização de Acesso: A315278

Data da Autorização de Acesso: 14/12/2020

Declaração de veracidade

☑ Declaro, sob as penas da lei, que todas as informações acima prestadas são completas e verdadeiras.

PETICIONAMENTO ELETRÔNICO Esta solicitação foi enviada pelo sistema Peticionamento Eletrônico em 09/12/2021 às 10:38, Petição 870210114409

Petição 870210114409, de 09/12/2021, pág. 6/55

Comprovante de Cadastro de Acesso

Cadastro nº A315278

A atividade de acesso ao Patrimônio Genético, nos termos abaixo resumida, foi cadastrada no SisGen, em atendimento ao previsto na Lei nº 13.123/2015 e seus regulamentos.

Número do cadastro:	**A315278**
Usuário:	**MARIA LIGIA RODRIGUES MACEDO**
CPF/CNPJ:	**221.061.703-00**
Objeto do Acesso:	**Patrimônio Genético**
Finalidade do Acesso:	**Pesquisa e Desenvolvimento Tecnológico**

Espécie

Inga cylindrica

Staphylococcus aureus

Staphylococcus epidermidis

Escherichia coli

Salmonella enterica

Enterobacter aerogenes

Pseudomonas aeruginosa

Candida albicans

Candida tropicalis

Candida buinensis

Fagopyrum tataricum

Spodoptera frugiperda

Galleria mellonella

Staphylococcus saprophyticus

Staphylococcus haemolyticus

Klebsiella oxytoca

Proteus mirabilis

Enterobacter aerogenes

Enterobacter cloacae

Klebsiella pneumoniae

Acinetobacter baumannii

Serratia marcescens

Candida krusei

Candida parapsilosis

Candida glabrata

Erythrina poeppigiana

Staphylococcus aureus (MR)

Enterolobium gummiferum

Clitoria fairchildiana

Vigna unguiculata

Cucurbita maxima

Listeria monocytogenes

Enterococcus faecalis

Inga laurina

 Enterolobium Timbouva

Título da Atividade:	**BUSCA DE SUBSTÂNCIAS BIOATIVAS DE ORIGEM NATURAL OU SINTÉTICA**

Equipe

Ana Paula Ramos Pereira	**UFMS**
Caio Fernando Ramalho de Oliveira	**UFMS**
Claudiane Vilharroel Almeida	**UFMS**
Maria Caroline de Moura Cavalheiro	**UFMS**
Janaína de Cássia Orlandi Sardi	**UFMS**
Jesus Rafael Rodriguez Amado	**UFMS**
Cláudia Magno Pereira de Brito	**UFMS**

Luís Henrique de Oliveira Almeida	**UFMS**
Graziele Custodia Sandim	**UFMS**
Amanda Carollina Borges da Silva	**UFMS**
Letícia Souza Lima	**UFMS**
Simone Maria Neto	**UFMS**
Matheus Maganha da Silva	**UFMS**
Suellen Rodrigues Ramalho	**UFMS**
Bruna Sanae Moroto	**UFMS**
Milenna Queiroz Tobias	**UFMS**
Paula Bêlit Mazacote Zenteno	**UFMS**
Ricardo Abreu de Oliveira	**UFMS**
Thaís de Oliveira Anastácio	**UFMS**
Queisielle Magalhães Carvalho de Souza	**UFMS**

Data do Cadastro: **14/12/2020 18:19:14**

Situação do Cadastro: **Concluído**

Conselho de Gestão do Patrimônio Genético
Situação cadastral conforme consulta ao SisGen em **7:57** de **06/08/2021**.

SISTEMA NACIONAL DE GESTÃO
DO PATRIMÔNIO GENÉTICO
E DO CONHECIMENTO TRADICIONAL
ASSOCIADO - **SISGEN**